1-1-2004

Development of an Analytical Method for Distinguishing Ammonium Bicarbonate from the Products of an Aqueous Ammonia Co2 Scrubber and the Characterization of Ammonium Bicarbonate

Lingyu Meng
Western Kentucky University

DEVELOPMENT OF AN ANALYTICAL METHOD FOR DISTINGUISHING AMMONIUM BICARBONATE FROM THE PRODUCTS OF AN AQUEOUS AMMONIA CO_2 SCRUBBER AND THE CHARACTERIZATION OF AMMONIUM BICARBONATE

A Thesis

Presented to

The Faculty of the Department of Chemistry

Western Kentucky University

Bowling Green, Kentucky

In Partial Fulfillment

of the Requirements for the Degree

Master of Science

by

Lingyu Meng

December, 2004

DEVELOPMENT OF AN ANALYTICAL METHOD FOR

DISTINGUISHING AMMONIUM BICARBONATE FROM

THE PRODUCTS OF AN AQUEOUS AMMONIA CO_2 SCRUBBER AND

THE CHARACTERIZATION OF AMMONIUM BICARBONATE

Date Recommended 12/15/2004

Dr. Wei-Ping Pan, Director of Thesis

Dr. Stuart Burris

Dr. M. Thandi Buthelezi

Elmer Gray, Dean of the Graduate College, (December 16, 2004)

ACKNOWLEDGEMENT

I would like to express my deep appreciation to Dr. Wei-Ping Pan, my academic advisor and director of my thesis, for his instruction, encouragement and patience through the past one and a half years. This work would not have been accomplished without his expertise, guidance and assistance. I want to acknowledge Dr. Stuart Burris and Dr. M. Thandi Buthelezi for their wise and valuable suggestions. Thank Brimrose Corporation of America for their support of Near Infrared analysis. Additionally, I sincerely thank Dr. Qiao He, Dr. Xiaochang Wang, Dr. Weibing Xu, Mr. Dong Li and other researchers for their kind support during these one and half years. And also, I really appreciate the help from Nathan Whitely, my best friend. I wish to acknowledge my gratitude to all the faculty and staff members of the Department of Chemistry. I need to acknowledge the financial support for this study from Small Business Innovation Research (SBIR) of Department of Energy (Project Number: DE-FG02-03ER83740). Finally, I wish to show my innermost acknowledgement to my parents and my dearest wife. To all of the above, I appreciate what I got and what I did in the one and half years. Without the assistance and guidance from all of you, this thesis would have been a mission impossible.

Lingyu Meng

TABLE OF CONTENTS

Chapter Page

I. INTRODUCTION……1

A. Background……..1

B. Theory of the NH_3-CO_2 Reaction……6

C. Theory of the TGA Kinetics ……10

D. Research on the Analytical Method of Ammonium Bicarbonate and Characterization of Ammonium Bicarbonate ……...13

E. Objective of This Study……14

II. EXPERIMENTAL……..15

A. Bench Scale Aqueous Ammonia CO_2 Capture Experimental System……...15

B. Samples.……18

C. Instrumentation and Analytical Methods…….....18

D. Ammonium Bicarbonate Decomposition Kinetics by Thermogravimetric Methods ……..26

III. RESULTS AND DISCUSSION……..……....30

A. Development of an Analytical Method for Distinguishing Ammonium Bicarbonate from the Products of An Aqueous Ammonia CO_2 Scrubber……..……..30

B. Thermal Stability Analysis of Ammonium Bicarbonate

and Long Effect Ammonium Bicarbonate……..……..75

C. Kinetic Study of of Ammonium Bicarbonate and

Long Effect Ammonium Bicarbonate……...83

IV. CONCLUSIONS……...94

V. BIBLIOGRAPHY…..……....97

LIST OF TABLES

Tables Pages

1. Bench Scale Aqueous Ammonia CO_2 Capture Experimental System Operation Conditions ……17
2. TGA Kinetics Numerical Integration Constants……29
3. Summary of DSC Data ……43
4. XRD Data from Samples ……56
5. XRD Data from Library……56
6. C H N Concentration (Weight%) in Standard by Calculation. ……60
7. Quantitative Results of Two Unknown Samples by C H N Element Analysis ……60
8. NIR Prediction Results of WKU samples……74
9. Summarized Weight Losses of ABC and LEABC at Different Temperatures……78
10. Summarized Weight Losses of ABC and LEABC at Different Air Flow Rates ……82
11. ABC Isothermal 30^{o}C Experimental Data……84
12. LEABC Isothermal 30^{o}C Experimental Data……84
13. ABC Kinetic Parameters at Different Conversion Levels……91
14. LEABC Kinetic Parameters at Different Conversion Levels……91

LIST OF FIGURES

Figures Pages

1. Janecke NH_3-CO_2- H_2O three-phase diagram……..…..8
2. Activation energy of an exothermic reaction……....11
3. Schematic diagram of experiment setup of bench scale aqueous

   Ammonia CO_2 capture …….....…….....16
4. Example of DSC curve…….....20
5. Example of TGA curve……..21
6. Schematic of acousto-optic tunable filter (AOTF) …….....25
7. FTIR spectrum of sample NH_4HCO_3 standard at room temperature ……...31
8. FTIR spectrum of sample $(NH_4)_2CO_3$ standard at room temperature……...32
9. FTIR spectrum of sample $NH_2CO_2NH_4$ standard at room temperature……....33
10. Overlaid spectra of NH_4HCO_3 standard, $(NH_4)_2CO_3$ standard

    and $NH_2CO_2NH_4$ standard…….34
11. FTIR spectrum of sample LEABC at room temperature…..…….…….…….....35
12. Overlaid FTIR spectrum of sample ABC and LEABC…….....36
13. FTIR spectrum of sample 01050401 at room temperature……....38
14. FTIR spectrum of sample 01060401 at room temperature……....39
15. DSC curve for NH_4HCO_3 standard……....40

16. DSC curve for $(NH4)_2CO_3$ standard…….…....41

17. DSC curve for $NH_2CO_2NH_4$ standard…….…...42

18. DSC curve for sample 01050401…….....45

19. DSC curve for sample 01060401…….…....46

20. Overlaid TGA curves for ABC and ACN at 300@10°C/min ……47

21. Overlaid m/z curves for NH_3, H_2O and CO_2 from the decomposition of

ABC by mass …….....48

22. Overlaid m/z curves for NH_3 and CO_2 from the decomposition of

Ammonium Carbonate by mass …….....49

23. TGA curve for sample 01050401…….....50

24. TGA curve for sample 01060401……....51

25. XRD spectrum of NH_4HCO_3 standard ……...53

26. XRD spectrum of $(NH4)_2CO_3$ standard……..54

27. XRD spectrum of $NH_2CO_2NH_4$ standard……...55

28. XRD spectrum of sample 01050401...…… …….....57

29. XRD spectrum of sample 01060401…...……....58

30. NIR absorbance spectra of samples….....…….....63

31. Absorbance spectra after a second derivative pretreatment……...64

32. Second derivative spectra between 1400 nm and 1550 nm……....65

33. Scores plot of PCA……66

34. Variance plot of variables……...68

35. Variance plot of particle size……69

36. X-Loadings for regression model……..…70

37. Predicted versus measured plot for calibration……..…71

38. Predicted versus measure plot of cross validation……....…72

39. Overlaid TGA curves of ABC at different temperatures…….....76

40. Overlaid TGA curves of LEABC at different temperatures…….....……77

41. Overlaid TGA curves of ABC at different flow rates…….....……80

42. Overlaid TGA curves of LEABC at different flow rates…….....……81

43. Overlaid weight loss curves for ABC…….……86

44. Overlaid weight loss curves for LEABC……87

45. The logarithm of the heating rate versus the corresponding

reciprocal temperature at various conversion of ABC……....88

46. The logarithm of the heating rate versus the corresponding

reciprocal temperature at various conversion of LEABC……...89

47. Estimated lifetime of ABC…….....92

48. Estimated lifetime of LEABC…….....93

DEVELOPMENT OF AN ANALYTICAL METHOD FOR

DISTINGUISHING AMMONIUM BICARBONATE FROM

THE PRODUCTS OF AN AQUEOUS AMMONIA CO_2 SCRUBBER AND

THE CHARACTERIZATION OF AMMONIUM BICARBONATE

Lingyu Meng Date: Dec. 15, 2004 99 Pages

Directed by: Dr. Wei-Ping Pan, Dr. Stuart Burris and Dr. M. Thandi Buthelezi

Department of Chemistry Western Kentucky University

The link between anthropogenic emissions of CO_2 with increased atmospheric CO_2 levels and, in turn, with increased global temperature has been well established and accepted. Using aqueous ammonia to capture CO_2 and produce an inexpensive nitrogen fertilizer, ammonium bicarbonate (ABC) has been thought as a feasible approach to CO_2 sequestration.

Due to the different concentrations of reactants and reaction conditions, different carbon-ammonium composites can be produced. In view of achieving a maximum of NH_3 utilization in the capture of CO_2, the product of ABC will be ideal. Hence the ABC in the products needs to be identified. Various analytical techniques were used to distinguish the ABC. FTIR, DSC, TGA and XRD techniques were used to qualitatively distinguish the ammonium bicarbonate from the ammonium salts. The carbon, hydrogen and nitrogen element analysis and Near Infrared (NIR) techniques were used as quantitative analysis of ABC. The AOTF-NIR Free Space spectrometer is an ideal tool for real-time, on-line measurements of ABC. Sample 01050401 and Sample

01060401 from the CO_2 Scrubbing experiment by aqueous ammonia at WKU were determined by these techniques as ammonium bicarbonate and have very good quality as fertilizer in accordance with GB -3559-92 Agriculture Ammonium Bicarbonate National Standard of China.

During fertilizer storage and application, an amount of ABC will decompose into NH_3, H_2O and CO_2. Long-effect ABC (LEABC) is a product of co-crystallized dicyanodiamide (DCD) and ABC. In order to evaluate ABC fertilizer efficiency and its contribution to permanent carbon fixation, tests with Thermogravimetric Analysis (TGA) were conducted. The experiments by TGA indicated that the temperature and air flow rate have much less effect on the evaporation of the LEABC than on the ABC. Kinetic studies of ABC and LEABC gave their Activation Energy. At the 7.5% conversion rate, LEABC's Activation Energy is 111.9 kJ/mole, which is greater than ABC's Activation Energy 93.6 kJ/mole. The difference in Activation Energy explains the reason of different stability of ABC and LEABC.

I. INTRODUCTION

A. Background

It has been known for more than 100 years that carbon dioxide (CO_2) is a greenhouse gas and the release of CO_2 from fossil fuels may affect the climate of the earth.[1] The growing awareness of the risks of climate changes has generated public concerns and, since 1989, the interests of researchers in sequestering CO_2 has increased. As the world population increases and energy demand rises, increased burning of fossil fuels will continue to drive atmospheric CO_2 levels upward. The Inter-government Panel on Climate Change (IPCC) predicts that atmospheric CO_2 concentrations will be increased by approximately twice from the pre-industrial concentration of 270 ppm to a concentration of 530 ppm in 2050 and could potentially exceed 700 ppm by 2100.[2] This increase will significantly affect global weather and the physiological basis of plant production unless major changes are made. According to the United Nations Framework Convention on Climate Change (UNFCCC) at Kyoto,[3] a commitment to reduce CO_2 emissions t 6% below the year 1990's level was made by several countries. Industrialized countries should take the lead in comboating climate change and its adverse effects.

It has been noted that power production contributes one-third of the CO_2 released from fossil fuel combustion worldwide.[4] Future generation of CO_2 through combustion will be substantial. One way to manage carbon is to use energy more efficiently in order

to reduce the need for high carbon-fossil fuel combustion. Another way is to increase the use of low-carbon and carbon-free fuels and technologies (such as nuclear power, and renewable sources). The third way to manage carbon is CO_2 sequestration during combustion and post combustion processes. Capturing and securely storing carbon emitted from the global energy system is a truly novel concept. Fast CO_2 sequestration by physical or chemical means from combustion flue gas is highly desirable.

For CO_2 sequestration, the current technical focus is to determine a fast and inexpensive method to sequester carbon. There are two typical strategies to approach this task, one is to concentrate the CO_2 in-situ during the fuel conversion process, and the other one is to extract the CO_2 from the combustion flue gas. Since the fuel conversion process is usually very complex and difficult to control, the former technique is still highly investigative.[5] Several possibilities for the latter method have been proposed and developed, such as chemical solvents, physical absorption, cryogenic methods, membrane systems and biological fixation.[6-8] The chemical solvent methods are generally recognized as the most effective technologies at present. However, the cost for separation of CO_2 is high, typically in the range $40-200 /ton of carbon.[9] In addition, the chemical solvent method also has several major problems including a slow absorption rate, small solvent capacity, and special equipment requirements. To reduce the cost of capturing CO_2, a low cost solvent that can minimize the energy requirement, the equipment size, and equipment corrosion should be found. A novel approach that may provide a inexpensive and effective route of reducing CO_2 emissions from power plants is extracting CO_2 by an ammonia (NH_3) reagent in a wet scrubber.[10] Injection of NH_3 gas or aqueous NH_3 for removing NO_x (selective catalytic

reduction) from flue gas is a common process in power plants. Unlike the Monoethanolamine Process (MEA), the Aqueous Ammonia Process does not have absorbent degradation problems, which are caused by sulfur dioxide and oxygen in the flue gas and does not cause equipment corrosion, as in the case of MEA. In the work by Bai and Yeh,[11] based on breakthrough curves, the NH_3 scrubbing capacity was calculated to be around 0.35 mol of CO_2/mol of NH_3 on a molar basis, or 0.9 to 1.2 kg of CO_2/kg of NH_3 on a mass basis. The removal efficiency is approximate 99%. In the work by Smouse,[12] a multi-pollution control concept with spraying aqueous ammonia into actual flue gas to capture CO_2, SO_2 and NO_X emissions was proposed and developed. The capture efficiency of CO_2 in absorber was in the range from 76.4% to 91.7% at 35 ^oC.

The NH_3-CO_2 reactions are very complex. Many species co-exist in the solution in an unstable transition state. The products in the aqueous ammonia scrubber could include ammonium bicarbonate (ABC), ammonium carbonate, and ammonium carbamate (all in crystalline or aqueous solution forms), plus reactants CO_2, NH_3, and H_2O. Of these by-products, ammonium bicarbonate has been utilized by certain developing countries as a crop fertilizer for over 30 years with proven results.[13] As an alternative to using ammonium bicarbonate as fertilizer, the ammonia in ammonium bicarbonate can be regenerated. Ammonium bicarbonate decomposes at the relatively low temperature of 60^{o}C,[14] compared to a 120^{o}C regeneration temperature for MEA solutions. Ammonia is highly water soluble, thus ammonia and carbon dioxide can be separated.

During the regeneration process, the CO_2 can be released from heated ammonium salts, followed by removal of ammonia from evolved gases, with high-purity CO_2 as the final product. The thermal regeneration of NH_4HCO_3 to yield a concentrated stream of CO_2 has been demonstrated at National Energy Technology Laboratory (NETL).[12] Meanwhile, the ammonium-containing solution is recycled as a CO_2 absorbent. Also, the CO_2 can be scrubbed out in the form of ammonium bicarbonate and ammonium carbonate, thereby "fixing" or retaining the carbon in CO_2 in a stable chemical compound. As a fertilizer, especially in the form of the stable and long lasting fertilizer, long effect ammonium bicarbonate - LEABC, ammonium bicarbonate will dissociate into two ions, the ammonium (NH_4^+) and bicarbonate (HCO_3^-) ions. These two ions play distinct roles in carbon dioxide sequestration. The ammonium ion participates as a nitrogen fertilizer which enhances the carbon cycle, a biological change from CO_2 and water into biomass represented by $C[H_2O]_x$. The bicarbonate ion will most likely remain in the solution and move with the ground water down into the aquifer. The aquifer contains a significant amount of highly alkaline compounds, which will neutralize the bicarbonate ion and form stable carbonate salts, i.e., calcium carbonate, or limestone, as is seen in caves. Bicarbonate ions dissolved in water could be sequestered if the dissolved carbonate enters a deep groundwater system that has a residence time of hundreds to thousands of years.

This techniques presents many advantages for CO_2 capture over MEA process due to its lower costs, higher capacity and CO_2 absorption efficiency, lower decomposition temperatures of ammonium bicarbonate, less corrosive environment for the absorber material, and good performance of LEABC. As a CO_2 concentrator, it can absorb the CO_2 at the flue gas

concentration level with high absorption efficiency, and ultimately produce high purity CO_2. As a starting material for fertilizer synthesis, it could generate ammonium fertilizer with a long-lasting, stable performance in soil and at an inexpensive price.

There will be many advantages if ABC is the main product of the reactions. First is maximizing the NH_3 utilization in the capture of CO_2. Second is the production of a fertilizer of ABC, which can be modified to LEABC. Third is that high purity CO_2 can be regenerated with less energy. However, due to the different concentrations of reactants and reaction conditions, different carbon-ammonium composites can be produced. In particular, the site conditions at the utility boiler vary more than those in the laboratory. So the analysis of ABC in the products plays a very important role in sequestering CO_2 by aqueous ammonia, which can optimize the operating condition favoring the production of ABC and increase the sequestration efficiency. Although some analysis methods for ABC exist, there is no standard method. Further the analysis of mixtures of ABC with other ammonium salts is very challenging.

The process of CO_2 capture by aqueous ammonia and storage in the study can be divided into three stages, which include two cycles.[15] In the first stage, CO_2 capture, the CO_2 in power plant flue gas is captured by ammonium scrubbers and forms a fertilizer. The second stage, Short Term CO_2 Storage, focuses on how the captured carbon-fertilizer enhances plant photosynthesis to form biomass. The third stage involves another cycle, in which carbon in the soil system percolates to react with alkali cations in the soil and groundwater to form a permanent storage system.

In the second and third stage, the carbon stability in the fertilizer plays a very important role in the permanent sequestration of carbon dioxide as carbonate salts. Unstable fertilizer in the soil decomposes and releases CO_2 back to the atmosphere. After ammonium bicarbonate fertilizer is applied to soil, it is expected that it can remain stable in the soil long enough for the bicarbonate ion to percolate to react with free alkali cations and form precipitated salts, or move with the groundwater down into the aquifer. The stability of the fertilizers needs to be measured and evaluated.

B. Theory of the NH_3-CO_2 Reaction

CO_2 can be removed by ammonia scrubbing through chemical absorption at various temperatures and operating conditions. As illustrated by equation (1), ammonium carbamate (NH_2COONH_4) is the main product in dry conditions (without moisture) under ambient pressure. However, ammonium carbamate, is very soluble in water. Under moist condition, the hydration product of ammonium carbonate, $(NH_4)_2CO_3$, is produced at room temperature, as illustrated in equation (2).[10]

$$CO_2(g) + 2NH_3(g) \leftrightarrow NH_2COONH_4(s) \quad (1)$$

$$NH_2COONH_4(s) + H_2O(g) \leftrightarrow (NH_4)_2CO_3(s) \quad (2)$$

There are two major concerns; (1) there is an explosive problem with the dry CO_2-NH_3 reaction if the process is designed or operated improperly, as the explosive limit for NH_3 gas is 15~28% (v/v), and (2) passageway plugs in the reactor could cause the production to stop. To

be safe and simple, the wet method (i.e., using ammonia scrubbing instead of ammonia injection) will be used as the CO_2 capturing method for investigation and utilization.

The gas-liquid chemical reactions between NH_3 and CO_2 in the wet scrubber can be illustrated by the following equations:[10]

$$CO_2(g) + 2NH_3(g) \leftrightarrow CO(NH_2)_2(s) + H_2O(g) \quad (NH_3/CO_2 \text{ molar ratio} = 0.5) \quad (3)$$

$$CO_2(g) + 2NH_3(aq) \rightarrow NH_4^+(aq) + NH_2COO^-(aq) \quad (NH_3/CO_2 \text{ molar ratio} = 0.5) \quad (4)$$

$$2NH_3(g) + CO_2(g) + H_2O(g) \leftrightarrow (NH_4)_2CO_3(s) \quad (NH_3/CO_2 \text{ molar ratio} = 0.5) \quad (5)$$

$$NH_3(g) + CO_2(g) + H_2O(g) \leftrightarrow NH_4HCO_3(s) \quad (NH_3/CO_2 \text{ molar ratio} = 1.0) \quad (6)$$

$$2NH_3(aq) + CO_2(g) + H_2O(l) \leftrightarrow (NH_4)_2CO_3(s) \quad (NH_3/CO_2 \text{ molar ratio} = 0.5) \quad (7)$$

$$NH_3(aq) + CO_2(g) + H_2O(l) \leftrightarrow NH_4HCO_3(s) \quad (NH_3/CO_2 \text{ molar ratio} = 1.0) \quad (8)$$

At room temperature and atmospheric pressure, reactions (4)-(8) would occur. These reactions are very temperature sensitive. Reactions (7) and (8) are the dominant reactions for CO_2 removal by NH_3 in a scrubber.

The reaction between CO_2 and aqueous ammonia is very complex. As illustrated in the Janecke three-phase diagram of the NH_3-CO_2-H_2O system shown in Figure 1, [16] under various operating conditions, many species could co-exist in the solution. In this triangle diagram, the bottom line represents the NH_3 concentration dissolved in a water solution. The vertical line at the left represents the CO_2 concentration dissolved in the water solution. It can be seen from the phase diagram that many parameters could influence the reaction process, such as the ratios of reactants, reaction temperature, pressure, etc.

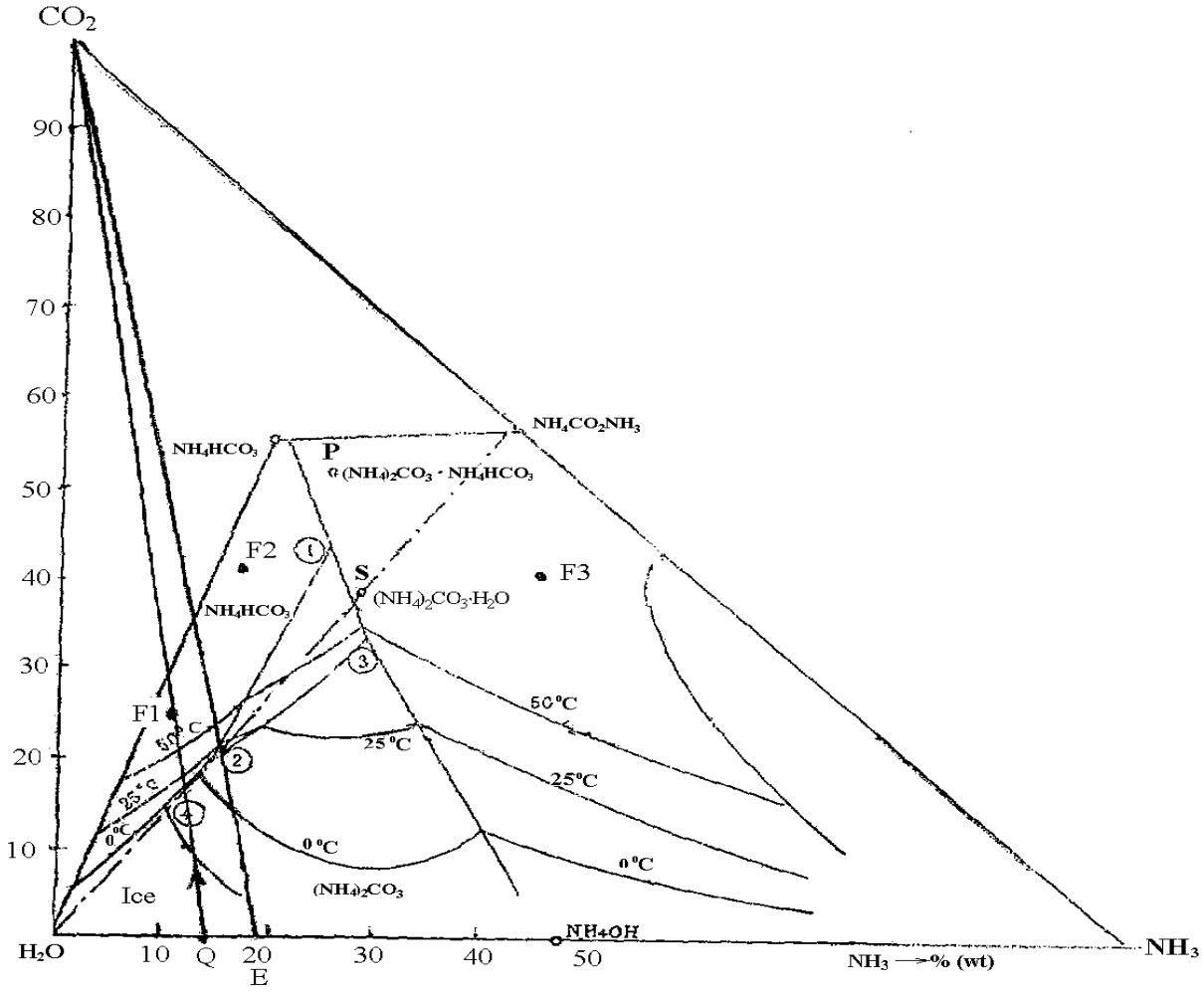

Figure 1. Janecke NH_3-CO_2- H_2O three-phase diagram.

The reactants consist of three materials: NH_3, CO_2 and H_2O. Due to the different concentrations of reactants and reaction conditions (temperature and pressure), different carbon-ammonium composites (i.e., different ammonium salts), can be obtained, as illustrated by equation (9):

$$aNH_3 + bCO_2 + cH_2O \rightarrow NH_4HCO_3(C-salt); \quad (NH_4)_2CO_3 \cdot H_2O(S-salt);$$

$$2NH_4HCO_3 \cdot (NH_4)_2CO_3(P-salt); \quad NH_4COONH_2(A-salt) \qquad (9)$$

All the products are white solids and may be a single salt or mixed salts. For example, if the ratios of reactants are at the location of F_1, F_2 in Figure 1,[16] ammonium bicarbonate will be generated from the reaction and crystallized from solution. For Point F_3, only ammonium carbonate will appear in a saturated solution.

In view of achieving a maximum of NH_3 utilization in the capture of CO_2 (minimum inventory required for CO_2 sequestration), reaction (8) will be ideal.[17]

Theoretically, a maximum 2.59 kg of CO_2/kg of NH_3 can be reached if only Reaction 8 occurs in the wet scrubber.

Ammonium fertilizer is usually very unstable, volatilizes and decomposes in soil easily, limiting its use. By stabilizing with dicyanodiamide [NH_2-C(NH_2)=N-CN] (DCD) fertilizer performance is greatly improved. This production technique has already been demonstrated extensively in China.[16-18] DCD is easily dissolved in ammonia solution. When introduced into the ammonium solution, it does not take part in the chemical reactions with the main components NH_3, CO_2 and H_2O. Therefore, the basic reaction equations among NH_3, CO_2 and H_2O are similar to the reactions illustrated in equations (1)-(8). A co-crystallization product,

NH_4HCO_3·DCD, is obtained during the reactions. It is a lamellar hexagon diamond crystal or acicular crystal in shape. It co-crystallizes with ammonia bicarbonate via mosaic and adsorbing ways. The general results can be expressed by using the following chemical equations.[17]

$$NH_3(l) + CO_2(g) + H_2O(l) + DCD \rightarrow NH_4HCO_3 \cdot DCD(s) \quad (10)$$

C. Theory of the TGA Kinetics

Before the reactants can be converted into products, the free energy of the system must overcome the activation energy for the reaction, as shown in Figure 2.[19] Activation energy is very important parameter for a reaction. It dictates the material stability: the higher the activation energy of the decomposition reaction, the more stable the material.

TGA measurements are used primarily to determine the composition of materials and to predict their thermal stability at elevated temperatures. However, with proper experimental procedures, additional information about the kinetics of decomposition and in-use lifetime predictions can be obtained.[20]

Isothermal and constant heating rate thermogravimetric analyses can be used to obtain kinetic information with the constant heating rate method developed by Flynn and Wall [21] being preferred because it requires less experimental time. The Flynn and Wall method is limited to well-resolved single step decompositions and first order kinetics.

The constant heating rate, or conventional TGA approach is based on the Flynn & Wall[21] method which requires three or more determinations at different linear heating rates, usually between 0.5 and 50^{o}C/minute.

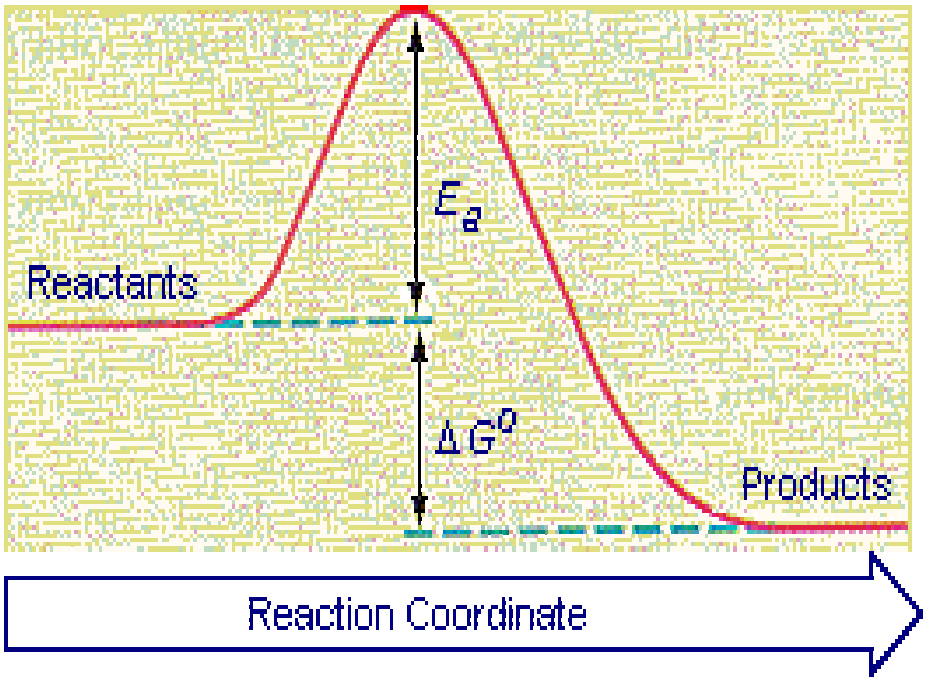

Figure 2. Activation energy of an exothermic reaction.

In kinetic analysis it is generally assumed that the rate of reaction can be described by two separable functions *k(T)* and *f(α)* such that [21]

$$\frac{d\alpha}{dt} = k(T) \cdot f(\alpha) \tag{11}$$

where dα /d*t* is the rate of reaction, *k(T)* is the temperature dependent rate constant, and *f(α)* corresponds to the reaction model. The temperature dependence of the reaction rate is commonly described by the Arrhenius equation

$$k(T) = A \cdot \exp\left(\frac{-E}{RT}\right) \tag{12}$$

where *R* is the universal gas constant, *E* is the activation energy and *A* is the preexponential factor.

For experiments in which samples are heated at a constant rate, the explicit time dependence in Equation (11) can be eliminated so that

$$\frac{d\alpha}{dT} = \frac{A}{\beta} \cdot \exp\left(\frac{-E}{RT}\right) \cdot f(\alpha) \tag{13}$$

where β= d*T*/d*t* is the heating rate.

A multivariate version of the Borchardt and Daniels method [22] is frequently used in the evaluation of dynamic data. In this method the kinetic parameters (*A*, *E*) are obtained by a linearizing transformation of Equation. (13) so that

$$\ln\frac{d\alpha / dT}{f(\alpha)} = \ln\left(\frac{A}{\beta}\right) - \frac{E}{RT} \tag{14}$$

This linear equation, which has the form $y = a_0 + a_1 x$ with $x = 1/T$, can be used to determine the optimal fit of the kinetic parameters by multiple linear regression. So

$$E = \frac{-R}{b}\left[\frac{d\log\beta}{d(1/T)}\right] \quad (15)$$

where: b = constant.

D. Research on the Analytical Method of Ammonium Bicarbonate and Characterization of Ammonium Bicarbonate

China has used ammonium bicarbonate as the mainstay of nitrogen fertilizers for many years. The analysis of the ammonium bicarbonate is mainly focused on the ammonia or nitrogen content because it is used as the nitrogen fertilizer. For example, the distillation & titration method distills the ABC in alkaline solution and absorbs the ammonia in standard sulfuric acid, then titrates the excess sulfuric acid with sodium hydroxide.[23] The nitrogen is calculated by the consumption of standard sulfuric acid. Another method puts ABC in excess standard sulfuric acid, then titrates the sulfuric acid with sodium hydroxide.[24]

In the experiment done by Diao et al.[25] to explore the possibility of using ammonia to capture CO_2 greenhouse gas, it is proved that the ammonia bicarbonate is the main product of the CO_2-NH_3 reaction. The crystal solids were identified using Fourier Transform-Infrared Spectroscopy (FTIR) analysis.

Bai, H.; Yeh, A. C[11] used the aqueous ammonia to remove the CO_2 from the simulated flue gas. The crystalline solids were obtained in the reaction products and were analyzed and determined by X-ray diffraction and SEM analyses. The experimental data were compared with standard data and the products identified as ammonium bicarbonate.

E. Objective of This Study

Using aqueous ammonia to sequester CO_2 in ammonium bicarbonate is an attractive method to capture carbon dioxide emitted from utilities using fossil-fuel combustion systems. The major objectives of this study are focused on the development of a method for measuring the ammonium bicarbonate in the products mixture, and characterizing the product. The goals of this study are:

1. To establish a laboratory analysis method to distinguish ABC from other synthesized products.
2. To obtain physical and chemical data of ABC.
3. To evaluate the stability at interested temperatures and flow rates of ABC and LEABC.
4. To help with the understanding of the chemical reaction mechanisms between CO_2 and aqueous ammonia under different conditions.
5. To develop an online quantitative measurement method for determining the percentage of ABC in the product mixture.
6. To find optimal conditions for capturing CO_2 and maximize the efficiency of aqueous ammonia.
7. To insure the quality of the product as a fertilizer.

II. EXPERIMENTAL

A. Bench Scale CO_2 Capture Experimental System by Aqueous Ammonia

The schematic diagram of the experimental system for studying the removal of CO_2 gas by ammonium scrubbing is shown in Figure 3.[26] The CO_2 scrubber was a glass container (I.D. 50mm) filling with 150 ml of 15 % ammonium solution. The CO_2 gas was fed from a simulated flue gas cylinder with CO_2 concentration 14.7 %. Two experiments used pure CO_2 gas. A mass flow controller was used to control the inlet CO_2 flow rate. A filter was placed after the scrubber to capture the escaped particles. Photoacoustic multi-gas analyzer (INNOVA 1312) was used for monitoring the outlet CO_2 and ammonium concentrations. A magnetic stirring system was used to help the reactants mix well. Experiments were conducted at room temperature (25 ± 1°C). The flow rate of the flue gas was kept at 3 L/min. The ammonia solution was obtained from a standard ammonia solution (Fisher Science, 29.7% (w/w)), which was usually diluted using DI water (in some cases spent-solution was used as the diluent). To investigate the influence of MEA on ammonia's CO_2 scrubbing, a few milliliters of MEA solution were used in one experiment. Some experiments used spent solution from previous experiments as the diluent for the standard ammonia solution instead of DI water. Two experiments started with ammonium bicarbonate in the ammonia solution make the initial ammonia solution. Eight were run with the stirring system at varying operating conditions. One experiment was operated without stirring. The operation conditions for all nine experiments are listed in Table 1.[26]

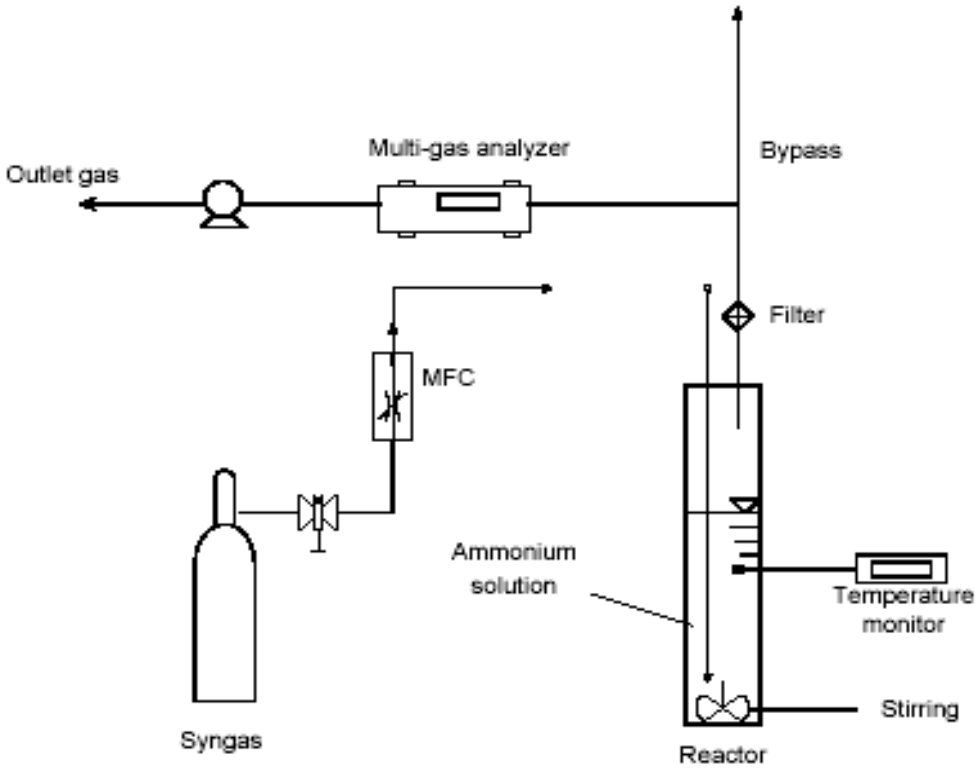

Figure 3. Schematic diagram of experiment setup of bench scale aqueous ammonia CO_2 capture.

Table 1. Bench Scale Aqueous Ammonia CO_2 Capture
Experimental System Operation Conditions

No.	$NH_3 \bullet H_2O$ (%)	CO_2 (%)	Additional MEA (ml)	Additional NH_4HCO_3 (g)	Spent-solution (ml)	Stirring
Exp 1	15	14.7	0	0	0	Yes
Exp 2	15	14.7	0	0	5	Yes
Exp 3	15	14.7	1.5	0	0	Yes
Exp 4	15	14.7	0	0	30	Yes
Exp 5	15	14.7	0	6	0	Yes
Exp 6	15	14.7	0	12.7	73	Yes
Exp 7	15	14.7	0	0	0	No
Exp 8	15	pure	0	0	0	Yes
Exp 9	15	pure	0	0	0	Yes

B. Samples

The ammonium bicarbonate standard, ammonium carbonate standard and ammonium carbamate were purchased from Aldrich, Acros Organics, and Alfa Aesar, respectively. The LEABC was obtained from China Fengcheng Fertilizer Works. Some samples were from CO_2 capture experiments at WKU.

C. Instrumentation and Analytical Methods

1. Fourier Transform-Infrared Spectroscopy (FTIR) Technique by Perkin Elmer 1600

FTIR spectroscopy measures the vibrational spectrum of a material by passing infrared radiation through a sample. The results are recorded as absorption of radiation by the molecule as a function of wavenumber (cm^{-1}). The spectrum obtained contains information about the structure and composition of the molecule and is used extensively in identifying or "fingerprinting" materials. Proof of identity can be established by comparing the sample spectrum with a library of spectra of frequently encountered materials.

The samples, each weighing approximately 10 mg, were mixed with 500 mg KBr to form a uniform mixture. For every FTIR test, the mixture was placed into an assembled compression module, and adequate pressure was placed on the module to ensure fusion of the KBr crystals.

2. Differential Scanning Calorimetry (DSC) TAI 2920

The DSC was used in this study for calorimetric analysis. The DSC reports the heat flow into and out of a sample associated with transitions in the material at various temperatures. Measurement of heat flow is accomplished by recording the amount of energy required to

maintain the sample temperature and holding a pan at the same temperature as that of an empty reference pan. The difference in energy supplied is due to the heat capacity of the sample and reflects chemical and physical changes occurring in the material. DSC results can be used to determine glass transitions, melting points, crystallization, heat capacity, oxidative stability, reaction kinetics, purity, and thermal stability.

Approximately 10 mg of each sample was used per run. Samples were analyzed in nitrogen atmospheres at a flow rate of 50 mL/min using a crimped aluminum sample pan. The sample chamber was purged for 30 minutes after loading each sample before beginning the analysis. The samples were heated from ambient temperature to 180°C at a heating rate of 10°C/minute. DSC results were reported as heat flow versus temperature. Exothermic peaks were indicated by an upward direction of the curve, while endothermic peaks were indicated by a downward direction. An example of the types of peaks indicated by a DSC curve is given in Figure 4.[27]

3. Thermogravimetric analysis (TGA) TAI Hi-Res 2950 TGA and TG-MS

The TGA reports the weight change, both gains and losses in the sample, as a function of temperature. The information obtained using TGA can be used to determined thermal stability, oxidative stability, decomposition kinetics, moisture and volatiles content, and composition of multi-component systems. An example of TGA results can be observed in Figure 5.[27]

The thermal stability characteristics were measured using a TAI 2950 TGA. A ceramic pan was used. Temperature influences were investigated by heating from room temperature to final temperatures (25 ^{o}C to 65 ^{o}C at 5 ^{o}C intervals) and holding for six hours. An Air

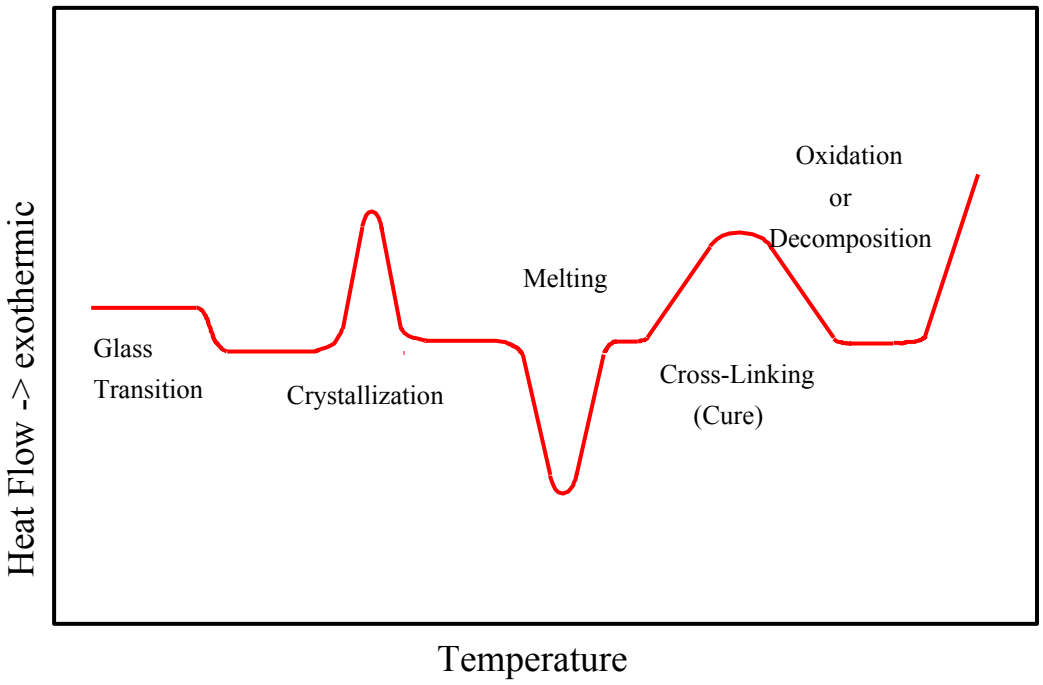

Figure 4. Example of DSC curve.

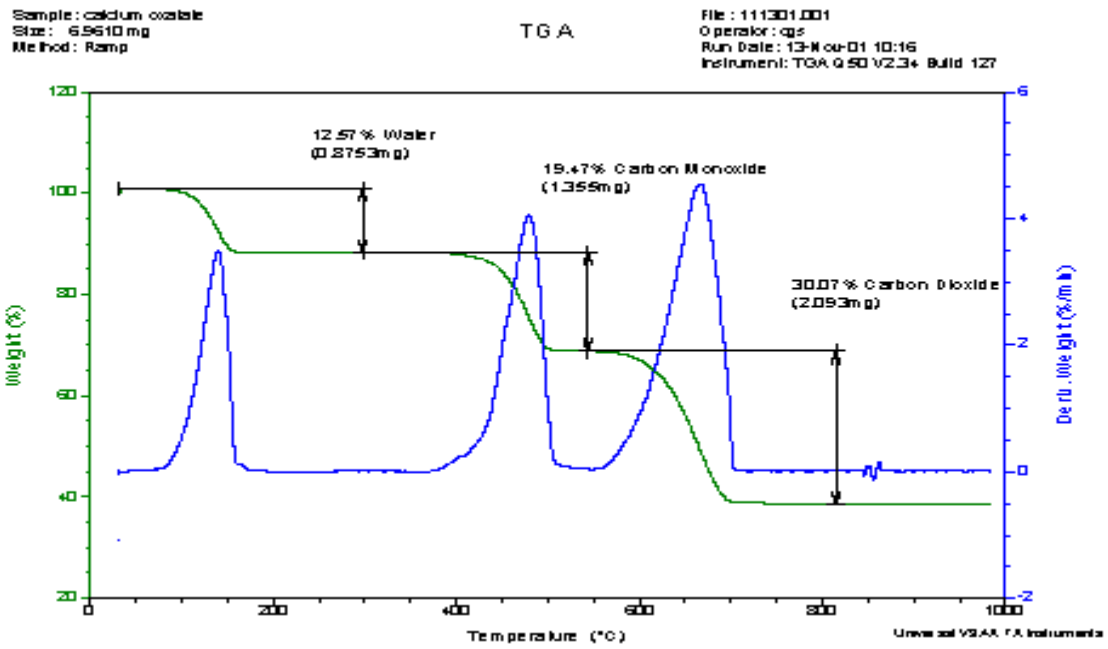

Figure 5. Example of TGA curve.

atmosphere was used at a rate of 50 mL/min. The air flow rate test samples were heated from room temperature to 30 ^{o}C and held for six hours. TGA data at 25, 50 and 75 mL/min were collected.

The ABC and ammonium carbonate decomposition characteristic were measured using TAI 2960 SDT interfaced to a Fisions VG Thermolab Mass Spectrometer by means of a heated capillary transfer line. The powder samples were heated from room temperature to 300 ^{o}C at the rate of 10 ^{o}C/min under flowing (50 mL/min) compressed nitrogen gas. The capillary transfer line was heated to 120ºC, and the inlet port on the mass spectrometer was heated to 150ºC. The Fisons unit is based on quadrupole design with a 1-300 amu mass range. The sample gas from the interface was ionized at 70 eV. The system was operated at a pressure of 1 X10^{-6} torr.

4. X-Ray Diffraction – Thermo XRD ARL X'TRA

Each crystalline solid has its unique characteristic X-ray powder pattern, which can be used as a "fingerprint" for its identification. XRD is one of the most important characterization tools used in solid state chemistry and materials science. It has been used in two main areas: "Fingerprint" characterization of crystalline materials and determination of crystalline materials' structure.

A tube voltage of 40 kV and a tube current of 20 mA were used for each sample. The samples were scanned every 0.04 degrees from 10 to 60 degrees. Three XRD spectra were compared. Different intensity (counts per second) at different angles were obtained for each standard chemical and used to qualitatively distinguish them.

5. CHN Element of Analysis - LECO CHN-2000

The samples combust in the furnace with oxygen gas and the carbon, hydrogen and nitrogen are converted into CO_2, H_2O, N_2 and NO_x. These gases are then passed through infrared cells to determine the carbon and hydrogen content and the NOx are reduced to N_2 and enter into a thermal conductivity (TC) cell to determine nitrogen. The furnace can be heated from 0^oC to 1000^oC. In general, a 0.100 g sample is loaded and analyzed. The test range (based on a 0.100 g sample) is 0.01-100 percent for carbon, 0.01-50 percent for hydrogen and 0.01-50 percent for nitrogen. The instrument has a 1 sigma accuracy at 0.001 for carbon and 0.01 for hydrogen and nitrogen.

6. Near Infrared Spectrometer - AOTF-NIR Free Space Spectrometer

The near infrared region of the spectrum extends from 800 nm to 2500 nm. The absorption bands that are most prominent in this region are due to overtones and combinations of the fundamental vibrations active in the mid-infrared region. The energy transitions are between the ground state and the second or third excited vibrational states. Because higher energy transitions are successively less likely to occur, each overtone is successively weaker in intensity. Because the energy required to reach the second or third excited state is approximately twice or three times that needed for a first order transition and the wavelength of absorption is inversely proportional to the energy, the absorption bands occur at about one-half and one-third the wavelength of the fundamental. In addition to the simple overtones, combination bands also occur. These usually involve a stretch plus one or more bending or rocking modes. Many different combinations are possible and therefore the NIR region is complex, with many band assignments unresolved.

Near infrared spectroscopy is currently being used as a quantitative tool, which relies on chemometrics to develop calibrations relating a reference analysis of the constituent to that of the NIR optical spectrum. The mathematical treatment of NIR data includes multi linear regression (MLR), principle component analysis (PCR), partial least squares (PLS) and discriminant analysis. All of these algorithms can be used singularly or in combination to yield the resultant goal of quantitative prediction and qualitative description of the constituents of interest.

The principle of the acousto-optic tunable filter (AOTF) is based upon the acoustic diffraction of light in an anisotropic medium. The device consists of a piezo-electric transducer bonded to a birefringent crystal. When the transducer is excited by an applied RF signal, acoustic waves are generated in the crystal. The propagating acoustic wave produces a periodic modulation of the refractive index. This provides a moving phase grating that under proper conditions will diffract portions of an incident light beam. For a fixed acoustic frequency, a narrow band of optical frequencies satisfies the phase matching conditions and be cumulatively diffracted. As the RF frequency is changed, the center of the optical bandpass is changed accordingly so that the phase matching condition is maintained. A schematic of the AOTF is shown in Figure 6.[28]

A Brimrose AOTF-NIR Free Space spectrometer was used to scan 63 samples of ammonia bicarbonate, ammonia carbamate, and ammonia carbonate mixtures. Three subsets in the sample set were created. One subset contained ammonia bicarbonate and ammonia carbamate in varying percentages by weight. Another subset contained ammonia bicarbonate

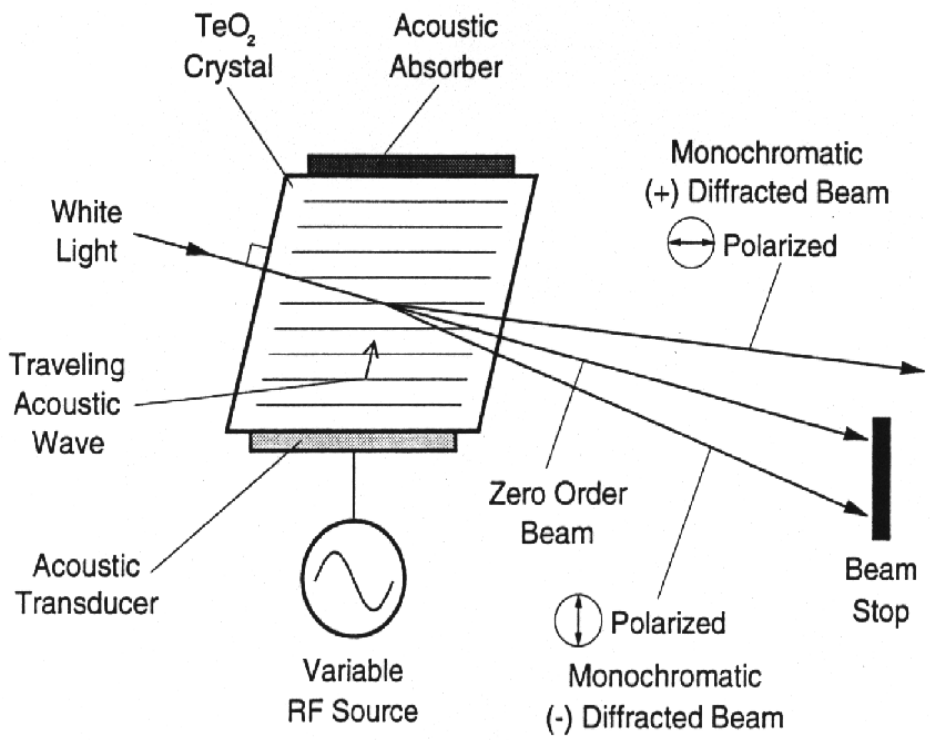

Figure 6. Schematic of acousto-optic tunable filter (AOTF).

and carbonate in varying percentages by weight. A third subset that contained ammonia bicarbonate, ammonia carbamate and ammonia carbonate in varying percentages by weight.

D. Ammonium Bicarbonate Decomposition Kinetics by Thermogravimetric Methods

1. Experimental

The kinetics characteristics were measured using a TAI 2950 TGA. A platinum pan was used. The sample size was 5 ± 1 mg. Decomposition profiles were obtained while heating at 1, 2, 5, 10 and 20°C/minute in nitrogen at a rate of 50 mL/min. Nitrogen gas is used as purge gas because air contains carbon dioxide. The partial pressure of carbon dioxide will depress the decomposition of ammonium bicarbonate. The profile during the first 20% of sample weight loss was used for subsequent calculations.

2. Calculation[29]

2.1 From each of the thermal curves obtained in part 1, determine the absolute temperature at constant conversion, α, was determined for each of the constant conversion values to be used in the calculations: 1, 2.5, 5, 7.5, 10, and 20 %.

2.2 The logarithm of the heating rate expressed as kelvins per minute was plotted against the reciprocal of the absolute temperature at which the conversion level, selected in 2.1, was reached. A straight line results.

2.3 Using the least-squares method to these data were fit to a straight line without weighing factors, and determine the slope; $\Delta \log\beta / \Delta 1/T$ was determined.

2.4 The following definitions apply to 2.3-2.6:

E = activation energy (J/mole)

A = pre-exponential factor, min^{-1},

R = gas constant, 8.314 J/(mol·K),

T = temperature (K) at constant conversion,

b = approximation derivative from Table 2 (use b = 0.457/K on first iteration),

a = approximation integral taken from Table 2

α = conversion value of decomposition, and

2.5 An estimation of the activation energy was calculated using equation 16, making use of the value of Δlogβ/Δ1/T determined in 2.3 and a value of 0.457/K for *b* in this first iteration:

$$E = -(R/b)* \Delta\log\beta/\Delta 1/T \qquad (16)$$

2.6 The value for E/RT_c, was calculated, where T_c = the temperature at constant conversion for the heating rate closest to the midpoint of the experimental heating rates.

2.7 Using the value for *Ee/RTc* obtained in 2.6, a new estimation of b was obtained from Table 2 and used as the value of b in Equation 16.

2.8 2.4 and 2.7 were repeated until the value for the activation energy change by less than 1 %. This refined value, E_r, is reported as the Arrhenius activation energy.

2.9 The mass loss curve for the heating rate nearest the midpoint of the experimental heating rates, was selected and the pre-exponential factor, A, was calculated using Equation 17 and the value of the exponent, *a*, was obtained from Table 2 for the refined value of E_e/RT_c determined in 2.7.[29]

$$A = -(\beta/Er)*R* \log(1- \alpha)*10^{a} \quad (17)$$

3.0 The above procedure was accomplished by the TA Specialty Software.

Table 2. TGA Kinetics Numerical Integration Constants.

E/RT	a	b (1/K)
8	5.3699	0.5398
9	5.8980	0.5251
10	6.4167	0.5187
11	6.926	0.511
12	7.433	0.505
13	7.933	0.500
14	8.427	0.494
15	8.916	0.491
16	9.406	0.486
17	9.890	0.484
18	10.372	0.482
19	10.851	0.479
20	11.3277	0.4770
21	11.803	0.475
22	12.276	0.473
23	12.747	0.471
24	13.217	0.470
25	13.686	0.469
26	14.153	0.467
27	14.619	0.466
28	15.084	0.465
29	15.547	0.463
30	16.0104	0.4629
31	16.472	0.462
32	16.933	0.461
33	17.394	0.461
34	17.853	0.459
35	18.312	0.459
36	18.770	0.458
37	19.228	0.458
38	19.684	0.456
39	20.141	0.456
40	20.5967	0.4558
41	21.052	0.455
42	21.507	0.455
43	21.961	0.454
44	22.415	0.454
45	22.868	0.453
46	23.321	0.453
47	23.774	0.453
48	24.226	0.452
49	24.678	0.452
50	25.1295	0.4515
51	25.5806	0.4511
52	26.0314	0.4508
53	26.4820	0.4506
54	26.9323	0.4503
55	27.3823	0.4500
56	27.8319	0.4496
57	28.2814	0.4495
58	28.7305	0.4491
59	29.1794	0.4489
60	29.6281	0.4487

III. RESULTS AND DISCUSSION

A. Development of an Analytical Method for Distinguishing Ammonium Bicarbonate from the Products of Aqueous Ammonia CO_2 Scrubber

1. FTIR Technique:

Figures 7, 8 and 9 are FTIR spectra of the ammonium bicarbonate, ammonium carbonate and ammonium carbamate respectively. Figure 10 is the overlaid spectra of the three chemicals. Figure 11 is the overlaid spectra of the LEABC and ABC standard.

As shown in the Figures 7, 8 and 9, the peak at wavenumber ~ 3098 cm^{-1} is due to the stretch of NH_4^+. In Figure 7, the peaks in the region of 1200-1450 cm^{-1} are the asymmetric stretch of O-C-O_2, and the peak at ~1600 cm^{-1} is the asymmetric stretch of CO_2. In Figure 8, the peaks in the region 1300-1600 cm^{-1} are the asymmetric stretch of CO_3^{2-}.

From Figure 9, the peak at about 3472 cm^{-1} is due to NH_2 stretch and it is not found in the spectra of NH_4HCO_3 and $(NH_4)_2CO_3$. Overlaid spectra of the three chemicals in Figure 10 show the difference. These spectra can be used to distinguish the ammonium carbamate from ammonium bicarbonate and ammonium carbonate.

Figure 11 shows the spectra of LEABC sample. The overlaid spectra of ABC and LEABC in Figure 12 indicate that no obvious differences exist between the two spectra of LEABC and ABC.

The spectra in Figures 7 and 8 are very similar and difficult to distinguish because of existence of broad peaks due to CO_3^{2-} and HCO_3^- both between 1200 ~1700 cm^{-1}. This can also be seen in Figure 10.

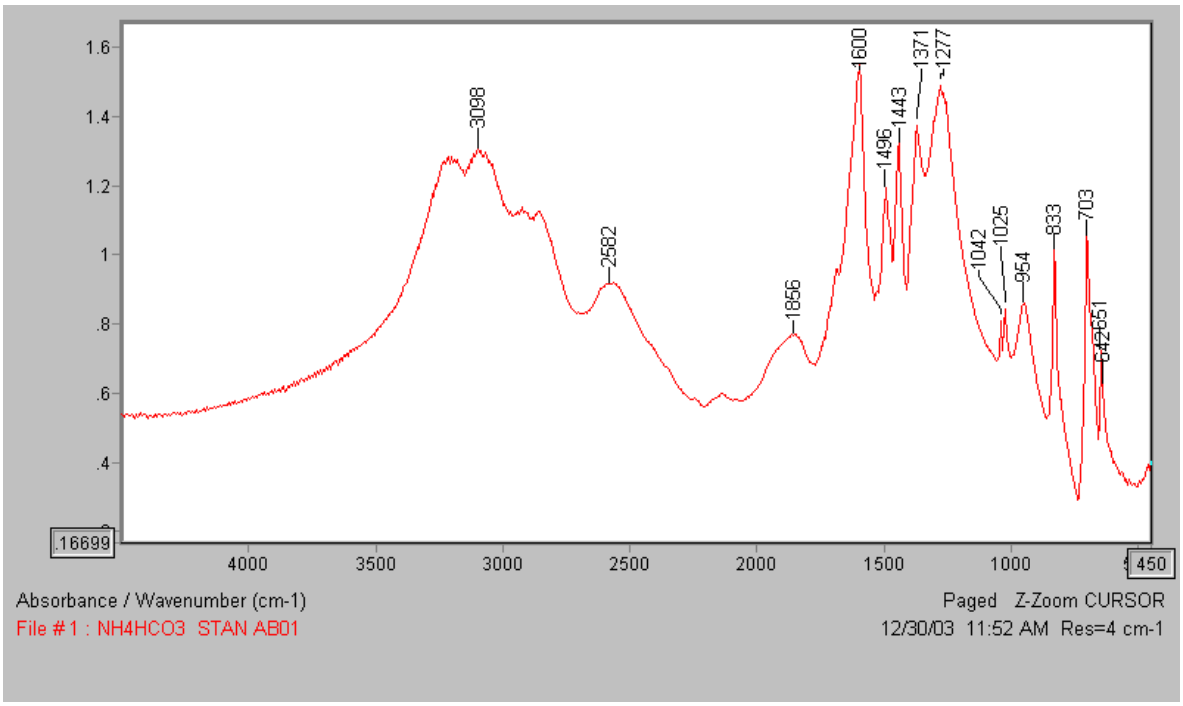

Figure 7. FTIR spectrum of NH_4HCO_3 standard at room temperature.

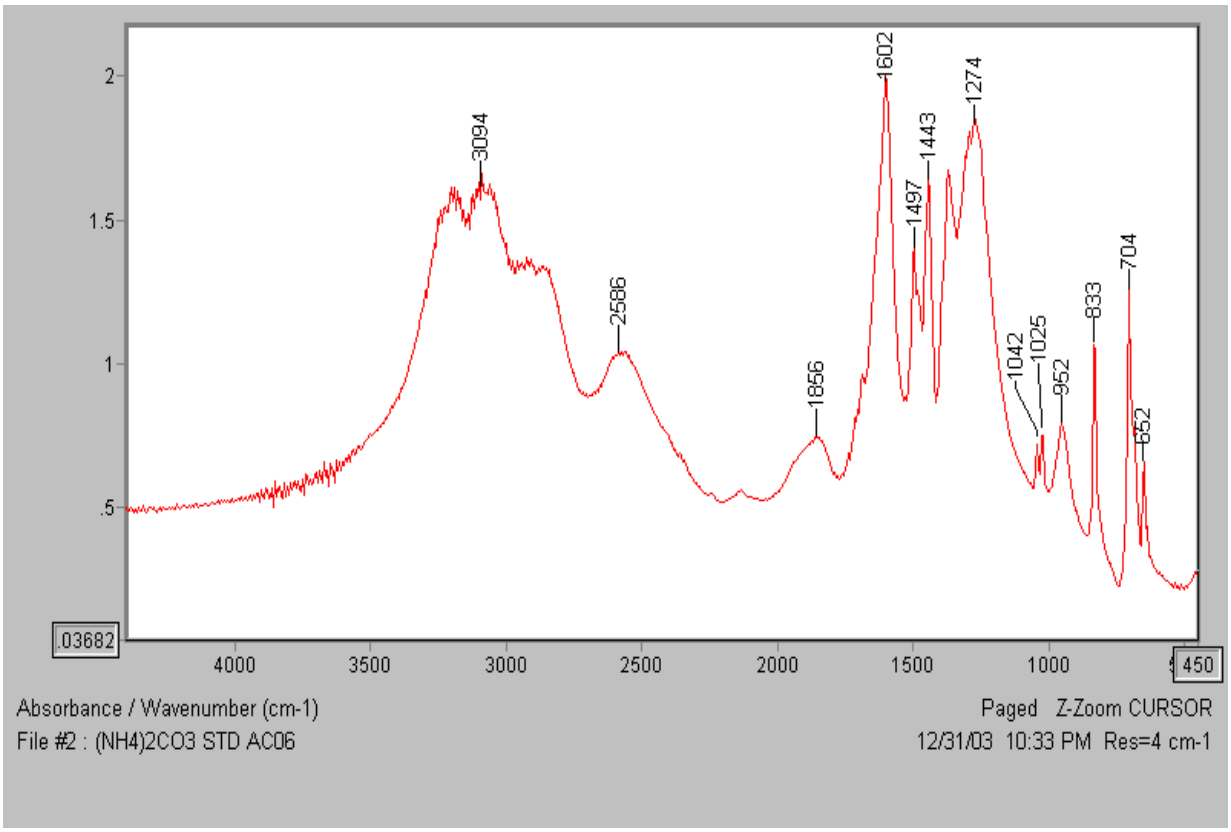

Figure 8. FTIR spectrum of $(NH_4)_2CO_3$ standard at room temperature.

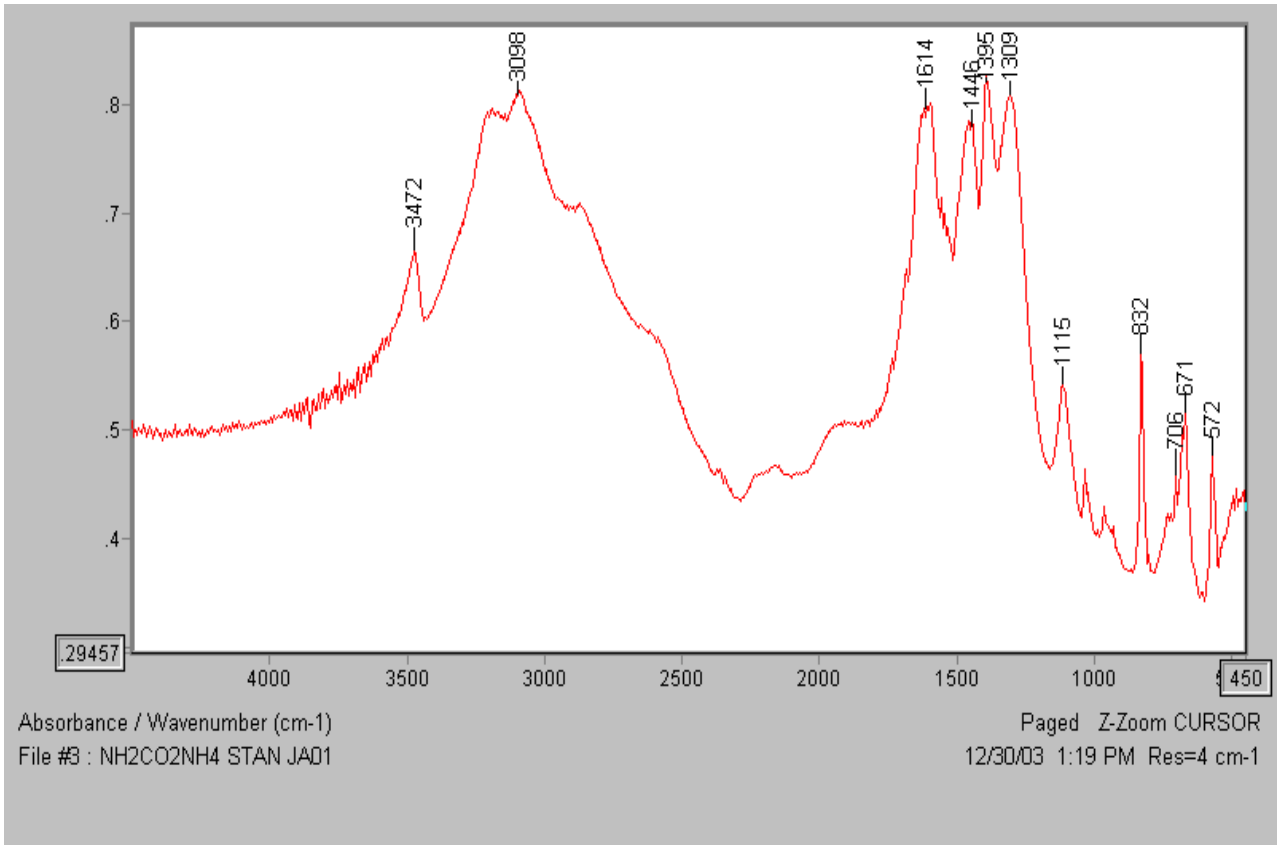

Figure 9. FTIR spectruma of $NH_2CO_2NH_4$ standard at room temperature.

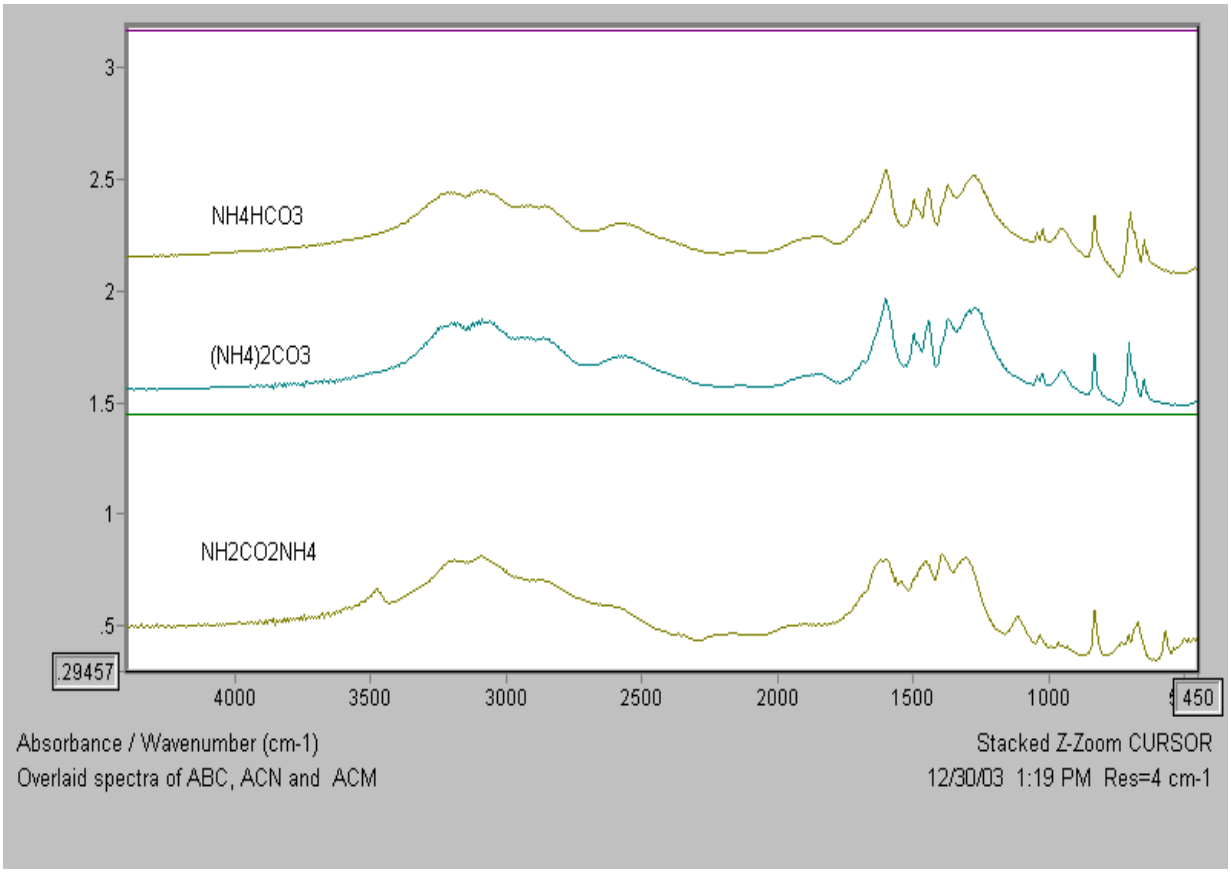

Figure 10. Overlaid spectra of NH_4HCO_3 standard, $(NH_4)_2CO_3$ standard and $NH_2CO_2NH_4$ standard.

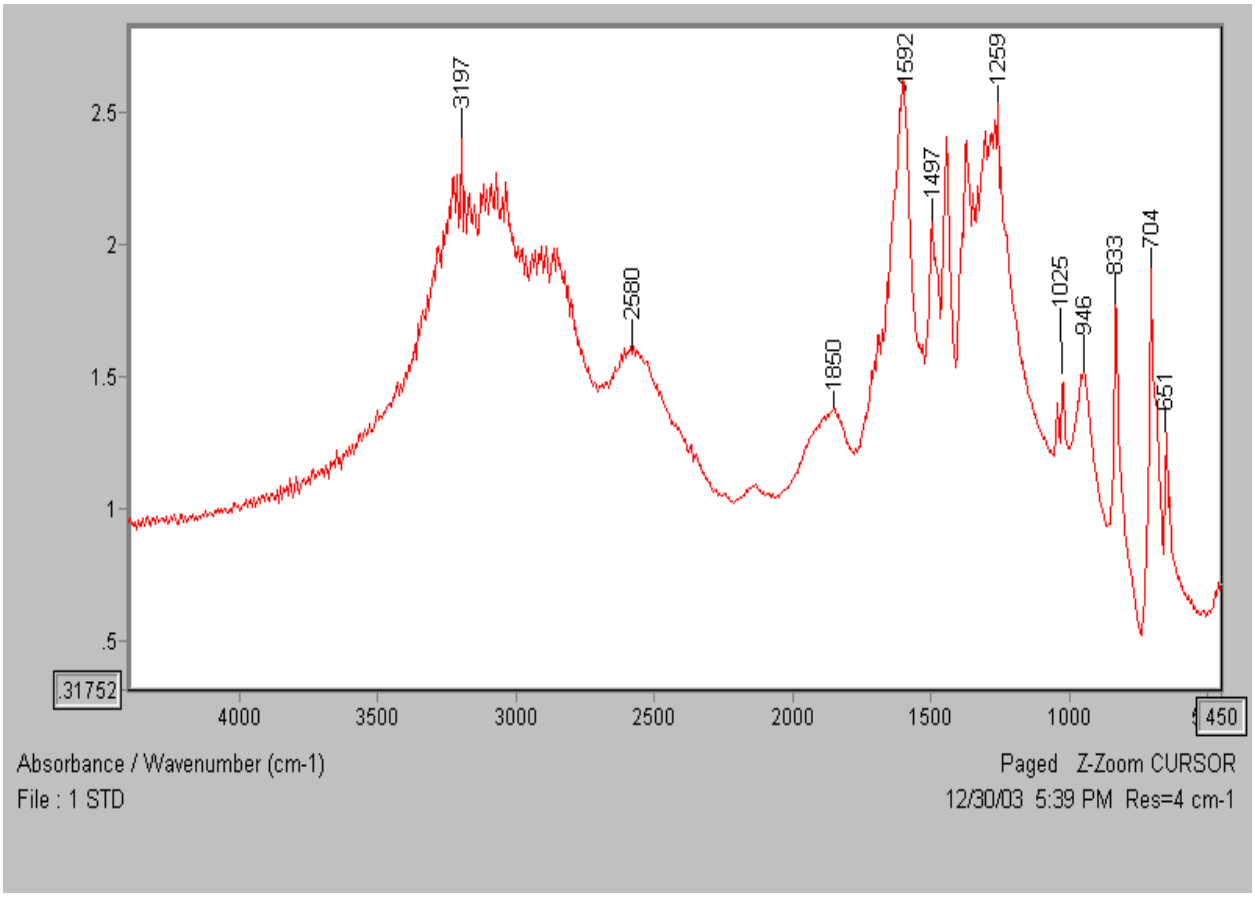

Figure 11. FTIR spectrum of LEABC at room temperature.

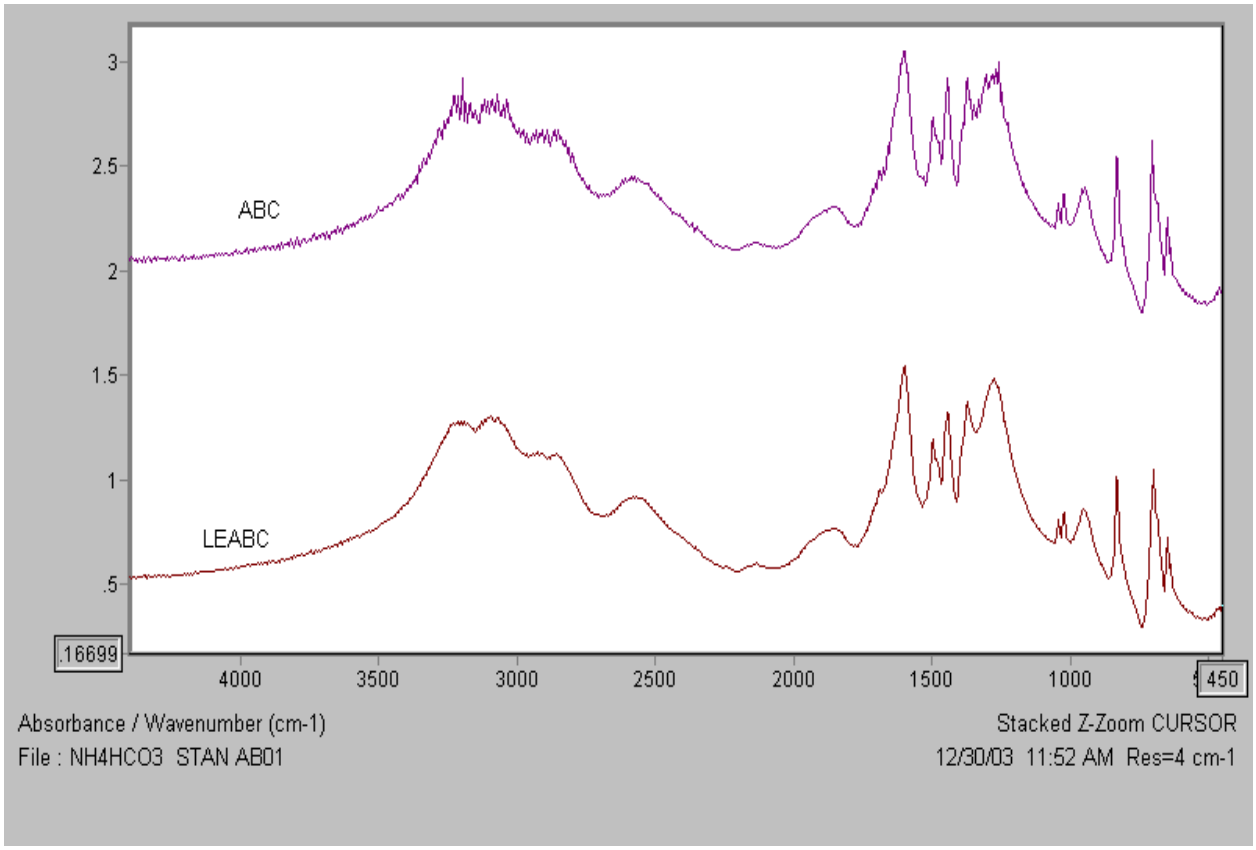

Figure 12. Overlaid spectra of ABC and LEABC.

Figures 13 and 14 are FTIR spectra of sample 01050401 and sample 01060401 from the CO_2 capture experiments. The spectra are very similar to the spectra of the NH_4HCO_3 and $(NH_4)_2CO_3$ Standard and different from the $NH_2CO_2NH_4$ Standard. They are not $NH_2CO_2NH_4$. The product is either ABC or ammonium carbonate.

From the above discussion, it is clear that FTIR can be used to distinguish the ammonium carbamate from the ammonium bicarbonate and ammonium carbonate. However, it is difficult to distinguish the ammonium bicarbonate from ammonium carbonate by FTIR. Hence, other analytical techniques will be used to distinguish ABC from ammonium carbonate.

2. DSC Technique:

Figures 15, 16 and 17 represent the DSC curves for ABC, ammonium carbonate and ammonium carbamate respectively. It was found that the NH_4HCO_3 and $(NH4)_2CO_3$ standard begin decomposition at about 66°C and 63°C, respectively, and $NH_2CO_2NH_4$ begins to decompose at about 35°C. However a second endothermic peak is found in the $(NH_4)_2CO_3$ Standard. The Peak temperatures are about 105°C and 147°C.

The results of the DSC curves are summarized in Table 3.

During the regeneration process, the CO_2 can be released from heated ammonium salts, followed by removal of ammonia from evolved gases, with high-purity CO_2 as the final product. From Table 3, the decomposition reactions heat of the three ammonium salts are different and in the increase order of NH_4HCO_3: 122 kJ/mol < $(NH4)_2CO_3$: 155 kJ/mol < $NH_2CO_2NH_4$: 165 kJ/mol. The ABC has the lowest reaction heat per molar of regeneration of CO_2. This shows

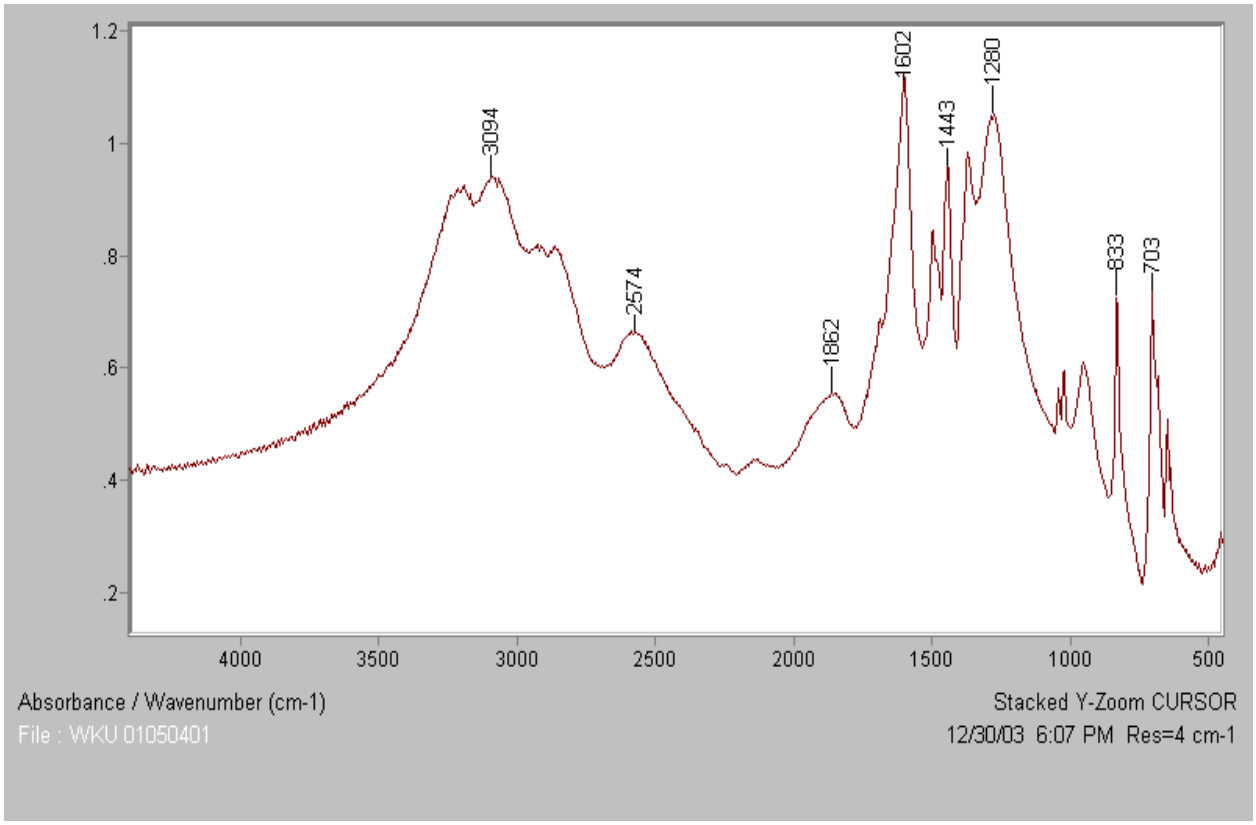

Figure 13. FTIR spectrum of sample 01050401 at room temperature.

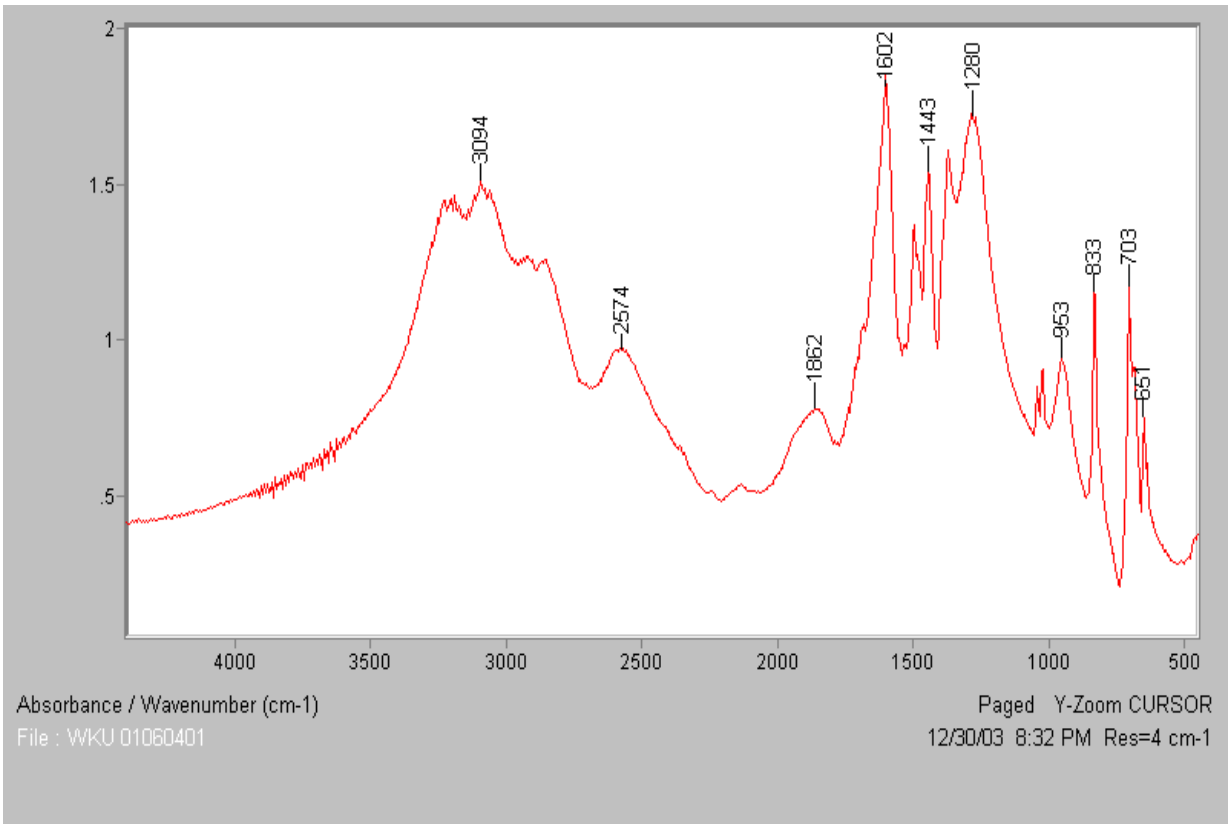

Figure 14. FTIR spectrum of sample 01060401 at room temperature.

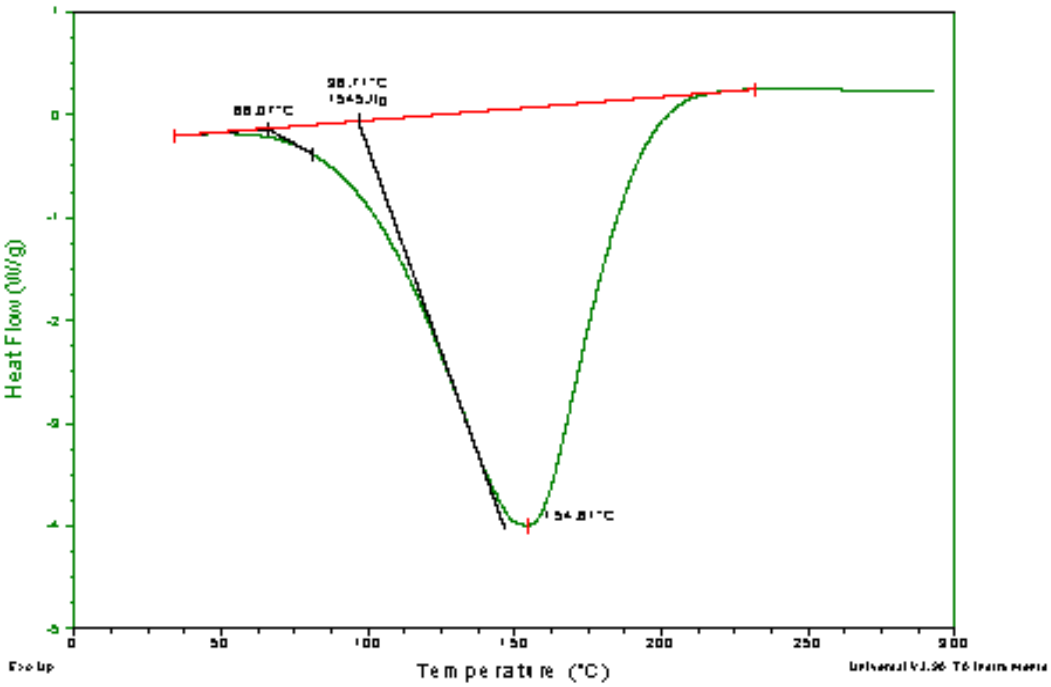

Figure 15. DSC curve for NH_4HCO_3 standard.

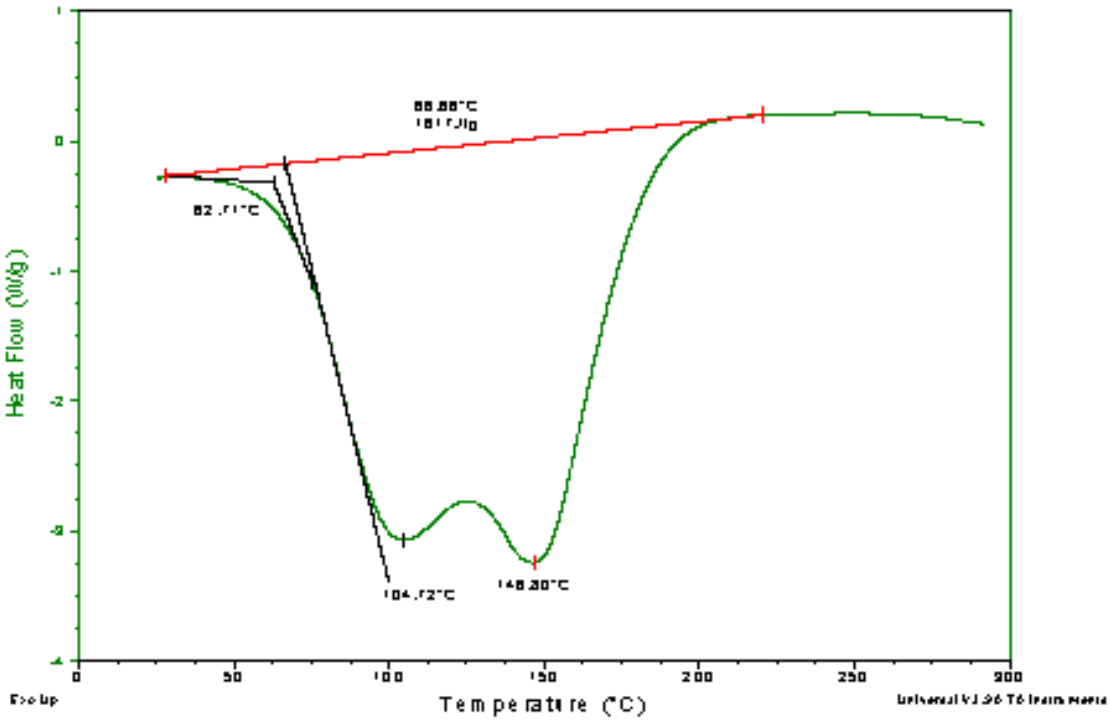

Figure 16. DSC curve for $(NH_4)_2CO_3$ Standard.

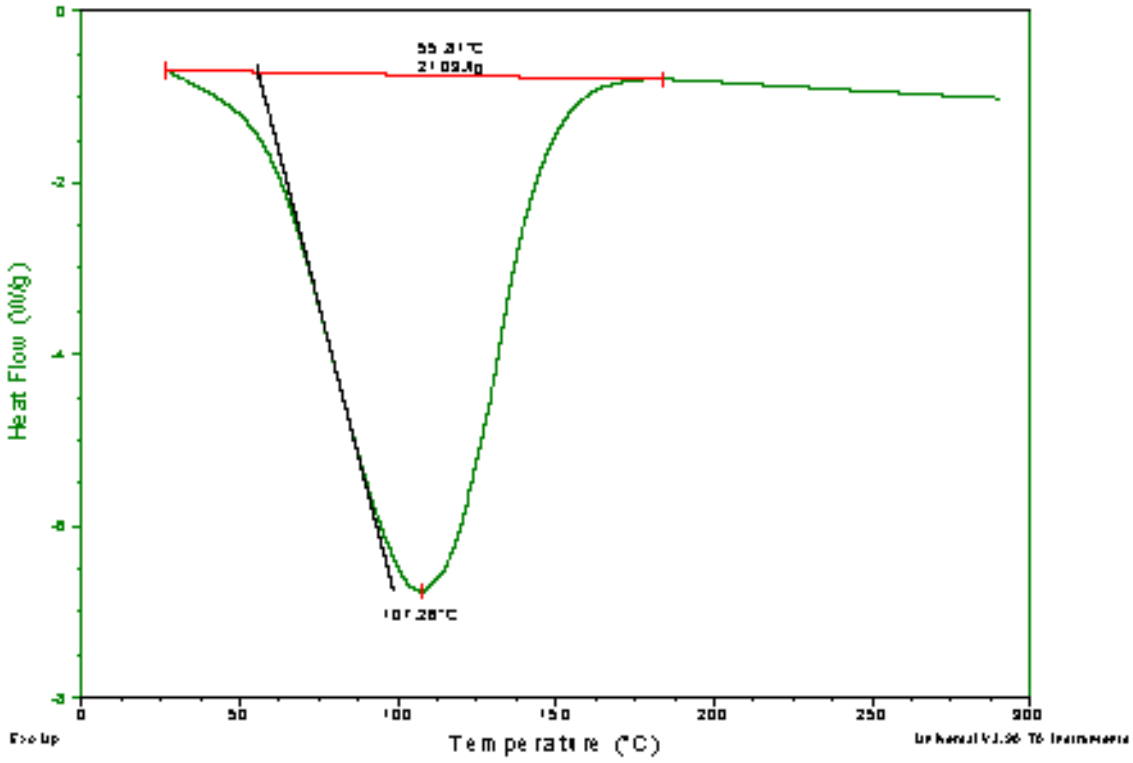

Figure 17. DSC curve for $NH_2CO_2NH_4$ standard.

Table 3. Summary of DSC Data.

Sample Name	Onset Temp. °C	Peak Temp. °C	Experimental Heat of RXN J/g	Experimental Heat of RXN J/mol
NH_4HCO_3 Standard	66	155	1545	122,055
$(NH4)_2CO_3$ Standard	63	#1: 105 #2: 147	1617	155,232
$NH_2CO_2NH_4$ Standard	35	107	2109	164,502

that ABC is the ideal product of the ammonia CO_2 scrubbing in addition to its other advantages.

Figures 18 and 19 are DSC curve of sample 01050401 and sample 01060401 from the CO_2 capture experiments. Only one peak is shown. The product is not ammonium carbonate. The DSC curve of ammonium carbonate shows double peaks, but ABC's DSC figure does not. Therefore DSC can be used to distinguish the ammonium bicarbonate from the ammonium carbonate.

3. TGA-MS Technique

Figure 20 shows the overlaid TGA curves of ammonium bicarbonate and ammonium carbonate. The samples were heated from room temperature to 300 ^{o}C at a rate of 10°C/min. The DTG curve of ammonium carbonate shows two peaks. The peak maxima are at about 95 °C and 145 °C. Two reasons are possible: either there are two steps of decomposition reaction or the sequence release of NH_3 and CO_2.

The DTG curve of ABC shows only one peak in Figure 20; the peak maximum is at 139°C. The overlaid m/z curves of NH_3, H_2O and CO_2 from the decomposition of ABC in Figure 21 show one peak. But the overlaid m/z curves of NH_3 and CO_2 from the decomposition of ammonium carbonate in Figure 22 show two peaks, corresponding to the DTG curve. This difference can be used to distinguish between ABC and ammonium carbonate.

Figures 23 and 24 are TGA curves of sample 01050401 and sample 01060401 from the CO_2 capture experiments. Only one peak is shown. The product is not ammonium carbonate.

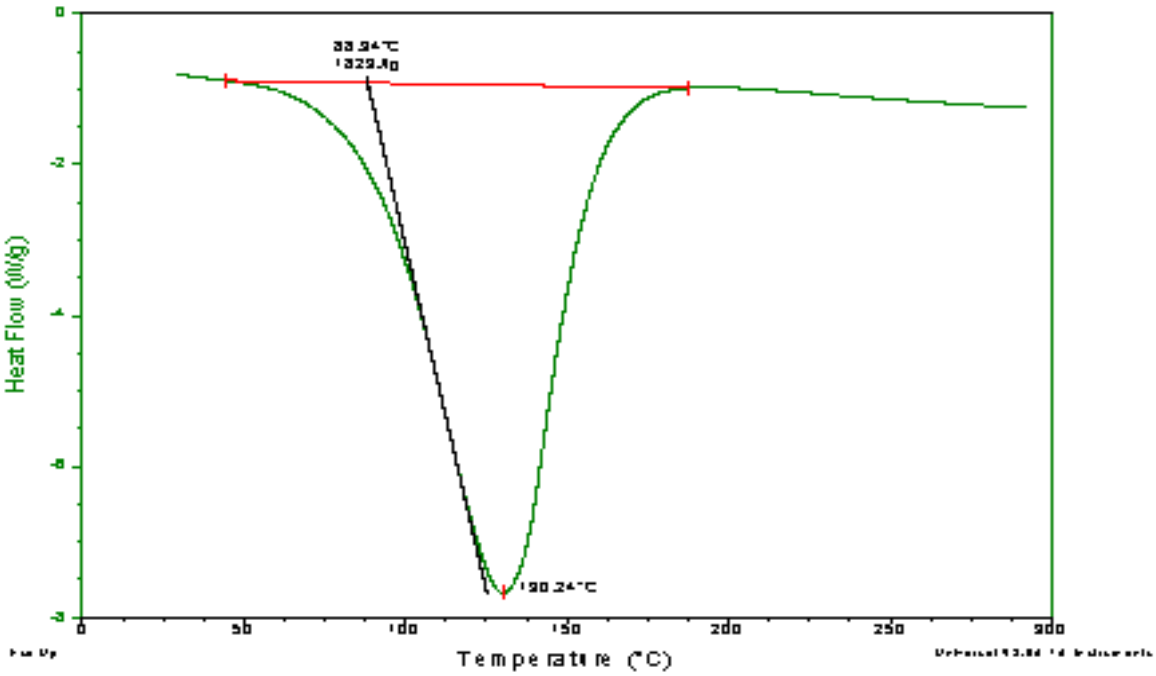

Figure 18. DSC curve for sample 01050401.

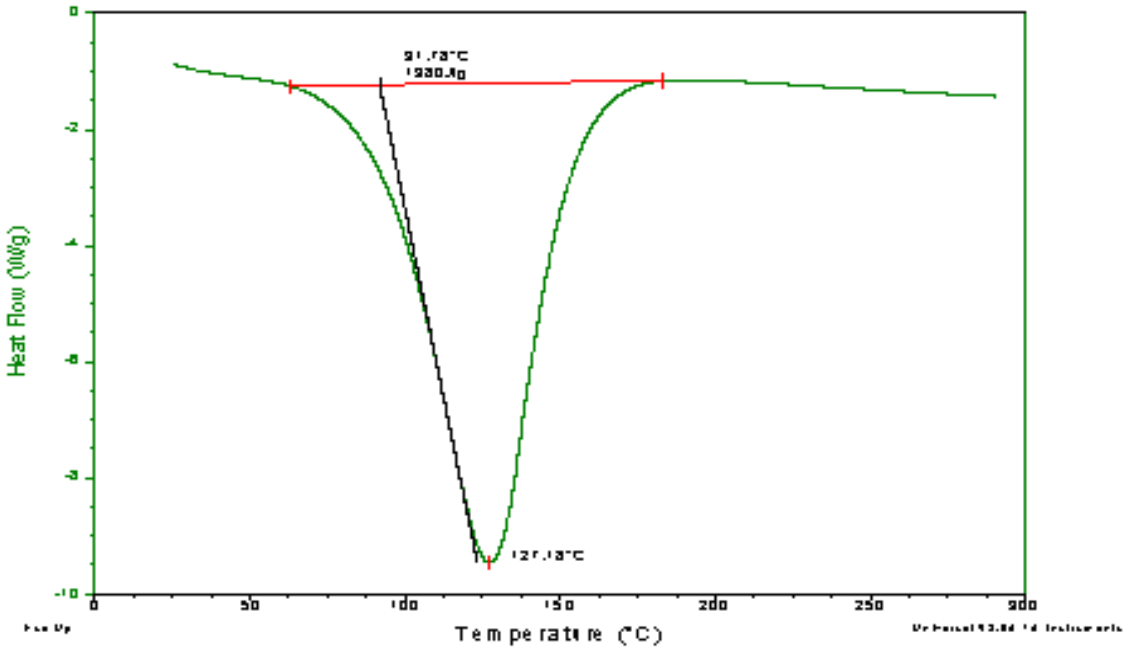

Figure 19. DSC curve for sample 01060401.

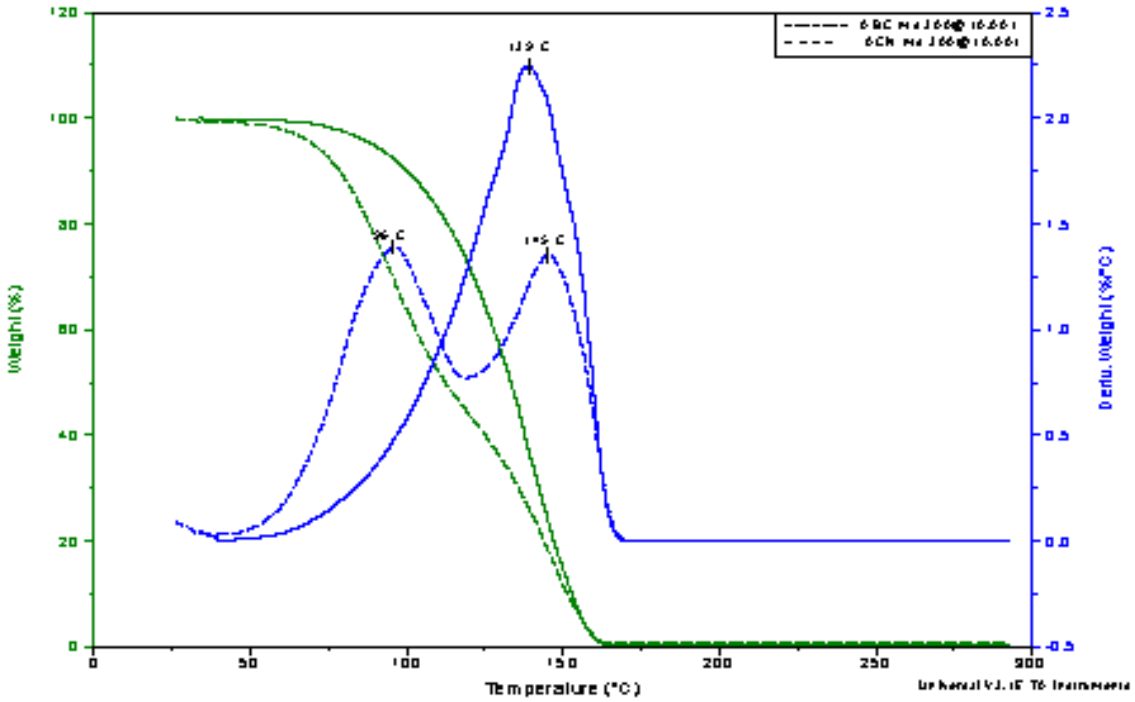

Figure 20. Overlaid TGA curves for ABC and ammonium carbonate at 300@10°C/min.

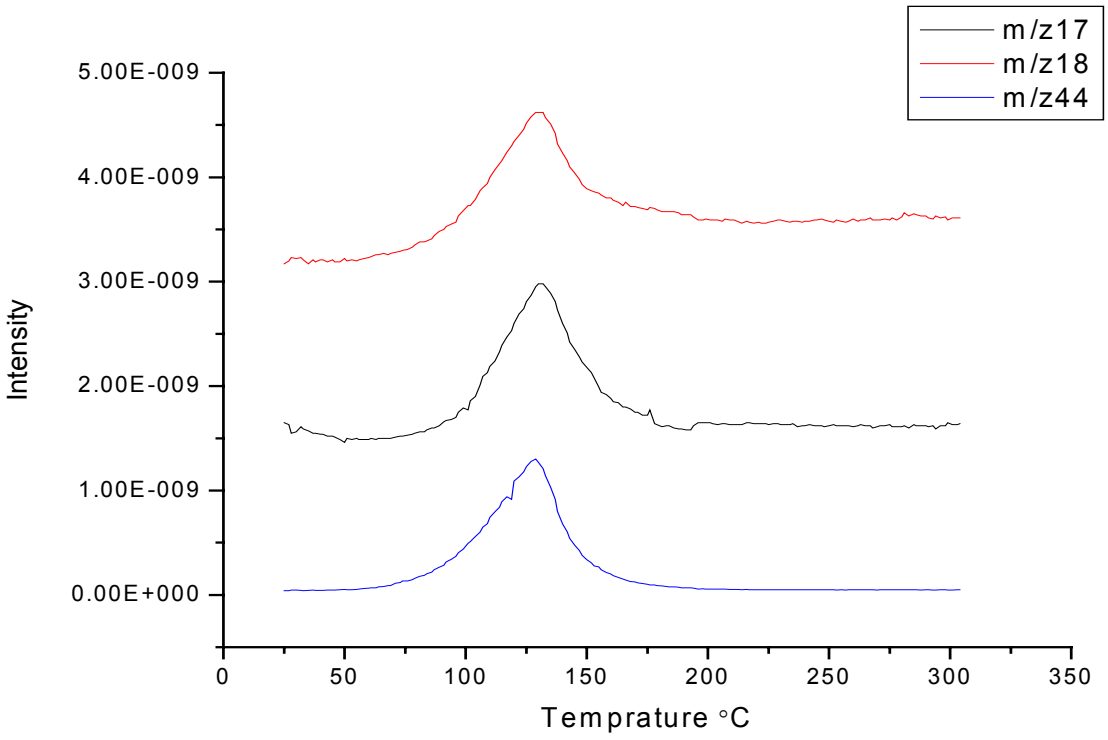

Figure 21. Overlaid m/z curves for NH_3, H_2O and CO_2 from the decomposition of ABC by mass.

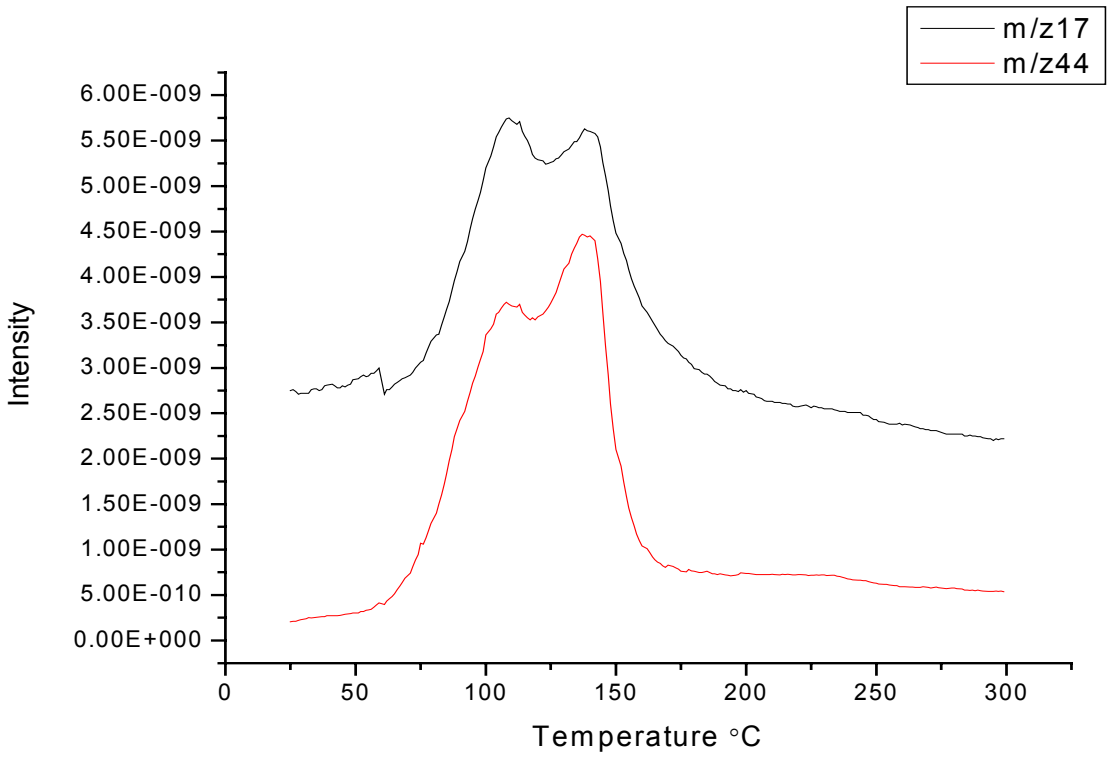

Figure 22. Overlaid m/z curves for NH_3 and CO_2 from the decomposition of ammonium carbonate by mass.

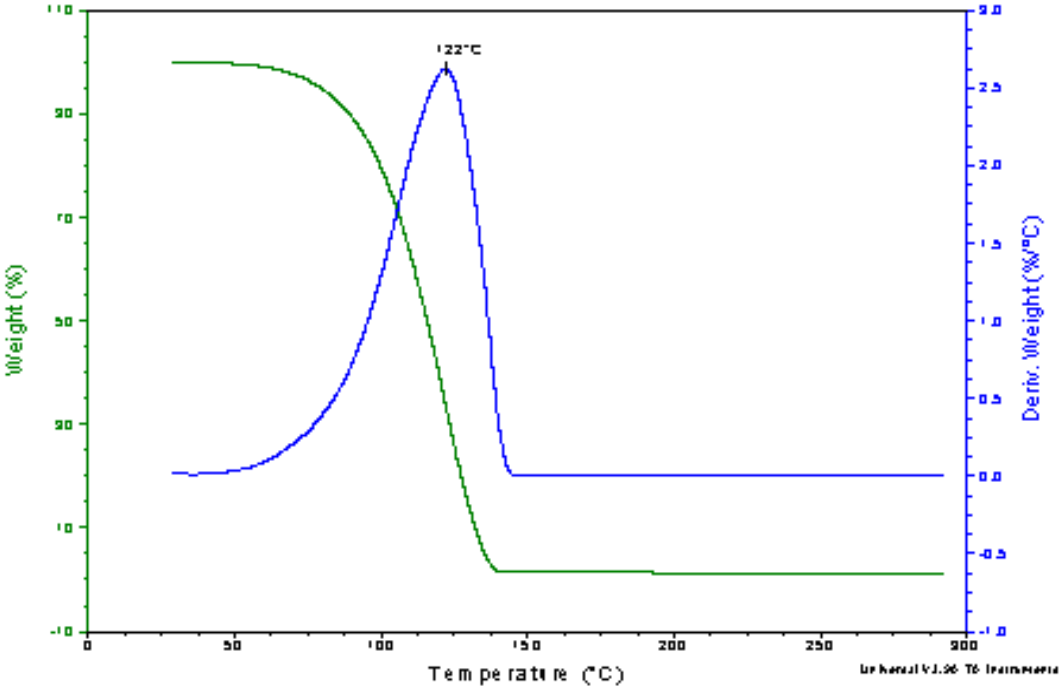

Figure 23. TGA curves for WKU sample 01050401 at 300@10°C/min.

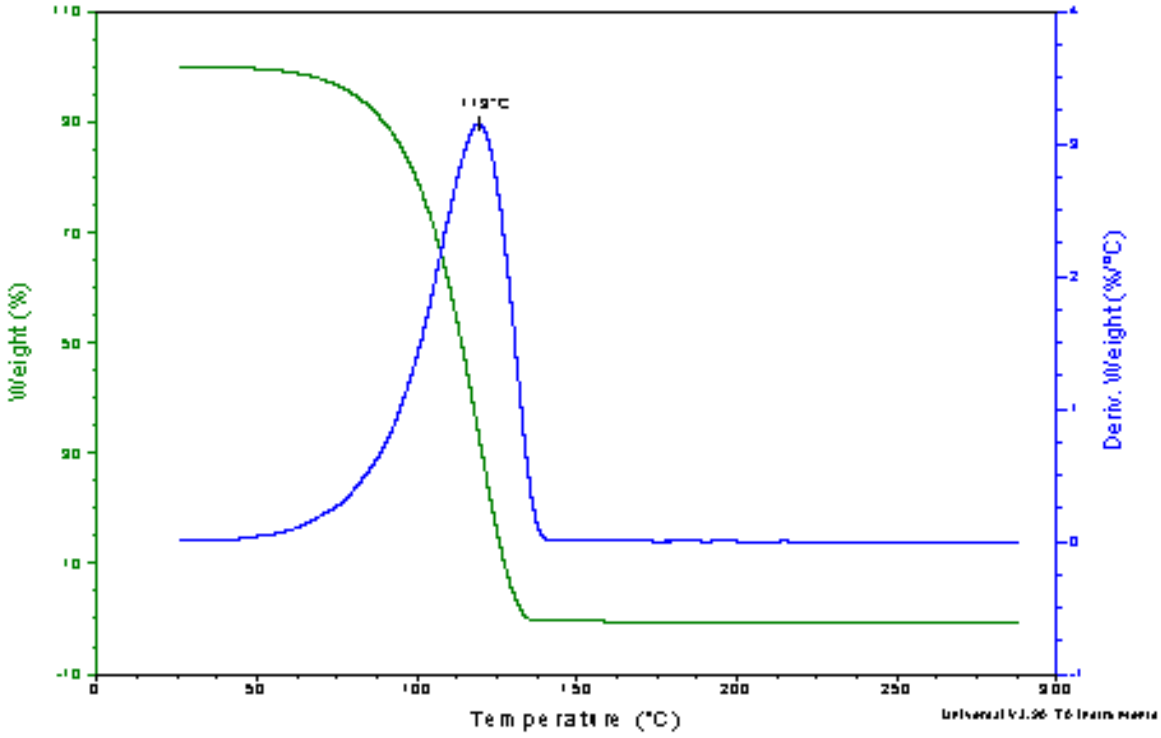

Figure 24. TGA curves for WKU sample 01060401 at 300@10°C/min.

From the above discussion, TGA can be used to distinguish the ammonium bicarbonate from ammonium carbonate. Double peaks in the TGA curve show the existence of ammonium carbonate.

4. XRD Technique

Figures 25, 26 and 27 represent the XRD spectra of ABC, ammonium carbonate and ammonium carbamate. The three highest peaks of ABC in Figure 25 are at 2θ: 29.7, 16.5, and 21.9, with relative intensity of 100%, 26.5%, and 19.43%. The three highest peaks of ammonium carbonate in Figure 26 are at 2θ: 29.6, 23.8, and 34.5, with relative intensity of 100%, 49.7%, and 42.8%. The three highest peaks of ammonium carbamate in Figure 27 are at 2θ: 30.4, 31.6, and 27.4, with relative intensity of 100%, 32%, and 5.98%. The three highest peaks 2θ and their relative intensity are summarized in Table 4. Table 5 shows the XRD spectral data from the Library. Comparison between the data indicate that the 2θ of the first strongest peaks are very close, although their relative intensities are different.

Figures 28 and 29 are XRD spectra of sample 01050401 and sample 01060401 from the CO_2 capture experiments. Both spectra show an obvious second highest peak at about 2θ: 16.5, which indicates these two samples are ammonium bicarbonate.

In the Table 4 and 5, it is found the following 2θ degree can be used to distinguish the NH4HCO$_3$, $(NH_4)_2CO_3$ and $NH_2CO_2NH_4$ samples: NH_4HCO_3 : 29.7, 16.5, and 21.9; $(NH4)_2CO_3$: 29.6, 23.8, and 34.5; $NH_2CO_2NH_4$: 29.7, 23.8, and 34.5.

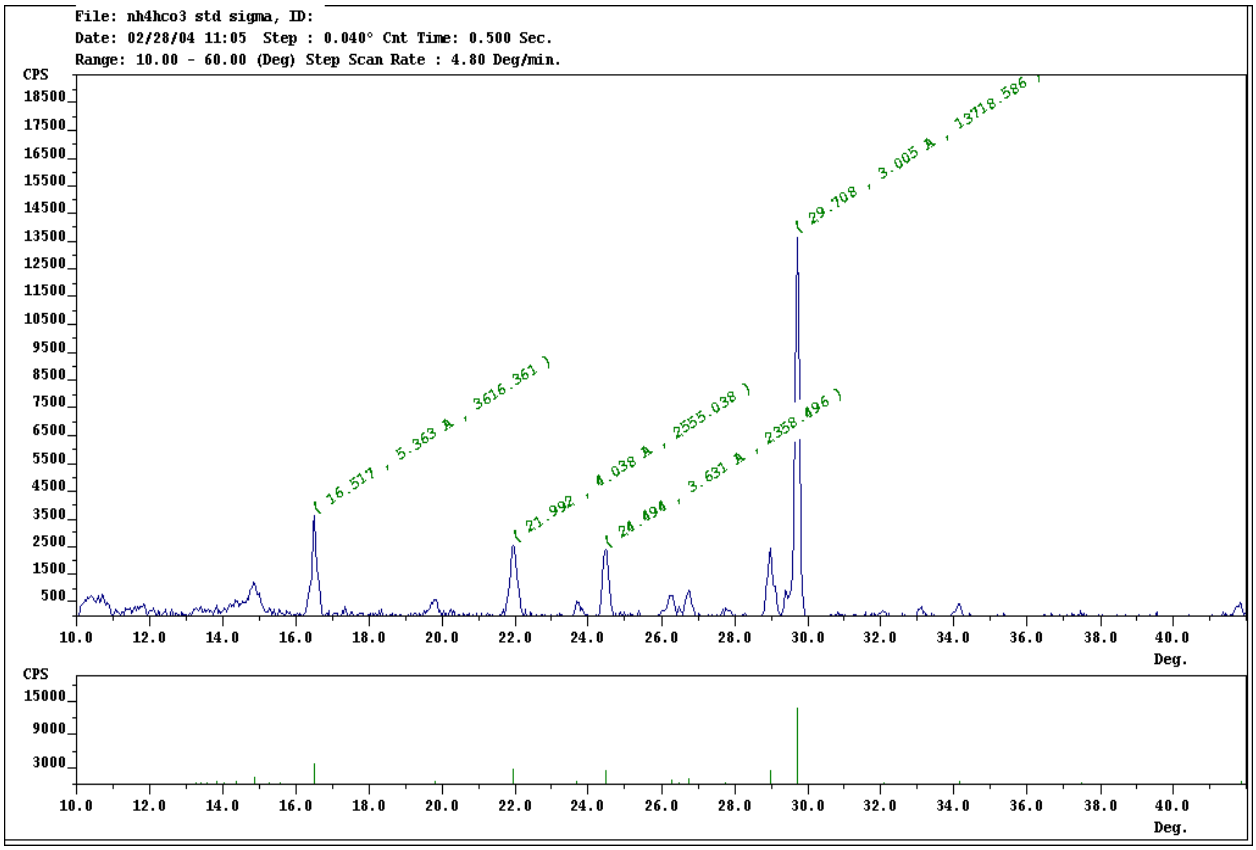

Figure 25. XRD spectrum of sample NH_4HCO_3 standard.

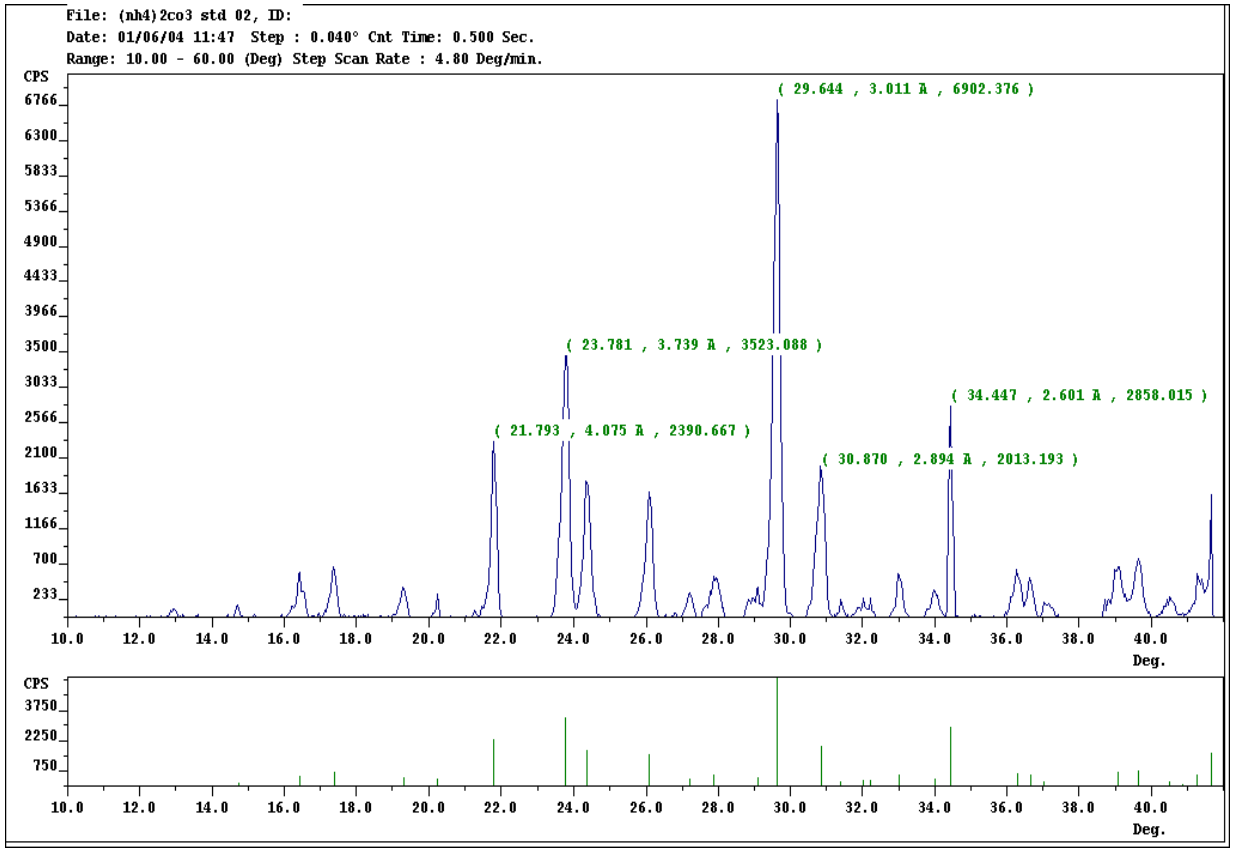

Figure 26. XRD spectrum of sample $(NH4)_2CO_3$ standard.

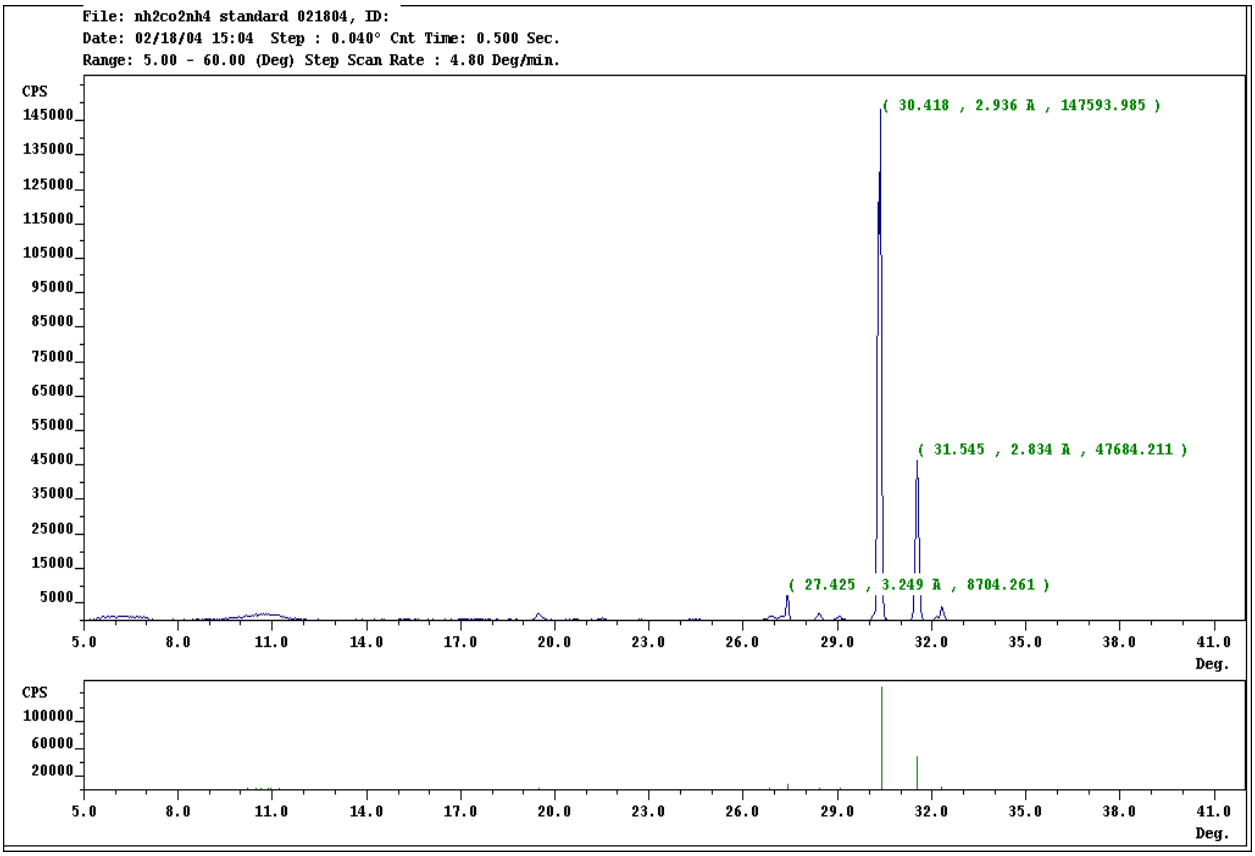

Figure 27. XRD spectrum of sample $NH_2CO_2NH_4$ standard.

Table 4. XRD Data from Samples (wavelength 1.54056Å)

Item	2θ	d spacing Å	Relative Intensity %
NH_4HCO_3 Standard	29.7	3.00	100
	16.6	5.36	26.5
	21.9	4.04	19.43
	24.5	3.63	18.02
$(NH4)_2CO_3$ Standard	29.6	3.01	100
	23.8	3.74	49.7
	34.4	2.60	42.8
$NH_2CO_2NH_4$ Standard	30.4	2.94	100
	31.6	2.83	31.95
	27.4	3.25	5.98

Table 5. XRD Data from ICDD Library
(wavelength 1.54056Å)

Item	2θ	D spacing Å	Relative Intensity
Ammonium Bicarbonate NH_4HCO_3 Card #01-0868	29.9	2.99	100
	16.7	5.30	42
	22.1	4.02	27
	24.6	3.61	27
Ammonium Carbonate Hydrate $(NH_4)_2CO_3$ H_2O Card #01-0858	29.7	3.00	100
	23.9	3.71	40
	26.2	3.40	30
	30.9	2.89	30
Ammonium Carbamate $NH_2CO_2NH_4$ Card #26-1565	30.5	2.93	100
	19.7	4.50	40
	27.0	3.30	40

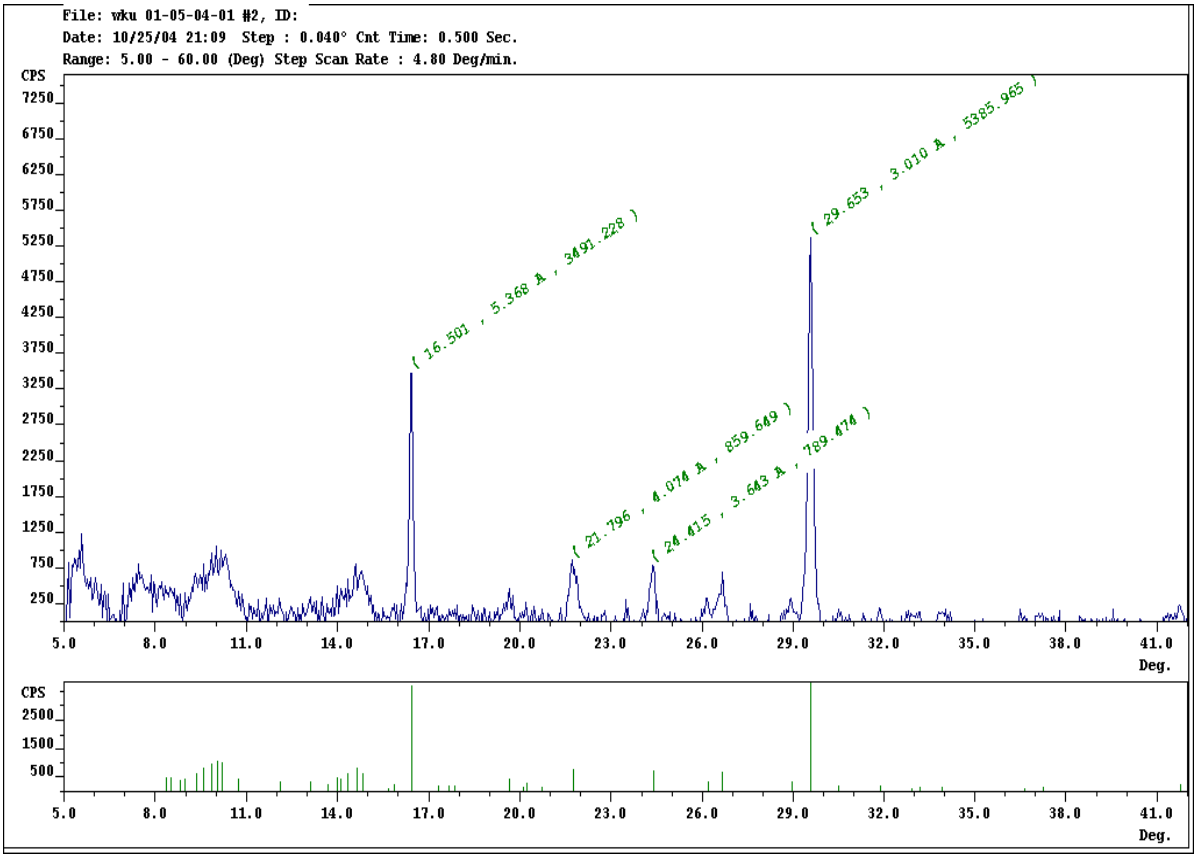

Figure 28. XRD spectrum of sample 01050401.

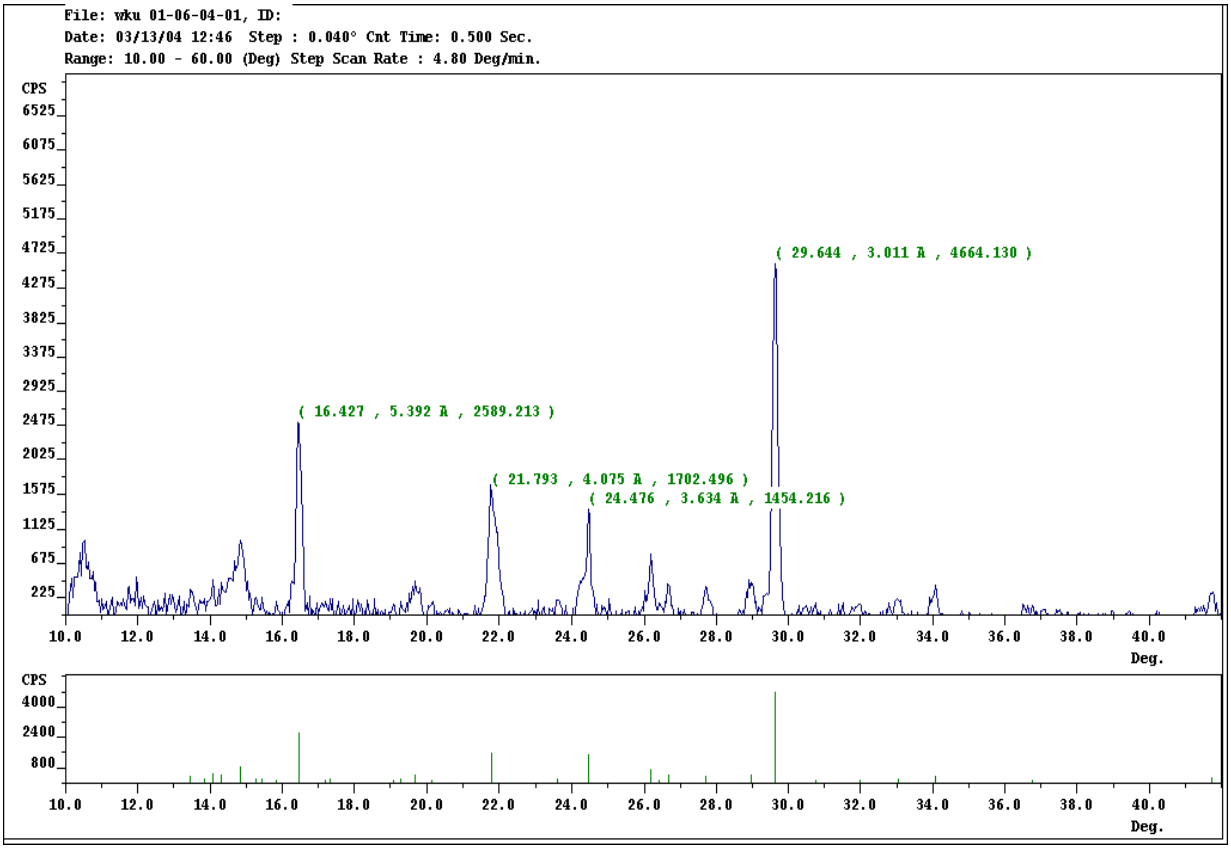

Figure 29. XRD spectrum of sample 01060401.

In conclusion, XRD provides obvious spectral difference among these three samples. Hence XRD can be used as an analysis method to differentiate the products of the CO_2 capture.

5. CHN Element Analysis

A LECO CHN-2000 carbon, hydrogen and nitrogen analyzer was used to analyze the C%, H% and N% in the ammonium salts. The C, H and N are the only elements in the products from the reaction of aqueous ammonia and CO_2. There are stoichiometric relations among these chemicals, which makes quantitative analysis of the ammonium bicarbonate in ammonium salt mixture by C H N element analysis possible. In accordance with the reaction mechanism between CO_2 and aqueous ammonia, the only products in solution are NH_4HCO_3 and $(NH_4)_2CO_3$ under the controlled conditions.

We can assume there are "X" Percentage of NH_4HCO_3 (MW: 79.06) and "Z" Percentage of $(NH_4)_2CO_3$ (MW: 96.09) in the mixture.

In the case of two components in chemicals mixture, the equations are:

$$X/79.06*12.01 + Z/96.09*12.01 = C \quad (18)$$

$$X/79.06*14.01 + Z/96.09*28.02 = N \quad (19)$$

The "C" and "N" are the percentage of carbon and nitrogen in the mixture by CHN2000.

So the solutions of the equation are as follows:

$$X = 79.06 * (2*C/12.01 – N/14.01) \quad (20)$$

$$Z = 96.09 * (N/14.01 – C/12.01) \quad (21)$$

C H N in standard chemicals by calculation is shown in Table 6.

C H N results in the samples from CO_2 Scrubbing by Ammonia are shown in Table 7.

Table 6. C H N Concentration (Weight%) in Standards by Calculation

	M.W.	C%	H%	N%
NH4HCO3	79.056	15.193	6.375	17.718
NH2CO2NH4	78.071	15.385	7.746	35.882
(NH4)2CO3	96.086	12.500	8.392	29.154

Table 7. Quantitative Results of Two Unknown Samples by CNH Element Analysis

Sample ID	C%	H%	N%	ABC %	Ave ABC%	Std Dev
01060401	15.083	6.212	17.76	98.30	97.93	0.53
	15.001	6.158	17.69	97.62		
	15.104	6.203	17.78	98.46		
	14.938	6.114	17.59	97.36		
01050401	15.025	6.178	17.82	97.18	97.55	0.29
	15.091	6.173	17.90	97.60		
	15.068	6.201	17.86	97.53		
	15.109	6.213	17.89	97.89		

Compared with Table 6 the C H N concentration in standard chemicals, the C H N concentrations in the product sample of Table 7 are very close to the standard C H N percentage in ABC.

Using equations 20 and 21, the calculated results are:

Sample 01060401: Average ABC 97.93% Standard Deviation 0.53

Sample 01050401: Average ABC 97.55% Standard Deviation 0.29

The nitrogen content of sample 01050401 and sample 01060401 are both above 17.2%, the index of good quality of ABC as stipulated in GB -3559-92 Agriculture Ammonium Bicarbonate National Standard of China [24]. Both products are of good quality.

Carbon, hydrogen and nitrogen are the predominant elements in the products from CO_2 scrubbing by aqueous ammonia. So elemental analysis can be used as quantitative analysis of ABC. A LECO CHN-2000 CHN Analyzer provides fast and accurate quantitative analysis of ABC.

The calculation results show that the ABC assay of Sample 01050401 and Sample 01060401 is above 97%. ABC is successfully produced by the CO_2 Scrubber.

6. NIR technique

The spectra collected from the Brimrose AOTF spectrometer were imported into the Unscrambler chemometric software package using a U5 file structure. A principle component analysis (PCA) was completed to attempt to separate the 3 subsets of samples. The results of the PCA indicated that samples with high percentages of bicarbonate were grouped together and not dependent on whether the remainder of the sample was comprised of carbamate or carbonate.

However as the percentage of either carbonate or carbamate increased, the samples were then separated into two groups. The samples that contained all three constituents were grouped together as well.

The same spectra were then used to perform a partial least squares regression (PLS) along with the constituent data that accompanied the samples. The constituent of interest in this study is bicarbonate. A regression was created that used three latent variables to explain 100 percent of both the spectra and constituent variation for bicarbonate.

NIR absorbance spectra of the samples are shown in Figure 30. Analysis of Figure 30 shows that there is a baseline ramp. This offset is most likely multiplicative in nature due to the fact that the samples were scanned using an overhead approach. This overhead approach allows for variability in the sampling pathlength. A corrective measure that can be implanted to correct for this baseline ramp is a second derivative pretreatment. The absorbance data was pretreated with a second derivative and the resultant spectra are shown in Figure 31.

At first, the resultant spectra appear to present excessive noise, but only a portion of the entire spectra are utilized. The structure of bicarbonate has one oxygen-hydrogen bonds. This bond would result in a peak at around 1450 nm. Figure 32 is an enlargement of the hydroxyl peak around 1450 nm. This is the region that is of most importance and is free of noise with spectral variation that could be used to perform a regression with.

Figure 33 was produced by a principal component analysis of the spectra using the wavelength region of 1400 nm to 1550 nm. This narrow range allows for fast analysis with the Brimrose Free Space Spectrometer. The red points in Figure 33 correspond to

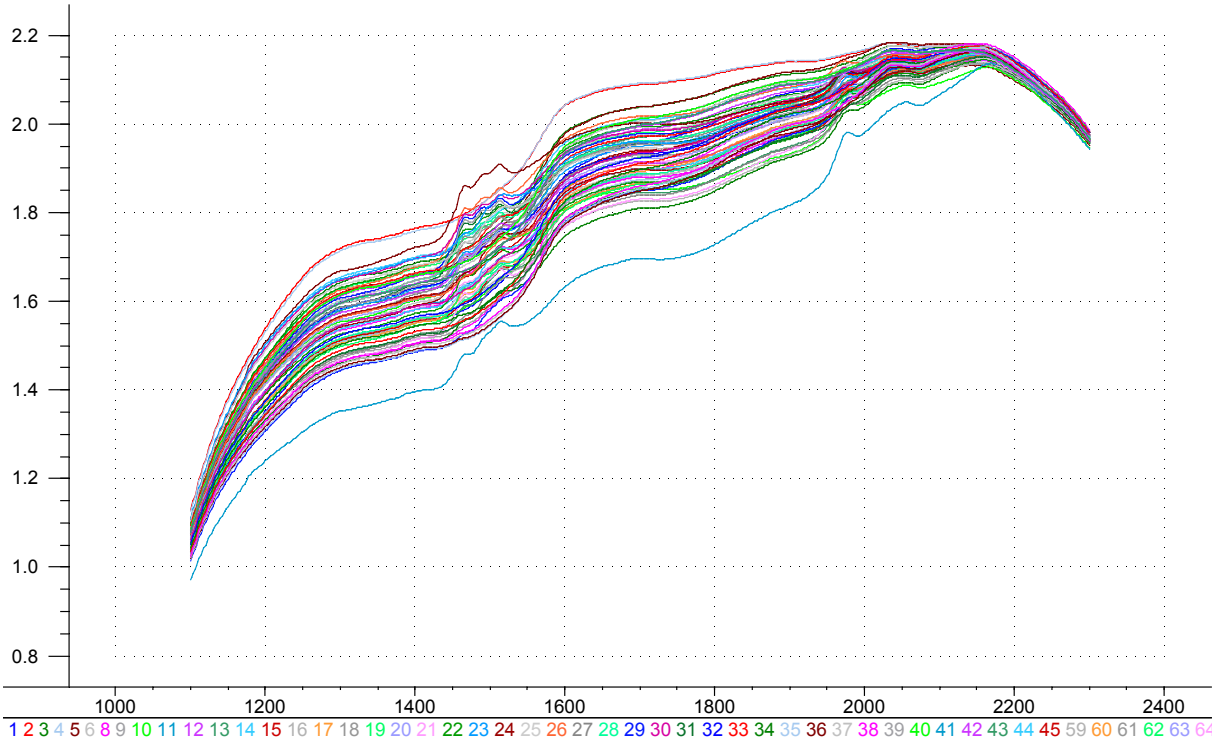

Figure 30. NIR Absorbance spectra of samples.

Figure 31. Absorbance spectra after a second derivative pretreatment.

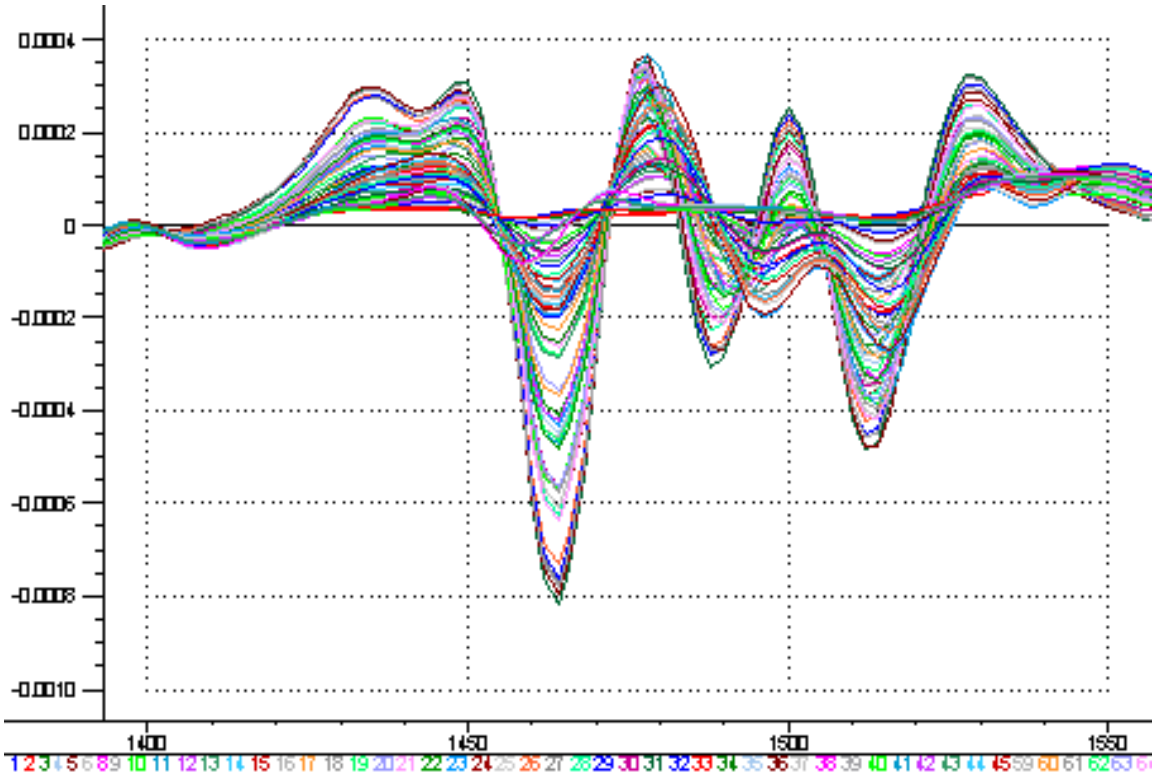

Figure 32. Second derivative spectra between 1400 nm and 1550 nm.

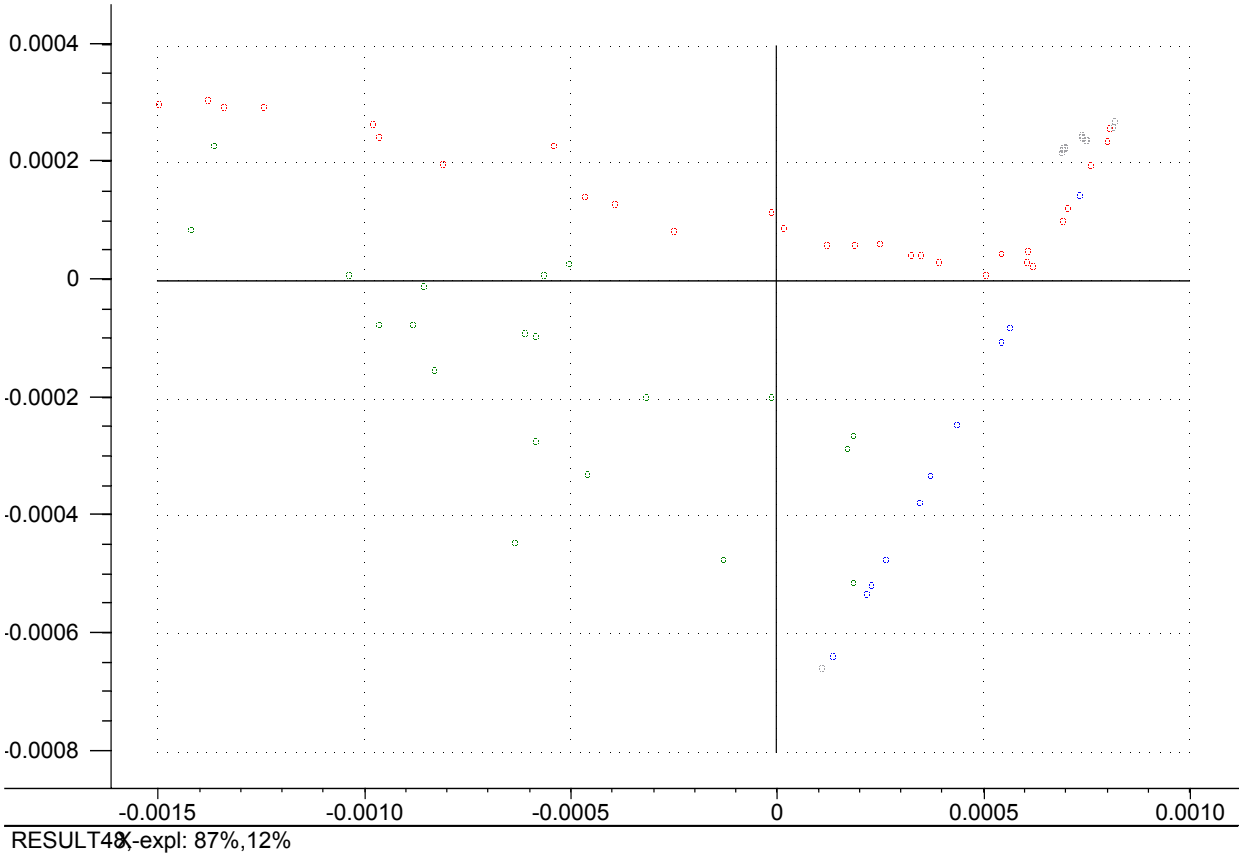

Figure 33. Scores plot of PCA.

bicarbonate/carbamate samples, the green points are the ternary samples, and the blue points are bicarbonate/carbonate samples. The grey points are the unknown samples that were provided and were used as test samples for the regression model. As indicated above, the three samples subsets can be separated by the spectral data in the range of 1400 to 1550 nm. The region of interest is where the samples are similar to the unknown samples. In this area of PC space, a PCA can not distinguish between bicarbonate/carbamate and bicarbonate/carbonate samples, due to the fact that the bicarbonate will dominate the spectra.

Figure 34 shows that 99.9 percent of the variance of the spectra is explained in the first three principle components. This is indicative of a robust model.

Figure 35 shows that 97 percent of the variance of the particle size is explained by the first three principle components. This plot is also indicative of robustness.

Figure 36 shows which wavelengths are used to determine the percentage of bicarbonate along with how strongly each variable affects the final results.

Figure 37 and Figure 38 show the predicted versus measured plot for calibration and predicted versus measure plot of cross validation, respectively. The regression model for percent bicarbonate indicates a strong correlation between the spectral data and reference values. The slope and bias for both calibration and cross validation are almost ideal. This translates into an accurate quantitative model from 0 % bicarbonate to 100 % carbonate. The residuals for both calibration and cross validation are small and show promise of a precise model.

The predicted versus measured plot for cross validation is almost identical to calibration. This would indicate the model is indeed robust, using only 3 principle

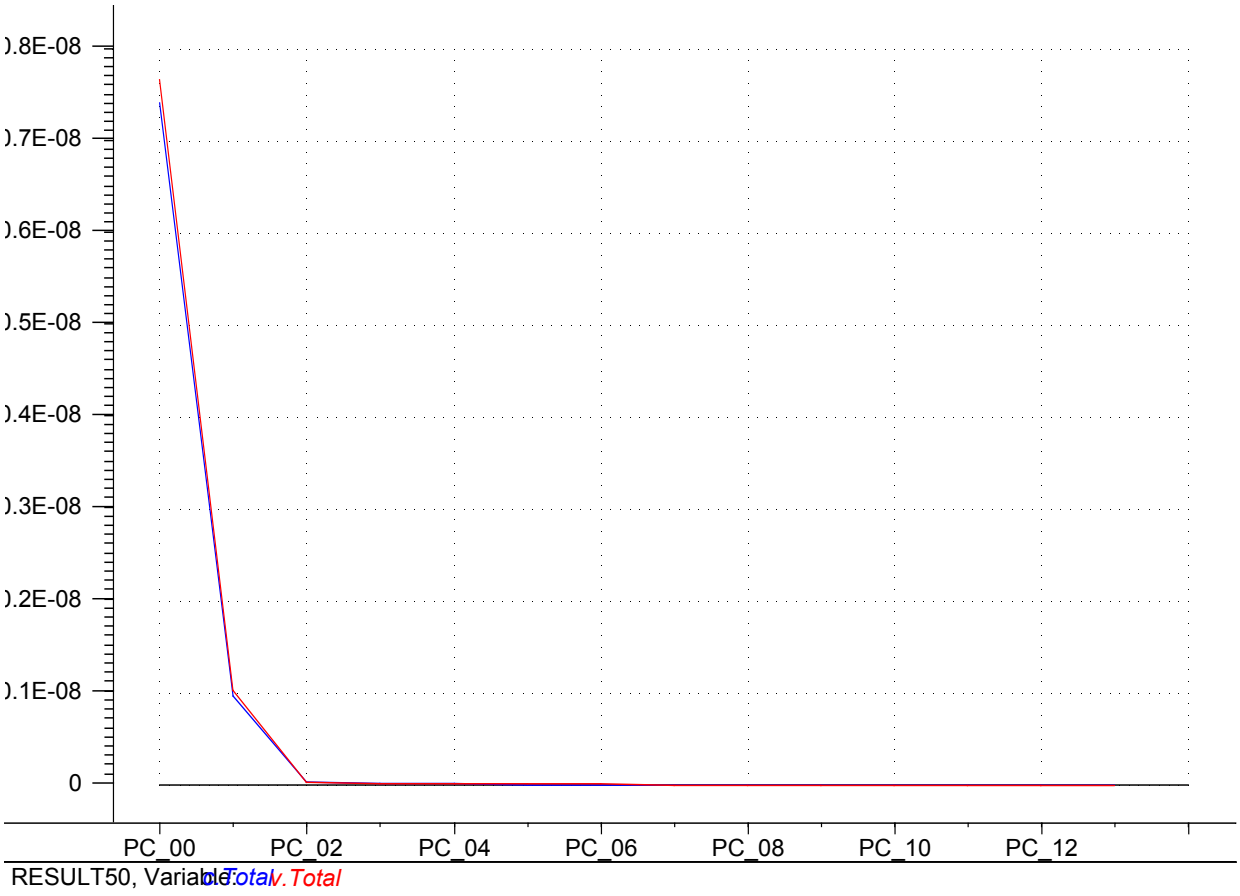

Figure 34. Variance plot of variables.

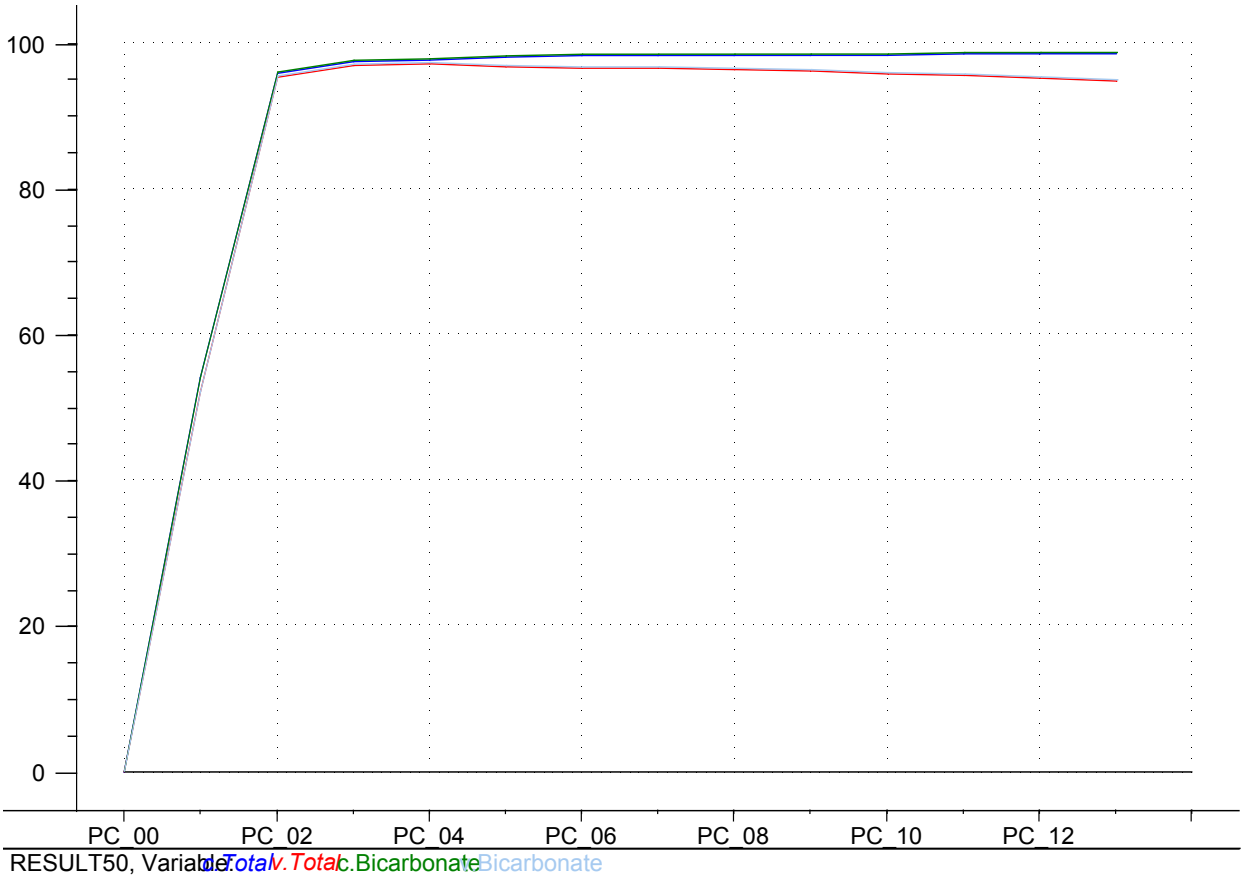

Figure 35. Variance plot of particle size.

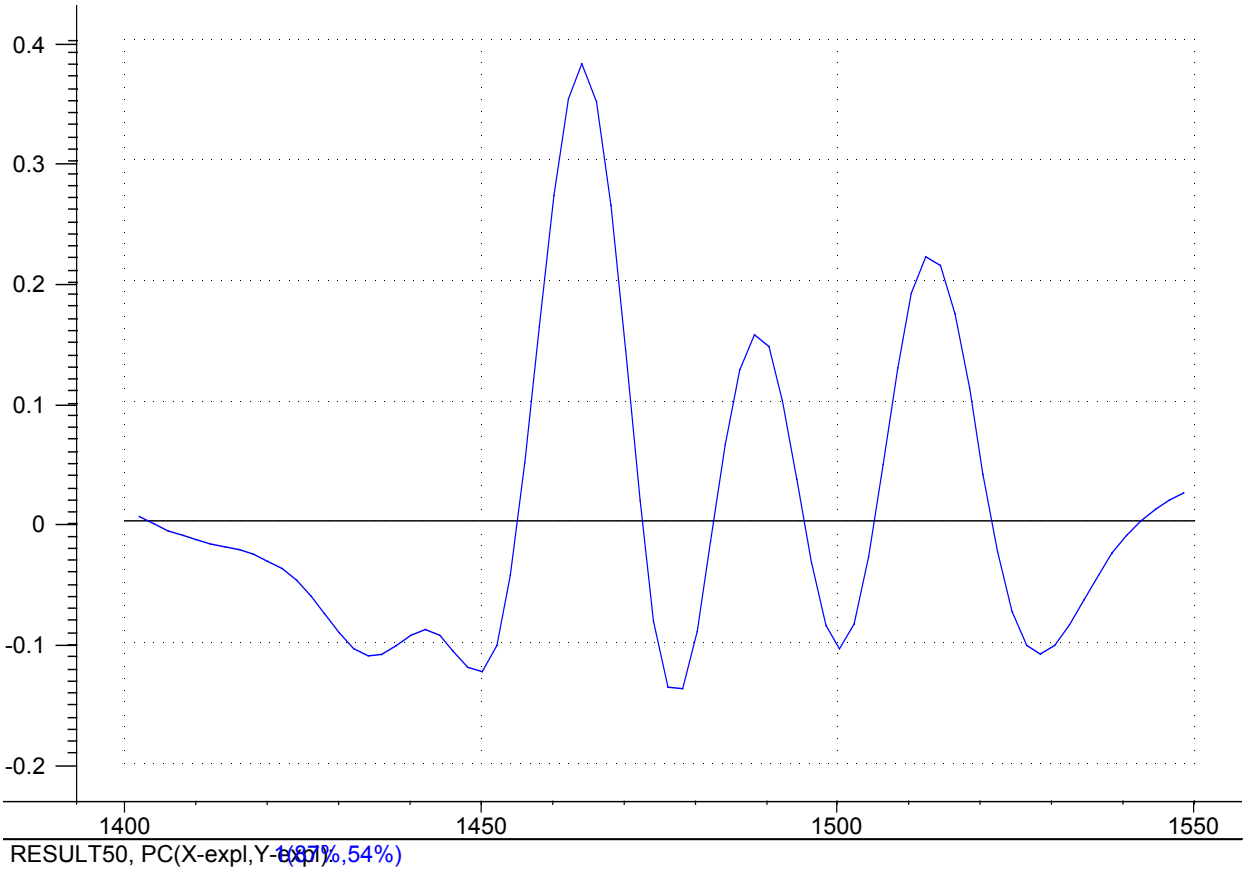

Figure 36. X-Loadings for regression model.

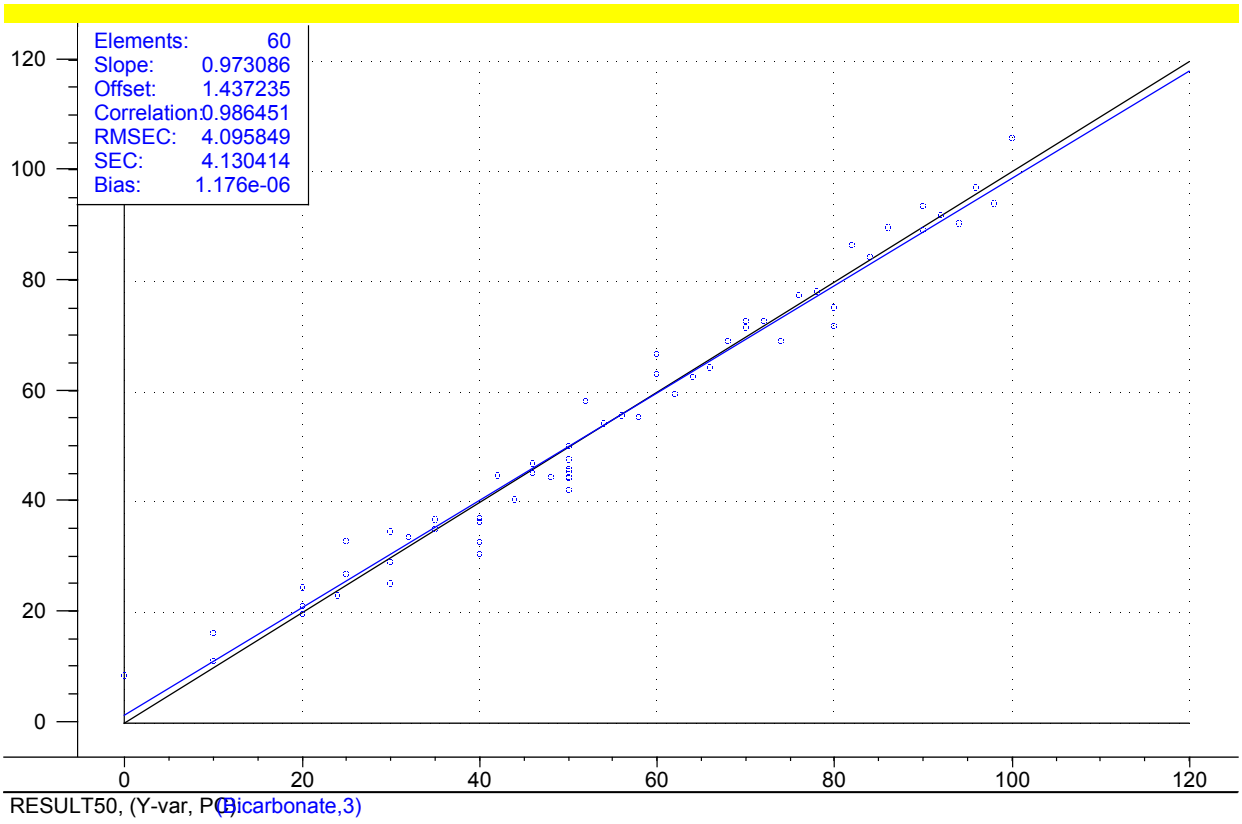

Figure 37. Predicted versus measured plot for calibration.

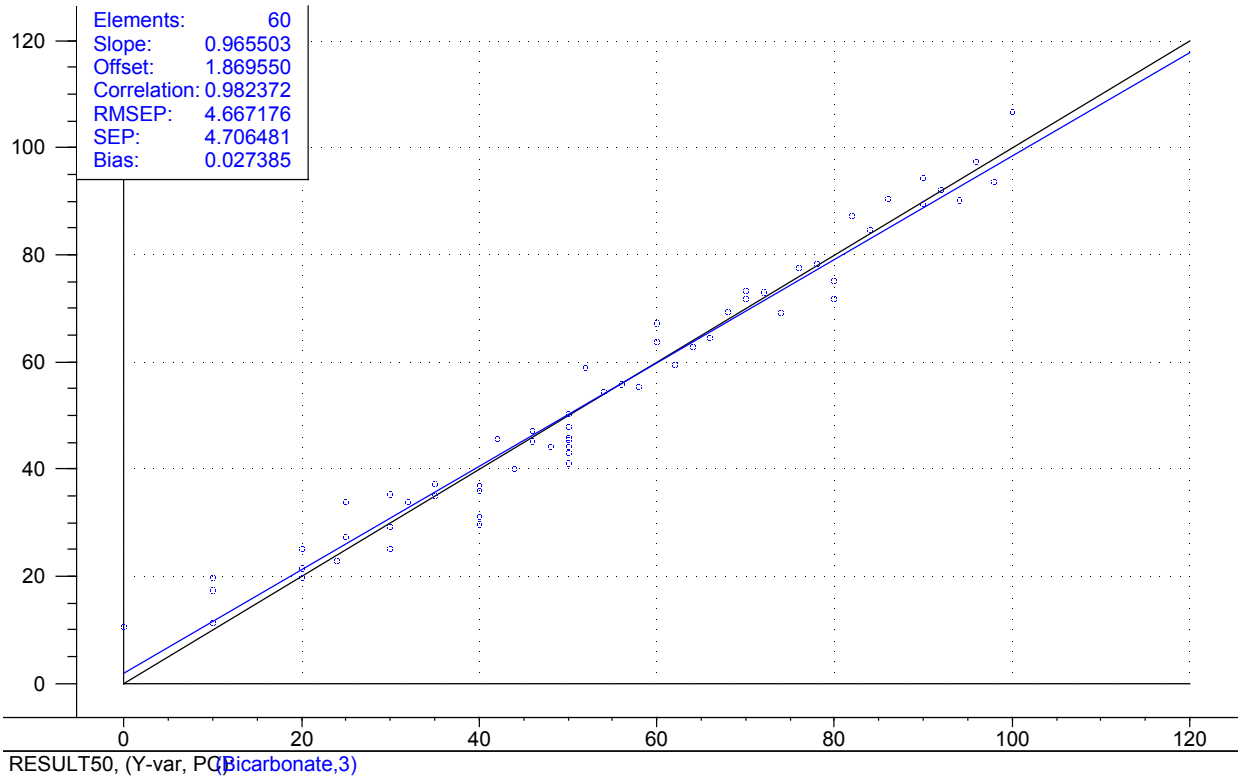

Figure 38. Predicted versus measure plot of cross validation.

components to explain all the variation between samples. The model produces an SEC of 4.1 and an SEP of 4.7.

Table 8 shows the results of a prediction using the above regression model. The predicted results have the standard deviations of 0.26 and 0.17, which indicate the model and NIR technique have very good repeatability. When comparing NIR results with the results from the CHN analysis, it is found the difference of Sample 01050401 is -2.79 and relative error is 2.8%, and the difference of 01060401 sample is -0.48 and relative error is 0.49%. Both the CHN and NIR techniques indicated the ABC purities of two WKU samples are above 95% and gave very close ABC concentration.

Since the model is using a region of the spectrum that only contains 150 wavelengths, the method of analysis is extremely efficient, a typical analysis would only take about 1 second to produce accurate and precise results. If increased accuracy is needed the number of scans per sample can be increased without increasing the scanning time greatly.

The AOTF-NIR Free Space spectrometer is the ideal tool for real-time, on-line measurements. The AOTF technology allows for fast scanning using no moving parts and without the need to recalibrate the system. In this case, a free space spectrometer can be mounted above a production line and non-contact classification analysis can be performed. The spectrometer can send a signal to the process control system indicating the results of the classification. The results of this study proved the feasibility of determining percent bicarbonate of samples from spectral data collected using the NIR technique for either on-line or laboratory determination.

Table 8. NIR Prediction Results of WKU Samples.

Sample	Predicted	Average	Standard Deviation
wku01050401	95.73	95.64	0.26
wku01050401	95.61		
wku01050401	95.67		
wku01050401	95.23		
wku01050401	95.95		
wku01060401	98.26	98.36	0.17
wku01060401	98.64		
wku01060401	98.22		
wku01060401	98.38		
wku01060401	98.29		

B. Thermal Stability Analysis of Ammonium Bicarbonate and Long Effect Ammonium Bicarbonate

There are many factors that can affect the loss of carbon from ABC, such as temperature, environmental gas flow rate, humidity, stored volume, sealing conditions, application measures, and so on. Temperature and environmental air flow rate are two of the most important factors since volatilization rapidly increases with the temperature and flow rate. TGA is very suitable for the analysis of the influences of these two factors on the evaporation speed because temperature and gas flow rate can be easily controlled by TGA when measuring the weight loss. Figures 39 and 40 show experimental results on volatilization speed of ABC and LEABC at different temperature conditions with an air flow rate of 50 mL/min. The weight losses of ABC and LEABC are summarized in Table 9. As shown in Table 9, the evaporation speed of ABC is approximately 2.0 - 3.8 times higher than that of LEABC between 25 ^{o}C and 55 ^{o}C. The highest evaporation speed ratio of ABC to LEABC is at 30 ^{o}C, which is 3.8 times. However at 60^{o}C and 65^{o}C, the evaporation speeds are close and the ratios are 1.4 and 1.1 respectively. This is because the ammonium bicarbonate decomposes into ammonia, water and carbon dioxide at about 60^{o}C. LEABC does not increase the decomposition temperature of ABC. The comparison of evaporation speeds between ABC and LEABC at different temperatures indicates LEABC evaporates much slower than ABC.

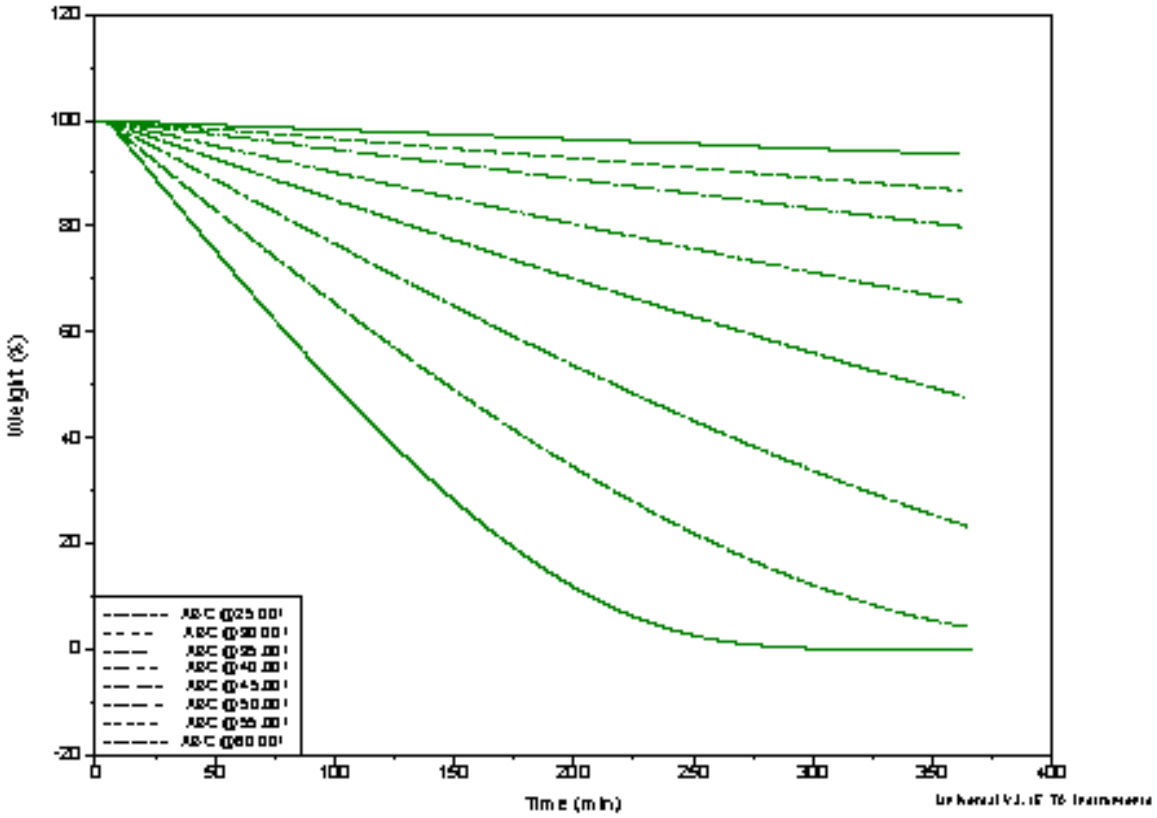

Figure 39. Overlaid TGA curves of ABC at different temperatures.

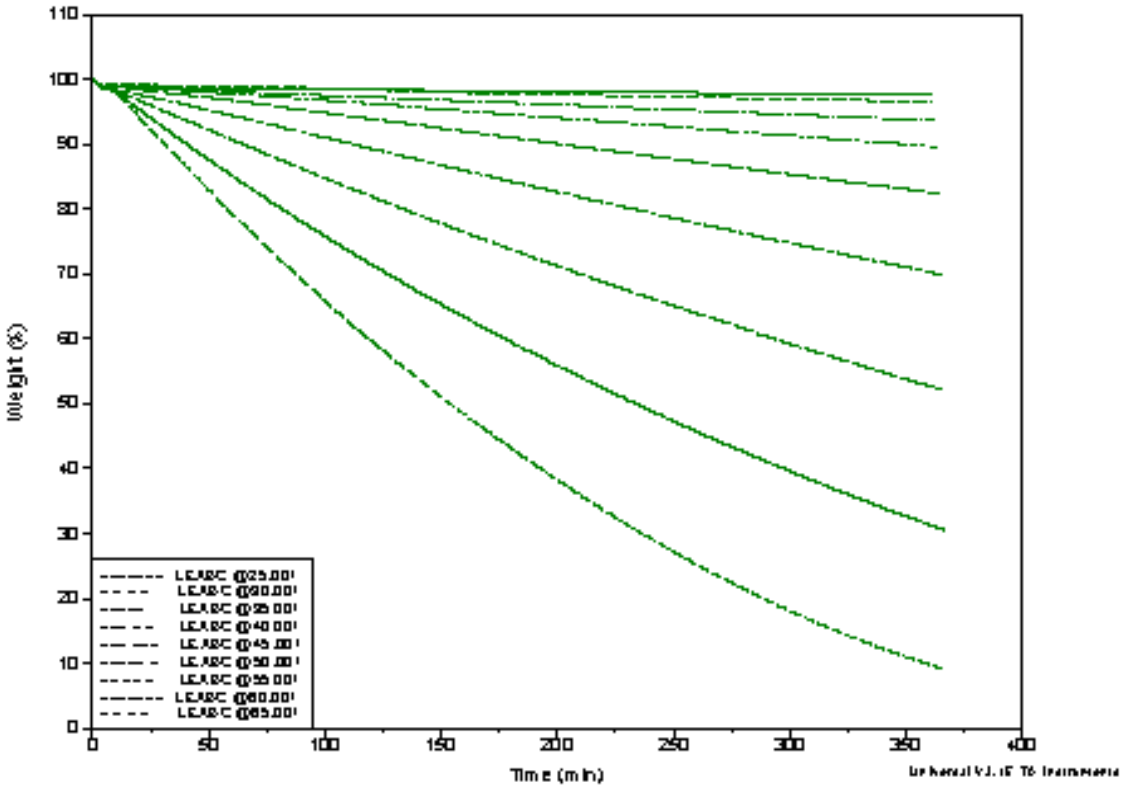

Figure 40. Overlaid TGA curves of LEABC at different temperatures.

Table 9. Summarized Weight Losses of ABC and LEABC at Different Temperatures

Temperature (ºC)	Volatilization speed (Weight Loss Percentage after 6 hrs)		
	ABC	LEABC	ABC/LEABC Ratio
25	6.4	2.4	2.7
30	13.3	3.5	3.8
35	20.1	6.3	3.2
40	34.3	10.4	3.3
45	52.2	17.5	3.0
50	76.7	30.0	2.6
55	95.8	47.8	2.0
60	100.0	69.4	1.4
65	100.0	91.0	1.1

Figures 41 and 42 show experimental results on volatilization speed of ABC and LEABC at 30 ^{o}C under different air flow rates conditions. The weight losses of ABC and LEABC are summarized in Table 10. It is shown that when the flow rate is from 25mL/min to 75mL/min, the weight loss changes from approximately 10% to 15% for ABC, and about 3.3% to 3.5% for LEABC, around one-third of ABC. Increasing air flow rate from 25mL/min to 75mL/min increases volatilization speed of ABC by nearly 50%, but only 6% for LEABC.

The results indicate that at different temperature and air flow rate conditions, volatilization speed of LEABC is much lower than ABC. Hence LEABC has good performance in retarding the release of CO_2 and has much better capacity for carbon fixation than ABC. There are three reasons. First, the hydrogen bonds between the DCD and the ABC affect physical properties of ABC, such as volatility and stability. Second the hydration of ABC is an irreversible reaction and ABC decomposes to NH_3, H_2O and CO_2. DCD decreases the hydration radius of $NH4^+$ and then reduces the free water and the release rate of CO_2. Third, the LEABC has a smaller surface area than ABC, which decreases the evaporation speed. Although LEABC improves carbon stability, it vaporizes slowly. It should be covered by soil immediately after application in the field, especially under conditions of high temperature. In order to reduce the release of CO_2, the short term storage of ABC should be in a dry environment with a low air ventilation rate.

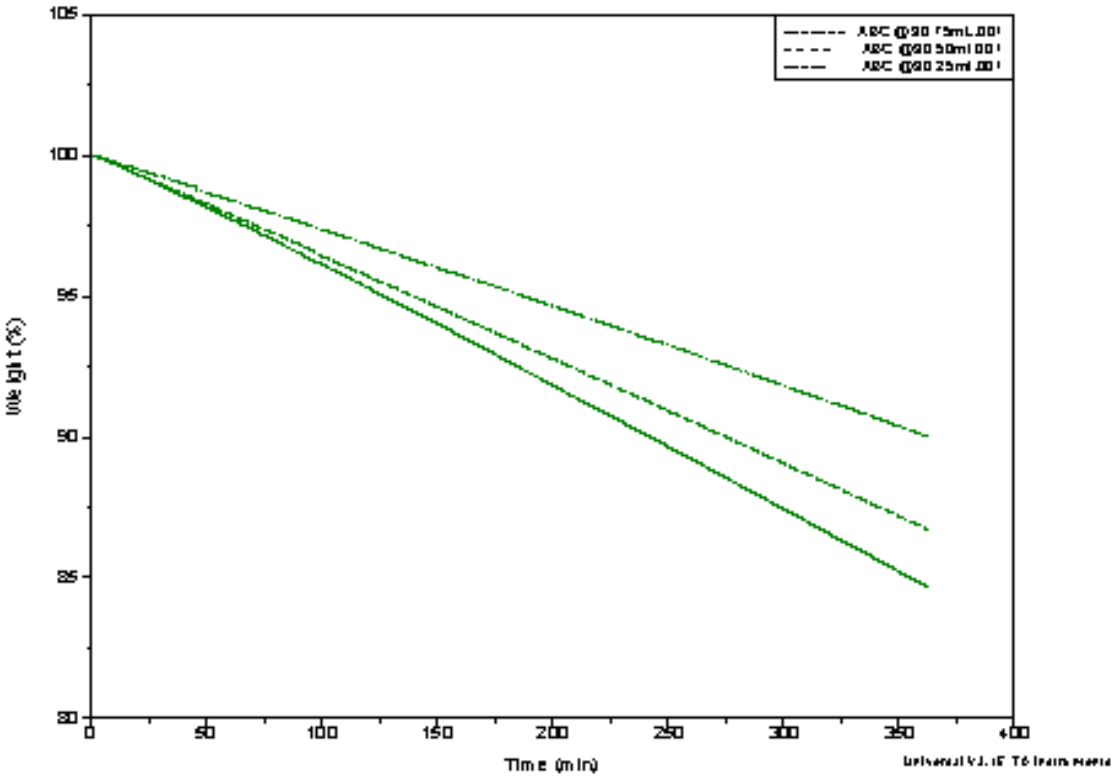

Figure 41. Overlaid TGA curves of ABC at different flow rates.

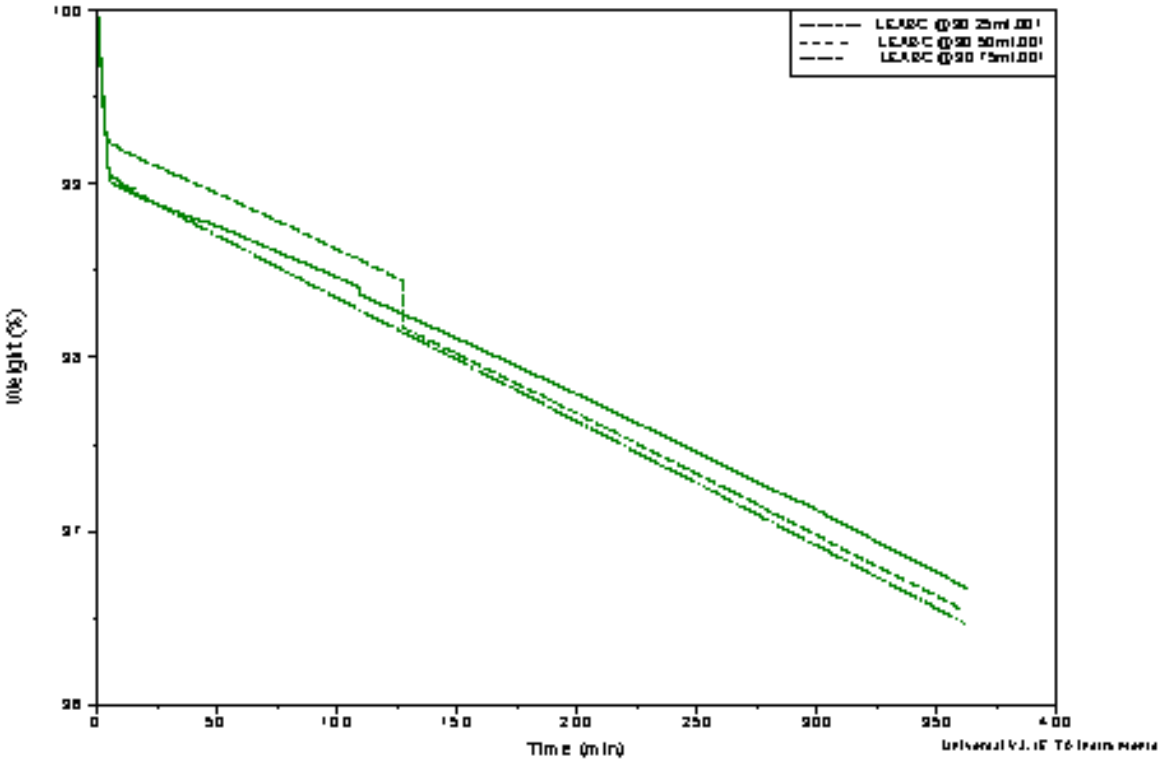

Figure 42. Overlaid TGA curves of LEABC at different flow rates.

Table 10. Summarized Weight Losses of ABC and LEABC at Different Air Flow Rates

Flow Rate (mL/min)	Volatilization speed (Weight Loss Percentage after 6 hrs)		
	ABC	LEABC	ABC/LEABC Ratio
25	10.0	3.3	3.0
50	13.3	3.5	3.8
75	15.3	3.5	4.3

C. Kinetic Study of Ammonium Bicarbonate and Long Effect Ammonium Bicarbonate

The Flynn and Wall[21] method is limited to well-resolved single step decompositions and first order kinetics. Before using this method, it is necessary to test the studied reaction for first order kinetics.

Consider the reaction: A → Products (23)

If first order kinetics is followed, then the rate of the reaction is proportional to the concentration of A:[30]

Rate = k x (conc. A) (24)

Let α be the concentration of A at t=o and (α -x) be the concentration of A at any other time denoted by t.

The reaction rate for decomposition is:

$dx/dt = k (\alpha - x))$ (25)

On Integration, this equation becomes:

$$k = \frac{1}{t}\ln\left(\frac{\alpha}{\alpha - x}\right) \quad (26)$$

Using values of α, α-x, and t from the ABC and LEABC isothermal 30°C experimental curve shown in Figures 39 and 40, the rate constant, k, can be calculated at any point in the reaction. The data is shown in Table 11 and 12.

Within experimental accuracy, the data are consistent with first order kinetics at least up to t = 90 min.

Table 11. ABC Isothermal 30°C Experimental Data (Starting Wt. 81.6656mg)

t (min)	α-x (mg)	k (min^{-1})
30	80.7977	0.000356
60	79.9296	0.000358
90	79.0471	0.000362
120	78.1253	0.000369

Table 12. LEABC Isothermal 30°C Experimental Data (Starting Wt. 92.0377mg)

t (min)	α-x (mg)	k (min^{-1})
30	91.8572	0.000065
60	91.6941	0.000062
90	91.5188	0.000063
120	91.3343	0.000064

Figures 43 and 44 display the overlaid weight loss curves for the ABC and LEABC at several different heating rates. The first step in the data analysis process is the choice of level of decomposition. Typically, a value early in the decomposition profile is desired since the mechanism here is more likely to be that of the actual product failure. On the other hand, taking the value too early on the curve may result in the measurement of some volatilization (e.g. moisture) which is not involved in the decomposition mechanism. ABC and LEABC are materials with high volatile matter (about 6.4% and 2.4%), as shown in Part B: Thermal Stability Analysis of ABC and LEABC. So a value of 7.5% decomposition level (sometimes called "conversion") is the chosen value.

Using the selected value of conversion, the temperature (in kelvin) at that conversion level is measured for each thermal curve. A plot of the logarithm of the heating rate versus the corresponding reciprocal temperature at constant conversion is prepared. The plotted data produce a straight line.

Figures 45 and 46 show a series of such lines created from the five curves shown in Figures 43 and 44 by plotting data at different conversion levels. If the particular specimens decomposition mechanism were the same at all conversion levels, the lines would all have the same slope. This is not the case here. The lines for the low conversion cases are quite different from those of 5% and higher conversion. This justifies the selection of 7.5% conversion as the "best" point of constant conversion for the purposes of this test.

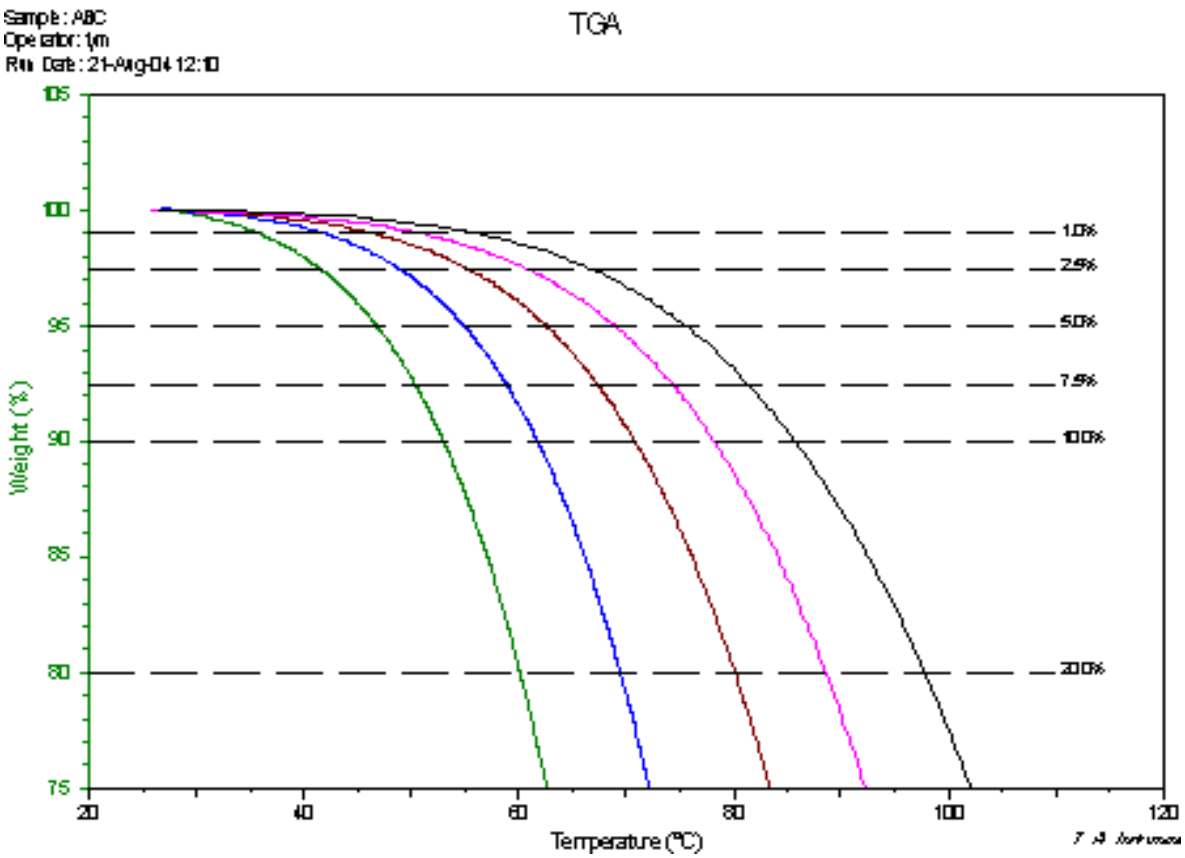

Figure 43. Overlaid weight loss curves for ABC.

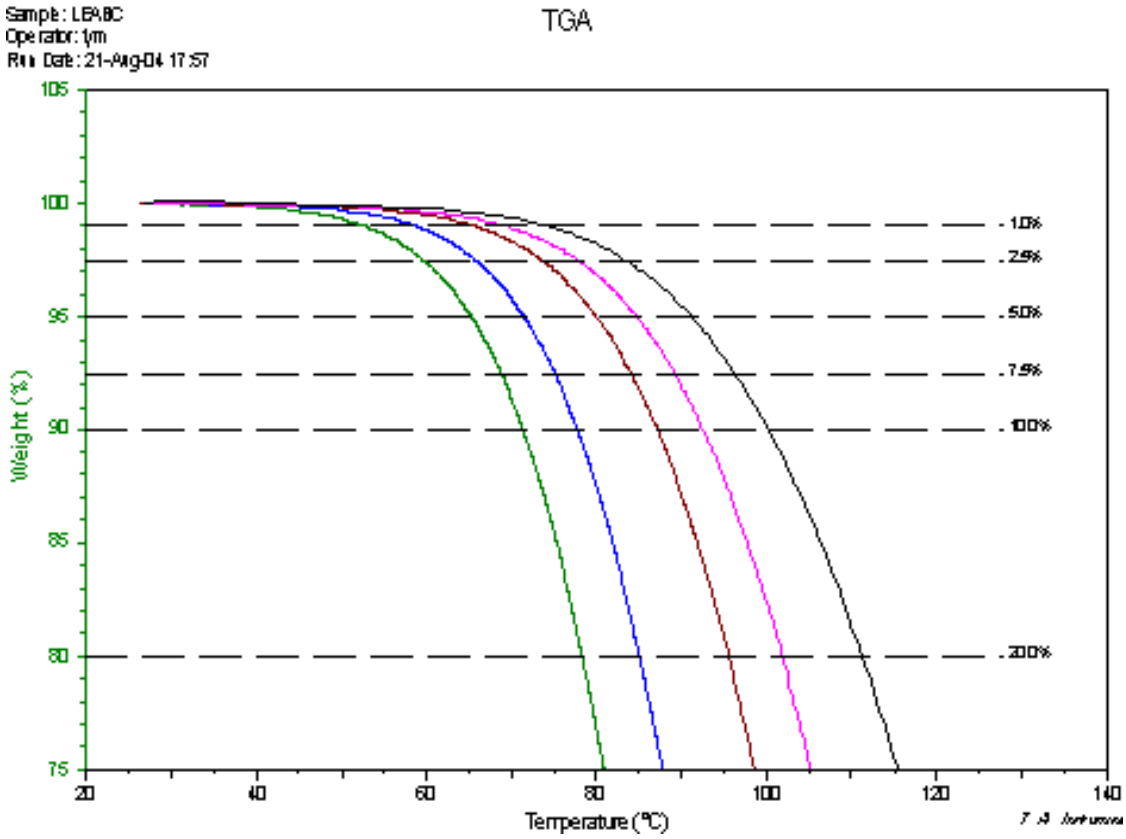

Figure 44. Overlaid weight loss curves for LEABC.

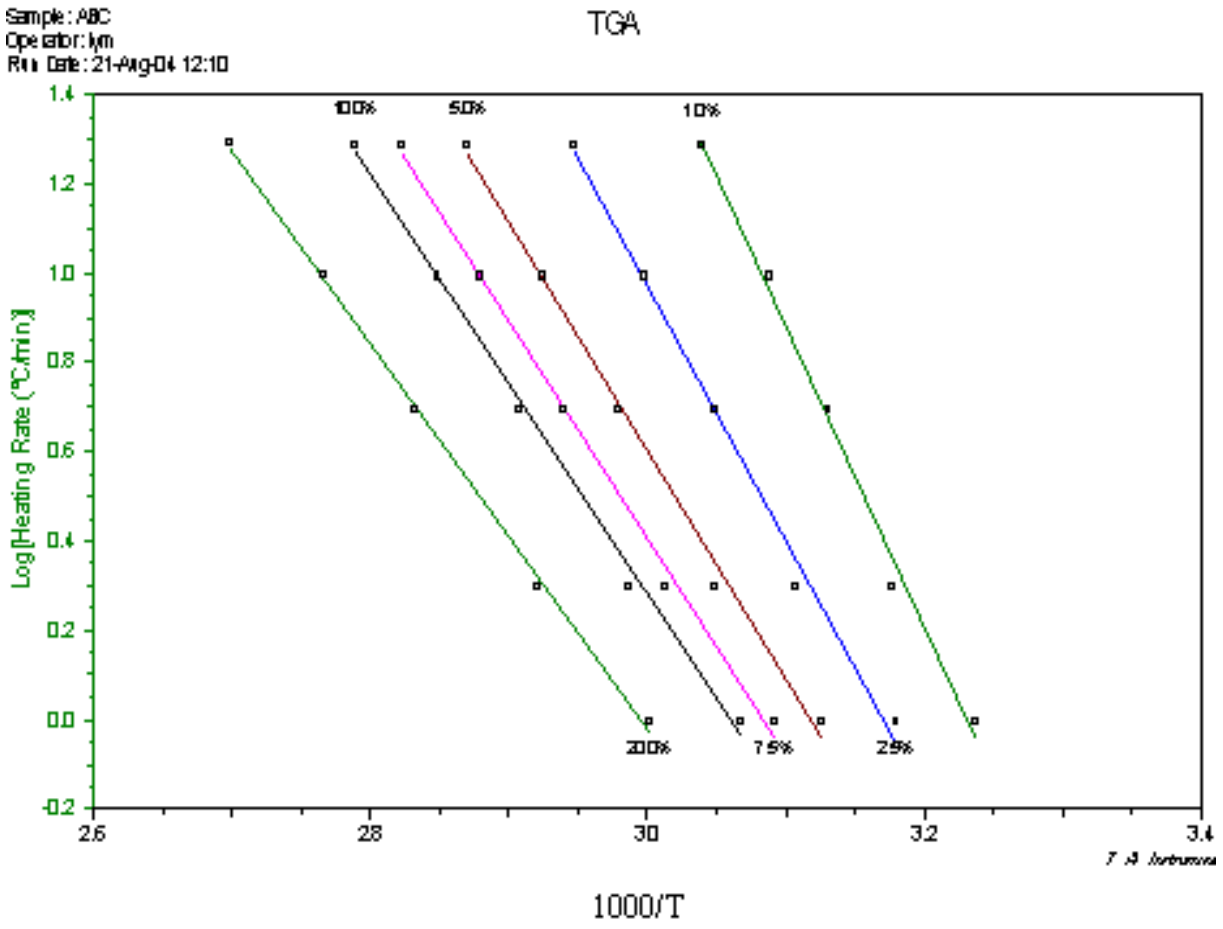

Figure 45. The logarithm of the heating rate versus the corresponding reciprocal temperature at various conversion of ABC.

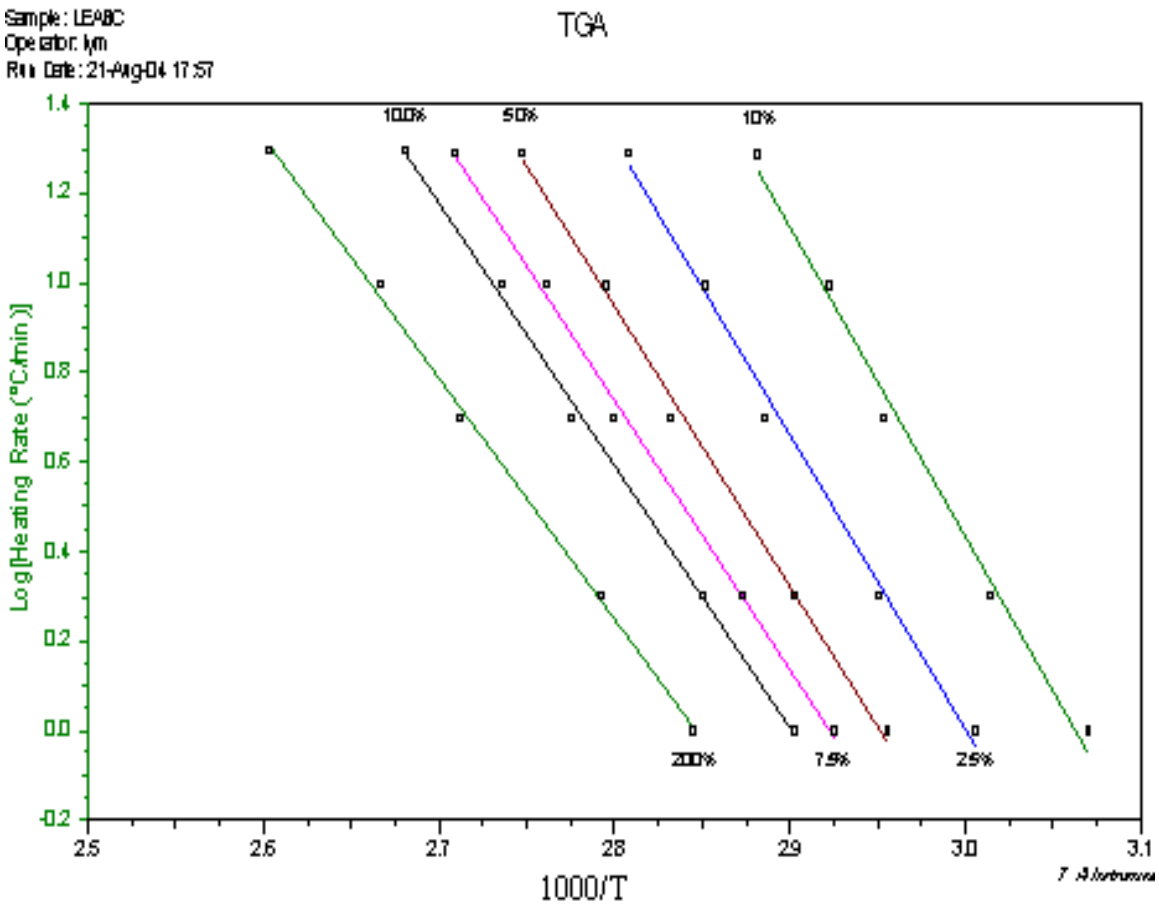

Figure 46. The logarithm of the heating rate versus the corresponding reciprocal temperature at various conversion of LEABC.

The next step in the process is the calculation of activation energy (E) from the slope in Figures 45 and 46 using the method of Flynn and Wall[21].

Tables 13 and 14 summarized the kinetic parameters at different conversion levels for ABC and LEABC. At the 7.5% conversion rate, LEABC's activation energy is 111.9 kJ/mole, which is greater than ABC's activation energy 93.6 kJ/mole. LEABC has higher activation energy, the decomposition reaction rate of LEABC is lower than that of ABC. This explains the reason why LEABC is more stable than ABC. In addition, the activation energy plays an important role in the engineering design such as sizing the CO_2 regeneration reactor as well as optimizing the its operation condition.

Figures 47 and 48 display the estimated lifetime of ABC and LEABC. They are used to predict the amount of time that the material will remain stable at specified storage temperatures. For example, at 15^{o}C, the ABC predicted lifetime is about 30 hrs, but the LEABC predicted lifetime is about 400 hrs. LEABC obviously has better stability performance than ABC.

Table 13. ABC Kinetic Parameters at Different Conversion Levels

Conversion %	Activation Energy kJ/mole	Log[Pre-exp Factor1/min]	60 min Half- Life Temp °C
1.0	118.1	17.18	49.0
2.5	106.8	15.19	52.5
5.0	97.6	13.64	54.2
7.5	93.6	12.96	55.0
10.0	89.5	12.29	55.3
20.0	79.3	10.70	54.9

Table 14. LEABC Kinetic Parameters at Different Conversion Levels

Conversion %	Activation Energy kJ/mole	Log[Pre-exp Factor 1/min]	60 min Half-Life Temp°C
1.0	139.6	9.47	67.5
2.5	129.9	7.85	69.7
5.0	118.4	6.04	70.8
7.5	111.9	5.05	71.1
10.0	105.7	4.10	71.1
20.0	92.1	2.08	70.2

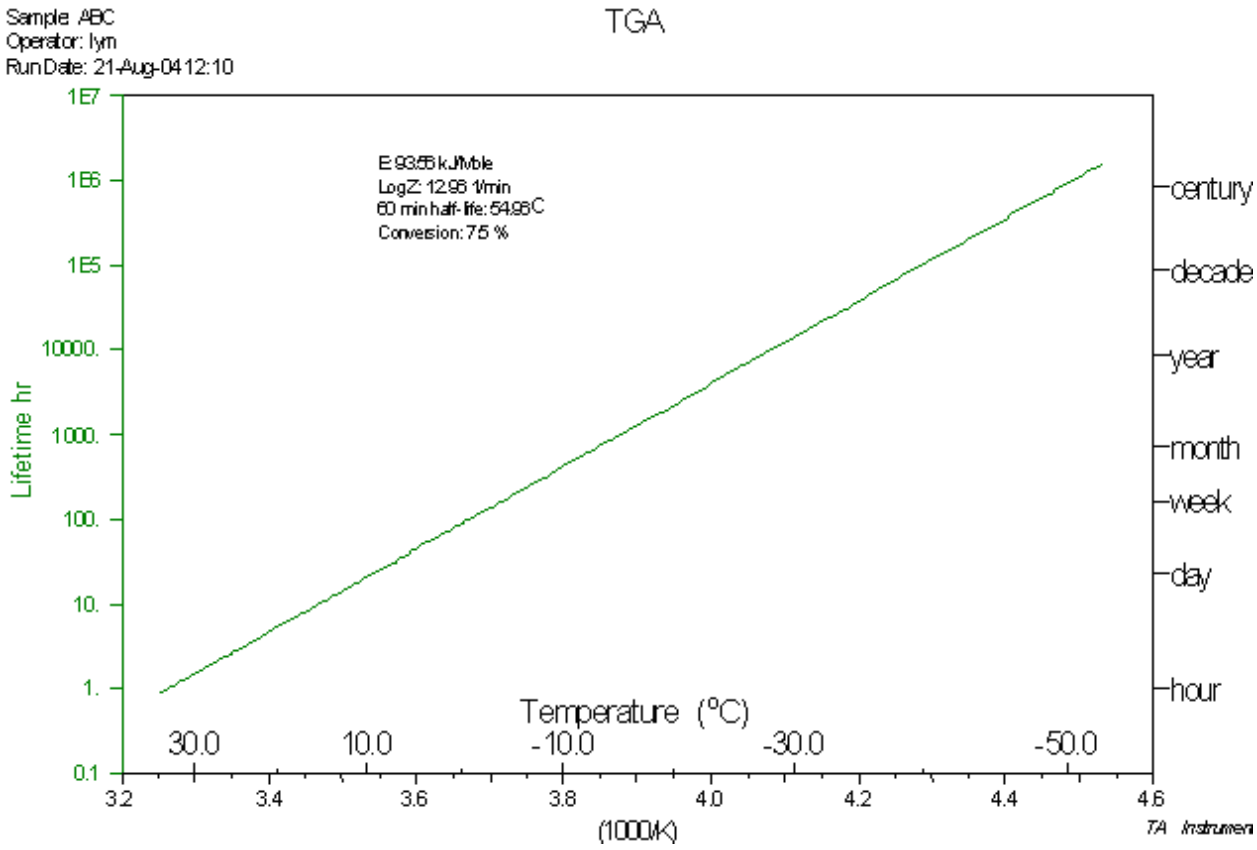

Figure 47. Estimated lifetime of ABC.

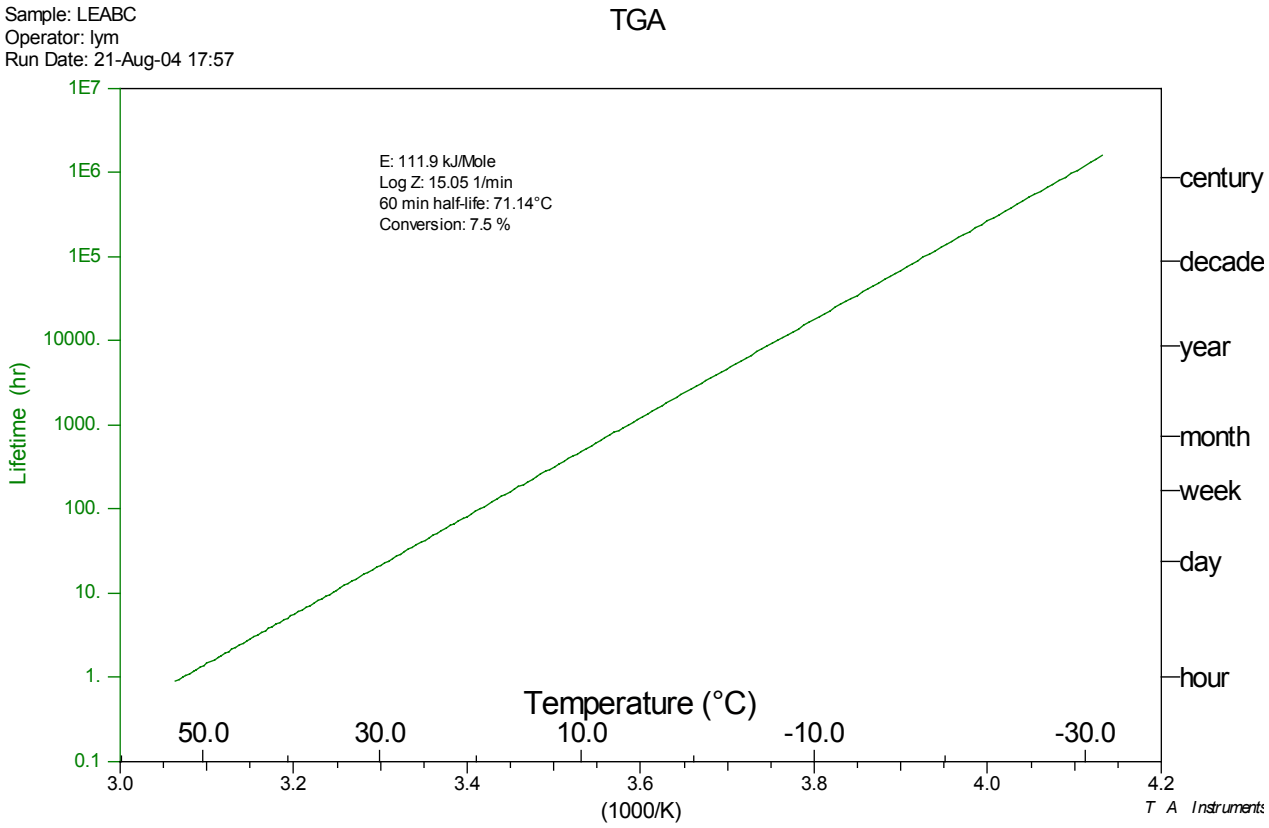

Figure 48. Estimated lifetime of LEABC.

IV. CONCLUSIONS

Various analytical techniques were used to measure the ammonium bicarbonate in the products of CO_2 scrubbing by aqueous ammonia.

FTIR can be used to distinguish the ammonium carbamate from the ammonium bicarbonate and ammonium carbonate because the spectrum of ammonium carbamate has the NH_2 peak at about 3472cm^{-1}. However, it is difficult to distinguish the ammonium bicarbonate from ammonium carbonate by FTIR.

The DSC curve of ammonium carbonate shows double peaks. The DTG curve of ammonium carbonate also shows double peaks. But ABC's DSC and TGA curve do not. Hence DSC and TGA techniques can be used to distinguish the ammonium bicarbonate from ammonium carbonate.

XRD provides obviously different spectra among ABC, ammonium carbonate and ammonium carbamate. The following 2θ angles can be used to distinguish NH4HCO_3, $(NH_4)_2CO_3$ and $NH_2CO_2NH_4$ samples: NH_4HCO_3 : 29.7, 16.5, and 21.9; $(NH4)_2CO_3$: 29.6, 23.8, and 34.5; $NH_2CO_2NH_4$: 29.7, 23.8, and 34.5. XRD can be used as the main analysis method to differentiate the products the CO_2 capture.

Carbon, hydrogen and nitrogen are the predominant elements in the products from CO_2 scrubbing by aqueous ammonia. The elemental analysis can be used as quantitative measure of ABC. A LECO CHN-2000 CHN Analyzer provides fast and accurate quantitative analysis of ABC.

The AOTF-NIR Free Space spectrometer is the ideal tool for real-time, on-line measurements of ABC. The AOTF technology allows for fast scanning using no moving parts and without the need to recalibrate the system. A Free Space spectrometer can be mounted above the CO_2 capture device and non-contact classification analysis can be performed. NIR can be used to determine percent bicarbonate of the products on-line.

Sample 01050401 and Sample 01060401 from the CO_2 scrubbing experiment by aqueous ammonia at WKU were determined to be ammonium bicarbonate. The nitrogen content of Sample 01050401 and Sample 01060401 are both above 17.2%, the index of good quality of ABC as stipulated in GB -3559-92 Agriculture Ammonium Bicarbonate National Standard of China[24]. When NIR results are compared with the results from the CHN analysis, both the CHN technique and NIR technique indicated the ABC purities of the two WKU samples are above 95% and gave very close ABC concentrations.

ABC thermal stability by TGA indicated that the evaporation speed of ABC is approximately 2.0 - 3.8 times higher than that of LEABC between 25 ^{o}C and 55 ^{o}C under the air flow rate of 50 mL/min. The evaporation speed of LEABC is approximately one-third of ABC between 25 mL/min and 75mL/min. The temperature and air flow rate has much less influence on the evaporation of the LEABC than on the ABC.

A kinetic study of ABC and LEABC gives their activation energy. At the 7.5% conversion level, LEABC's activation energy is 111.9 kJ/mole, which is greater than ABC's activation energy 93.6 kJ/mole. The decomposition reaction rate of LEABC is lower than that of

ABC. In addition, the activation energy plays an important role in engineering design such as sizing the CO_2 regeneration reactor as well as optimizing its operating condition.

LEABC has a much better effect than ABC on retarding the release of CO_2 and is suitable for short-term storage of CO_2 scrubbed by aqueous ammonia from the flue gas of power plants.

V. BIBLIOGRAPHY

1. Arrhenius, S. "On the Influence of Carbonic Acid in the Air upon the Temperature of the Ground," *The London, Edinburgh and Dublin Philosophical Magazine and Journal of Science*, Fifth series, **1896,** *41* 237-277.

2. IPCC – Intergovernmental Panel on Climate Change, *Climate Change. The IPCC Scientific Assessment*, Cambridge University Press, **1990**, XXXIX +358.

3. UNFCCC, *Kyoto Protocol to the United Nations Framework Convention on Climate Change,* FCCC/CP, **1997**, L.7/Add.1, Bonn.

4. Herzog, H.; Eliasson, B.; Kaarstad, O., "Capturing Greenhouse Gases," *Scientific American*, **2000**, *282(2),* 72-79.

5. Andres L.; Bo L.; Tobias, M. "A Fluidized-bed Combustion Process with Inherent CO2 Separation; Application of Chemical-looping Combustion," *Chem. Eng. Sci*., **2001**, *56,* 3101-3113.

6. Wolsky, A.M.; Daniels, E.J.; Jody, B.J. "CO_2 Capture from the Flue Gas of Conventional Fossil-fuel-fired Power Plants," *Environ. Prog*. , **1994,** *13*, 214.

7. Nishikawa, N.; Hiroano, A.; Ikuta, Y.; et al. "Photosynthetic Efficiency Improvement by Microalgae Cultivation in Tubular-type Reactor," *Energy Convers. Manage*, **1995,** *36*, 681.

8. Kimura, N.; Omata, K.; Kiga, T.; Takano, S.; Shikisima, S. "The Characteristics of Pulverized Coal Combustion in O2/CO2 Mixtures for Recovery," *Energy Convers. Manage*., **1995,** *36*, 805.

9. Freund, P. "Abatement and Mitigation of Carbon Dioxide Emissions from Power Generation," Power-gen 98 Conference, Milan, June, **1998**, http://www.ieagreen.org.uk/pge98.htm

10. Yeh, J. T., et al. "Aqua Ammonia Process for Simultaneous Reduction of CO_2, SO_2, and NO_x," *Proceedings,* 19th Annual International Pittsburgh Coal Conference, Pittsburgh, PA, September 23-27, **2002** .

11. Bai, H.; Yeh, A. C. "Removal of CO_2 Greenhouse Gas by Ammonia Scrubbing," *Industrial and Engineering Chemistry Research*, **1997,** *36*(6), 2490-2493.

12. Scott M. Smouse, James M. Ekmann, and et al. "Experimental study to capture CO_2 in the flue gas from a coal-fired research facility by spraying aqueous ammonium to produce a modified NH_4HCO_3 fertilizer", Second Annual Conference on Carbon Sequestration: Developing & Validating the Technology Base to Reduce Carbon Intensity, Virginia, May 5-9, 2003

13. NPCC, "Study on CO_2 Sequestration by Spray Concentrated Aqueous NH_3 and Production of Modified NH_4HCO_3 Fertilizer," a proposal for US-China joint research. State Engineering Technology Research Center of Combustion of Power Plants (NPCC), China, 2000.

14. Shale, C.C.; Simpson, D.G.; Lewis, P.S. "Removal of Sulfur and Nitrogen Oxide from Stack Gases by Ammonium," *Chem. Eng. Prog. Symp. Ser*., **1971,** *67*, 52-58.

15. Qiao He, John T. Riley, Kunlei Liu, Wei-Ping Pan, "Development of a Method for Measuring Carbon Balance in the Chemical Sequestration of CO_2", Technical Proposal for Phase II for Small Business Innovation Research (SBIR) of Department of Energy, 2004.

16. Zhang Z.M.; Feng Y.Q.; et al. *New Nitrogen Fertilizer-Long Efficiency Ammonium Bicarbonate*, Press of Chemistry Engineering of China, 1998.

17. Qiao He, John T. Riley, Kunlei Liu, Wei-Ping Pan, Technical Proposal for Phase Diagram Study of the Reaction of NH_3, H_2O and CO_2 for Small Business Innovation Research (SBIR) of Department of Energy, 2003.

18. Jiang W.D.; Pao, H.P.; He, Q., "The Production of Ammonium Bicarbonate as Fertilizer in China," *Technical Report* of General Technology, Inc., No. 02-1, **2002**.

19. The Activation Energy of Chemical Reactions, http://chemed.chem.purdue.edu/genchem/topicreview/bp/ch22/activate.html.

20. S. Sauerbrunn & P. Gill, TA Application 075: Decomposition Kinetics Using TGA, TA Instrument .

21. Flynn and Wall, *Polymer Lett.,* **1966,** *19*, 323.

22. Borchardt, H. J.; Daniels, F. J Am Chem Soc, **1957**, *79*, 41-46.

23. *Soil Agriculture Chemical Analytical Method*, China Soil Society, 1992, 358-359.

24. GB -3559-92 Agriculture Ammonium Bicarbonate National Standard of China, 1992.

25. Yong-Fa Diao, Xian-Yu Zheng, Bo-Shu He, Chang-He Chen and Xu-Chang Xu Li, X.; "Experimental Study on Capturing CO_2 Greenhouse Gas by Ammonia Scrubbing"**,** *Energy Conversion and Management*, August **2004,** *13-14(45)*, , 2283-2296.

26. Q. He, M. Chen, L. Meng, K. Liu and W. Pan, "Study on Carbon Dioxide Removal by Absorption of Ammonium Solution", Third Annual Conference on Carbon Capture and Sequestration, May 2004.

27. Wei-Ping Pan, NATAS Short Course Handout, Thermal Analysis Laboratory, Western Kentucky University, 2003.

28. H. Bui, S. Burris, L. Meng and W. Pan, Analytical Report of Ammonium Salts, Brimrose Corporation of America & Thermal Analysis Laboratory at Western Kentucky University, 2004.

29. ASTM E 1641 – 99 Standard Test Method for Decomposition Kinetics by Thermogravimetry.

30. Kinetics of Drying by Thermogravimetric Analysis, Thermal Analysis Application Brief, Number TA-134.